ÇUKUROVA UNIVERSITY
INSTITUTE OF NATURAL AND APPLIED SCIENCES

MSc THESIS

Akın İLHAN

EFFICIENCY ANALYSIS OF AN INSTALLED WIND FARM

DEPARTMENT OF MECHANICAL ENGINEERING

ADANA, 2014

ÇUKUROVA UNIVERSITY
INSTITUTE OF NATURAL AND APPLIED SCIENCES

EFFICIENCY ANALYSIS OF AN INSTALLED WIND FARM

Akın İLHAN

MSc THESIS

DEPARTMENT of MECHANICAL ENGINEERING

We certify that the thesis titled above was reviewed and approved for the award of degree of the Master of Science by the board of jury on 25/08/2014.

………………...................	……………………………….	……………...............................
Prof. Dr. Beşir ŞAHİN	Prof. Dr. Hüseyin AKILLI	Assoc. Prof. Dr. Mehmet BİLGİLİ
SUPERVISOR	MEMBER	MEMBER

This MSc Thesis is written at the Department of Institute of Natural And Applied Sciences of Çukurova University.
Registration Number:

Prof. Dr. Mustafa GÖK
Director
Institute of Natural and Applied Sciences

ABSTRACT

MSc THESIS

EFFICIENCY ANALYSIS OF AN INSTALLED WIND FARM

Akın İLHAN

ÇUKUROVA UNIVERSITY
INSTITUTE OF NATURAL AND APPLIED SCIENCES
DEPARTMENT OF MECHANICAL ENGINEERING

Advisor : Prof. Dr. Beşir ŞAHİN
Year: 2014, Pages: 81
Jury : Prof. Dr. Beşir ŞAHİN
: Prof. Dr. Hüseyin AKILLI
: Assoc. Prof. Dr. Mehmet BİLGİLİ

In this study, energy analysis and efficiency study of turbines of a wind farm were performed using data of wind speed, wind direction, air temperature and electric generation, of five selected turbines. Wind energy losses of the plant, monthly and daily performance of turbines were carried out. Parameters influencing the results were also examined in detail. Aerodynamic analysis of turbines was conducted using data of five turbines.

Analysis of factors affecting system performance, Betz criteria, power coefficient, energy balance and exergy balance were conducted. Magnitude of wind speeds where turbines start and stop energy generation and influences of these wind speeds on power production and energy losses of five turbines were examined. Consequently, clarifications on the reasons of the losses during conversion of wind power into electric energy, and clarifications on the reasons of instantaneous fluctuations in efficiencies were aimed to be explained. Interactions between aerodynamic parameters during power generation were also reported.

Key Words: Exergy, wind power, wind turbine

ÖZ

YÜKSEK LİSANS TEZİ

KURULU BİR RÜZGÂR ÇİFTLİĞİNİN VERİM ANALİZİ

Akın İLHAN

ÇUKUROVA ÜNİVERSİTESİ
FEN BİLİMLERİ ENSTİTÜSÜ
MAKİNE MÜHENDİSLİĞİ ANABİLİM DALI

Danışman : Prof. Dr. Beşir ŞAHİN
Yıl: 2014, Sayfa: 81
Jüri : Prof. Dr. Beşir ŞAHİN
: Prof. Dr. Hüseyin AKILLI
: Assoc. Prof. Dr. Mehmet BİLGİLİ

Bu çalışmada bir rüzgâr çiftliğinin 5 adet türbinine ait rüzgâr hızı, rüzgâr yönü, güç üretimi ve hava sıcaklığı verileri kullanılarak ilgili türbinlerin enerji ve ekzerji analizi ve türbinlere ait verimlilik çalışması yapılmıştır. Santralin enerji kayıpları ayrıntılı bir şekilde incelenmiştir; enerji ve ekzerji analizlerinin, türbinlerin aylık ve günlük performans değerlendirmesindeki önemi araştırılarak, sonuçlara etkiyen parametreler ayrıntılı bir biçimde ele alınmıştır. Türbinlerin aerodinamik analizi ise dört türbine ait veriler kullanılarak yapılmıştır.

Sistemin performansına etkiyen, Betz kriteri, güç katsayısı, enerji dengesi ve egzerji dengesinin analizi yapılmıştır. Türbinlerin enerji üretimine başladığı ve üretimi sonlandırdığı hız aralığının, çalışmada dikkate alınan beş adet türbin üzerindeki güç üretimini ve enerji kayıplarını nasıl etkilediği anlatılmıştır. Sonuç olarak, rüzgâr enerjisinin elektrik enerjisine dönüşümünde, meydana gelen enerji kayıplarının, verimdeki anlık çalkantıların sebeplerine açıklık getirilmeye çalışılmıştır. Üretim esnasındaki aerodinamik verilerin birbirleriyle karşılıklı olarak nasıl değiştiği gösterilmiştir.

Anahtar Kelimeler: Egzerji, performans analizi, rüzgar enerjisi, rüzgar hızları

ACKNOWLEDGEMENTS

Warm thanks to my advisors dear Prof. Dr. Beşir ŞAHİN, Prof. Dr. Hüseyin AKILLI and Doç. Dr. Mehmet BİLGİLİ who had given me the thesis named "Efficiency Analysis of an Installed Wind Farm", never had begrudged their helps at every section of my study and always guided me by their creative and leading ideas.

CONTENTS **PAGE**

ABSTRACT I
ÖZ II
ACKNOWLEDGEMENTS III
CONTENTS IV
LIST OF TABLES VI
LIST OF FIGURES VIII
NOMENCLATURE XII
1. INTRODUCTION 1
 1.1. Factors Affecting Wind Formation 1
  1.1.1. Relation of Topography and Wind 1
  1.1.2. Surface Roughness 2
 1.2. Wind Power Potential on Earth and in Turkey 3
  1.2.1. Wind Power Potential on Earth 3
 1.3. Wind Power Potential in Turkey 3
 1.4. Brief History of Wind Energy 5
 1.5. Exergy Analysis of Wind Turbines in Thermodynamic Aspect 8
  1.5.1. Definition of Exergy 8
2. LITERATURE SURVEY 9
 2.1. Historical Development of Wind Energy 9
 2.2. Preliminary Work 10
3. MATERIALS AND METHOD 13
 3.1. Air Density 14
 3.2. Calculation of Wind Power and Efficiency 15
 3.3. Computation of Wind Power Losses 17
 3.4. Wind Exergy 19
 3.5. Estimation of Wind Directions 20
 3.6. Relations for Wind Aerodynamics 20
4. RESULTS AND DISCUSSION 27
 4.1. Power and Efficiency Computations by Monthly Average Data 27

4.2. Power and Turbine Efficiency for Unrecorded Wind Direction.................... 29
4.3. Identification of Wind Directions for the Turbines 32
4.4. Introduction of Cut-In and Cut-out Speeds.. 35
4.5. Exergy Analysis.. 50
4.6. Aerodynamic Performance Analysis 52
5. CONCLUSIONS... 71
REFERENCES.. 73
CURRICULUM VITAE 77
APPENDICES 78

LIST OF TABLES **PAGE**

Table 3.1. Specifications of wind turbines considered in the present study 18
Table 3.2. Roughness lengths 20
Table 3.3. Wind direction values 20
Table 4.1. Power efficiencies of T01 and T02 27
Table 4.2. Power efficiencies of T03, T04, T05 and power efficiency according to the average data of all turbines 28
Table 4.3. Monthly power efficiency (C_p) for all turbines... 28
Table 4.4. Yearly efficiency of turbines for unrecorded wind direction.................... 29
Table 4.5. Power efficiencies of T01, T02, T03, T04, T05 and power efficiency according to the average data of all turbines.. 36
Table 4.6. Efficiency comparison for all turbines considering boundary limits........ 45
Table 4.7. Exergy of turbines T01, T02, T03, T04 and T05...................................... 50
Table 4.8. Total times of all turbines for zero production in a year........................... 52

LIST OF FIGURES **PAGE**

Figure 1.1. Modified wind map of Turkey (Kıncay, 2008) 4

Figure 1.2. Map of modified wind energy potential in Turkey at an elevation of 100 m. (Kıncay, 2008).. 4

Figure 1.3. Existing wind power modified (Tanriöven, 2011) 6

Figure 1.4. Relation of power with respect to the wind speed modified (Tanrıöven, 2011).. 6

Figure 1.5. Front and side views of modified wind turbine (Yılmaz et al, 2012)...... 7

Figure 1.6. Idealized flow passing through moveable disc at stream tube 7

Figure 3.1. Elevation used in computations (800 m above sea level)...................... 14

Figure 3.2. Helical vortex wake shed by rotor with three blades each with uniform circulation DG (Burton et al, 2011)....................................... 22

Figure 3.3. Simplified helical vortex wake ignoring wake expansion (Burton et al, 2011) 23

Figure 3.4. A blade element sweeps out an annular ring (Burton et al, 2011)......... 24

Figure 3.5. Blade Element Velocities and Forces (Burton et al, 2011) 24

Figure 4.1. Average wind speed of turbines for unrecorded wind direction............ 29

Figure 4.2. Average air temperatures for turbines according to the unrecorded wind direction... 30

Figure 4.3. Average wind power generations of turbines for unrecorded wind direction.. 30

Figure 4.4. Power analysis of turbines for unrecorded wind direction.................... 31

Figure 4.5. Monthly power efficiencies of turbines for unrecorded wind direction 32

Figure 4.6. Distributions of wind direction for turbines T01 and T02..................... 32

Figure 4.7. Distributions of wind direction for turbines T03, T04 and T05 33

Figure 4.8. Monthly distributions of wind direction for turbines T01, T02, T03 and T04 34

Figure 4.9. Monthly distributions of wind direction for turbine T05....................... 35

Figure 4.10. Monthly average wind speed for turbines T01, T02, T03 and T04....... 37

Figure 4.11. Monthly average wind speed for turbine T05 and monthly average wind speed according to the average wind speeds of all turbines......... 38
Figure 4.12. Monthly average air temperature for turbines T01 and T02.................. 38
Figure 4.13. Monthly average air temperature for T03, T04, T05 turbines and monthly average air temperatures of wind farm 39
Figure 4.14. Monthly average measured wind power generations for T01, T02, T03 and T04 turbines 40
Figure 4.15. Monthly average power generation for turbine T05 and monthly average power generation of all turbines 41
Figure 4.16. Power analysis of T01, T02, T03 and T04 turbines 42
Figure 4.17. Power analysis of T05 and average power analysis according to the average powers of all turbines.. 43
Figure 4.18. Monthly efficiencies of turbines T01 and T02 43
Figure 4.19. Monthly efficiencies of turbines T03, T04, T05 and monthly average efficiencies according to the average data of all turbines 44
Figure 4.20. Comparison of efficiency of all turbines for one year........................... 45
Figure 4.21. Comparison of efficiency for all turbines considering average wind speeds 46
Figure 4.22. Comparison of efficiency for all turbines with separate average wind speeds related to each other... 47
Figure 4.23. Monthly average efficiency distribution for all turbines 47
Figure 4.24. Monthly average flow induction factor (a) distribution for all turbines 48
Figure 4.25. Distributions of monthly average thrust coefficient (C_T) for all turbines... 49
Figure 4.26. Monthly total electric generations and average wind speeds 49
Figure 4.27. Distributions of power coefficient, C_p with velocity ratio, λ 53
Figure 4.28. Distributions of thrust coefficient, C_T with velocity ratio, λ 53
Figure 4.29. Relation of power coefficient, C_p with flow induction factor, a............ 54
Figure 4.30. Thrust coefficient, C_T with flow induction factor, a.............................. 54
Figure 4.31. Variation of wake velocity, U_w and free-stream velocity, U_∞ 55
Figure 4.32. Distribution of speed on rotor, U_D with free-stream wind speed, U_∞ ... 56

Figure 4.33. Distribution of power generation, P with free-stream wind speed, U_∞ 56

Figure 4.34. Distributions of thrust force (T) with free-stream wind speed, U_∞ 57

Figure 4.35. Variation of mass flow rate $(\dot{m})$ with free-stream wind speed, U_∞ 58

Figure 4.36. Relations between rotor speed (Ω) and free-stream wind speed (U_∞) 58

Figure 4.37. Variations of tangential flow induction factor (a') with free-stream wind speed (U_∞) 59

Figure 4.38. Variations of flow induction factor (a), with free-stream wind speed (U_∞) 60

Figure 4.39. Variations of power coefficient (C_p) with tangential flow induction factor (a').. 61

Figure 4.40. Variations of thrust coefficient, C_T with tangential flow induction factor (a').. 61

Figure 4.41. Tangential flow induction factor (a') with flow induction factor (a) ... 62

Figure 4.42. Variations of flow induction factor (a) with velocity ratio (λ) 63

Figure 4.43. Variations of tangential flow induction factor (a') with velocity ratio (λ).. 63

Figure 4.44. Variation of bound circulation angle, ϕ and velocity ratio, λ 64

Figure 4.45. Variations of bound circulation angle, ϕ with free stream wind speed, U_∞ 65

Figure 4.46. Variation of bound circulation angle, ϕ with tangential flow induction factor (a')... 66

Figure 4.47. Variation of bound circulation angle, ϕ with flow induction factor (a) 66

Figure 4.48. Variation of bound circulation angle (ϕ) with rotor speed (Ω) 67

Figure 4.49. Variation of bound circulation angle, ϕ with resultant relative velocity, W 68

Figure 4.50. Variation of resultant relative velocity, W with free-stream wind velocity, U_∞ 68

Figure 4.51. Variations of total circulation, Γ with free-stream wind speed, U_∞ 69

Figure 4.52. Variation of power coefficient for BEM theory, C_p* with tip speed ratio, λ^* 70
Figure 4.53. Distributions of power coefficient for BEM theory, C_p* with wind speed on the rotor, U_D 70

NOMENCLATURE

C_p	:	Pressure coefficient
a	:	Flow induction factor
a'	:	Tangential flow induction factor
r	:	Density (kg/m^3)
v	:	Speed (m/s)
C_T	:	Thrust coefficient
P	:	Absolute pressure (1 atm)
^oC	:	Centigrade Celsius
R_{Rotor}	:	Radius of rotor (m)
T	:	Absolute temperature (K: Kelvin) $Kelvin = K = {}^oC + 273.15$
R	:	Ideal gas constant = $8.2056\,x10^{-5}\,[m^3.atm/Kelvin.mol]$
n	:	Mass (mol)
V	:	Volume (m^3)
Z_o	:	Coefficient of roughness length (m)
Z_1	:	Elevation of wind turbine hubs at sea level
Z_2	:	Elevation of wind turbine hubs in the wind farm
V_i	:	Wind Speed (m/s)
V_1	:	Wind speed at sea level (m/s)
V_2	:	Wind speed in the wind farm (m/s)
Vz,com_top	:	Interpolated wind speed due to hub heights and variety of terrain conditions (m/s)
V_{z,sea_level}	:	Interpolated wind speeds due to the hub heights of turbines at sea level (m/s)
V_r	:	Nominal Speed (m/s)
W_{tr-ex}	:	Exergy of wind turbine
P_R	:	Maximum power that can be taken from optimum wind turbine
P_{TH}	:	Theoretical power (Watt)

$C_{p\text{-}Betz}$	:	Maximum pressure coefficient that Betz foresees
P	:	Power (Watt)
Q	:	Torque (Joule)
T	:	Thrust (Newton)
$\dot{m}$	:	Mass flow rate (kg/s)
W_{KE}	:	Kinetic energy (Joule)
Kwh	:	Unit of energy
C_p	:	Turbine efficiency
A	:	Rotor sweeping area (m^2)
D	:	Rotor diameter (m)
G	:	Bound circulation (m^2/s)
W	:	Number of rotations (rpm)
W	:	Resultant relative velocity at the blade (m/s)
f	:	Angle at plane of rotation
a	:	Angle of attack
b	:	Resultant relative velocity angle
C_l	:	Lift coefficient
L	:	Lift force
C_d	:	Drag coefficient
D	:	Drag force
c	:	Chord length of blade
B	:	Number of blades
C_x	:	Coefficient giving relation between lift and drag
C_y	:	Coefficient giving relation between lift and drag
s_r	:	Chord solidity
U_D	:	Speed on the rotor
U_W	:	Speed far on the wake
Lapse rate	:	Change of temperature in troposphere due to the altitude
BEM	:	Blade element/momentum theory
C_P^*	:	Power coefficient for BEM theory

λ	:	Ratio of air speed far on the wake to air speed in front of the rotor
λ^*	:	Tip speed ratio

1. INTRODUCTION

Energy usage is important in enhancing the quality of life besides providing physical comfort and surviving of life. The usage of energy depends on resources and development of the proficiency of using these resources. Most of the energy sources used by humans was obtained from sun until the discovery of nuclear energy. Sun energy is absorbed and stored up by plants with the specific activity named photosynthesis in order to provide the energy found in foodstuff. Fossil fuels which are also derived from sun were also produced of rotten plants lived million years ago. Energy coming from sun also generates wind formation in the atmosphere. This operates wind rotors for years. Nowadays, the world demand of energy grows rapidly and this demand will continue to grow substantially in coming years because of high growth of populations, social, economic and industrial developments. High rate of energy demand, rapid increase of oil price and negative impact of fossil fuels on the environment gave tremendous attention to wind energy all over the world. In order to convert wind energy into electricity one need to use wind turbine. Wind turbine is equipment to be used to convert wind energy into electric energy. It is also referred to be inverter of wind energy to mechanical energy.

Wind is an indirect product of sun energy. There are lots of variations in wind speed from stagnant velocities to hurricanes.

1.1. Factors Affecting Wind Formation

1.1.1. Relation of Topography and Wind

If topography was plain and smooth everywhere on the earth surface, then wind variation from one point to another would be very small. With the participation of hills, valleys, river valleys, lakes, a complex and variable wind regime is formed. Forest and buildings can be added to this complexity.

Crests, plateaus, and cliffs are the locations where high wind speed can be found. Wind speed is lower in locations that are more enclosed and having lower altitudes. Nevertheless, it is not obligatory for wind speed to be low in whole valleys. When the valleys stand parallel to the wind flow, they can pretend as channels and can increase the magnitude of wind speed. A sudden contraction in section of valley can fortify wind flow in a narrow area by funneling air. This usually takes places in narrow mountain gates facing wind.

High altitude topographical features can speed up wind flow. When an approaching mass of air passes over climax point, it is usually compressed into a thin layer which increases its speed. Highest speed is obtained when wind blows perpendicular on the line of mountain ridge. Isolated hills and mountains accelerate winds less than mountain ridges, since more air tend to flow sides.

Land areas close to seas and big lakes can be good windy zones due to two reasons. Firstly, a water surface is much smoother than a land surface which results the air flowing on it to be exposed to lower friction. Best wind area is the coastal area where dominant wind direction is directed to the shore. Secondly, like as in a sunny summer day when the local wind is slight, local winds named to be sea or lake breezes are formed since heating of land and sea are in a different ratio. By the virtue of land heating is much quicker than water heating; colder air is moved from water to land instead of heated and raised air of land. Consequently, breezes of speeds varying from 13 to 20 km/h or higher are formed that are directed from sea through land. Since at nights, lands cool down faster compared with seas, breezes stop flowing or blow in the opposite direction.

1.1.2. Surface Roughness

Wind speed close to ground surface is as much lower with the same ratio of higher friction. Wind speed is affected by the surface on which it blows. Granular surfaces covered with trees and buildings will cause more friction and turbulence compared with plain surfaces like lakes or plain ground surface.

1.2. Wind Power Potential on Earth and in Turkey

1.2.1. Wind Power Potential on Earth

Earth wind power source is calculated to be 53 TWh/year, and by the year of 2020 World electric demand is predicted to increase by 25.579 TWh/year. Until the year of 2020, about 12 % of World electric consumption is predicted to be provided by wind energy. Amount of investment is expected to be nearly 692 billion $ in order to reach the target of 1245 GW electric energy received from Earth wind power production until the year of 2020. Within this time interval, production costs are foreseen to decrease from 3.79 e-cents/kWh to 2.45 e-cents/kWh. Within this time interval, 2.3 million job opportunities will be obtained worldwide from production, assembly and other branches of industries related with wind energy.

1.3. Wind Power Potential in Turkey

Production of energy (especially electrical) affair increasing in Turkey by recent years boosted dependency to abroad as in natural gas and consequently unbalances in energy productions grew out. Wind energy which is a category of renewable energy source has a great potential in our country, however the reality that we cannot benefit from this potential sufficiently is clear. Wind energy potential category intervals given by Turkish Government Electric Power Resources Survey and Development Administration (Figure 1.1) and based on stations of Turkish Government Meteorological Department Database at 50 m and 100 m altitudes (Figure 1.2) are shown in the following maps.

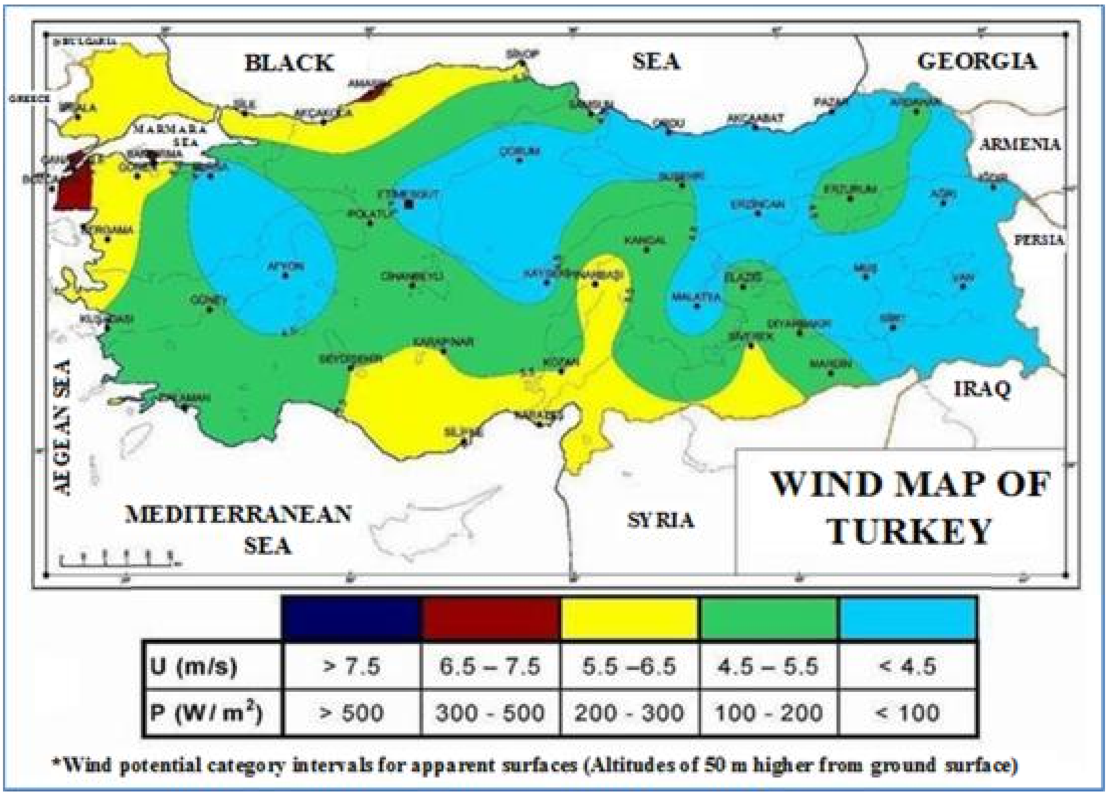

Figure 1.1. Modified wind map of Turkey (Kıncay, 2008)

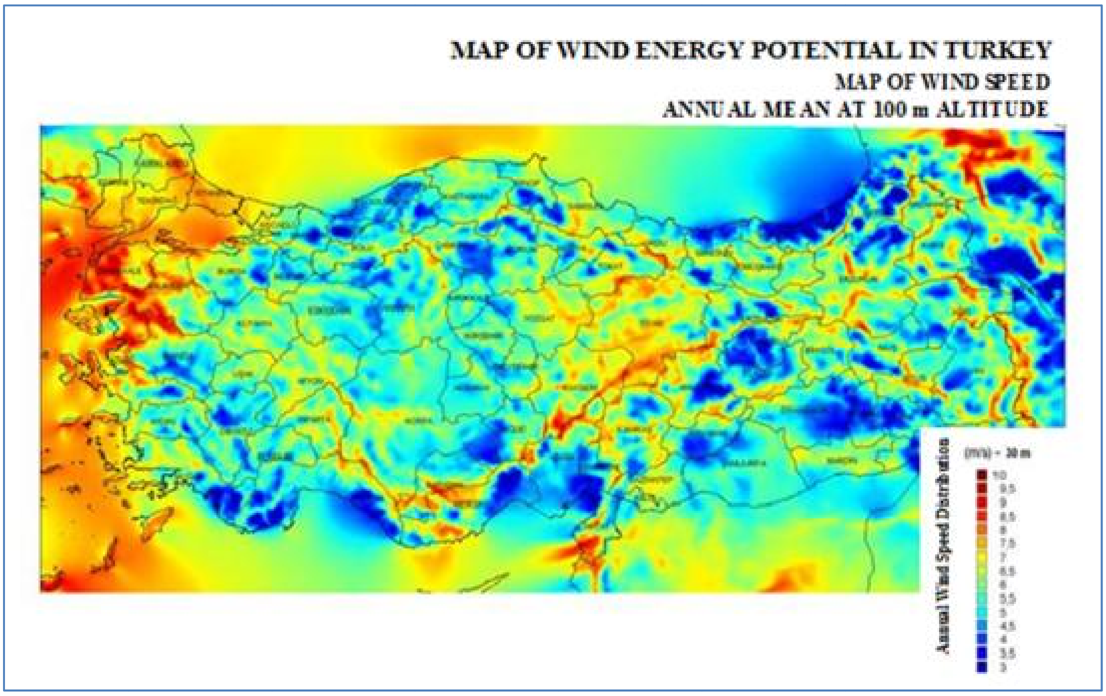

Figure 1.2. Map of modified wind energy potential in Turkey at an elevation of 100 m. (Kıncay, 2008)

1.4. Brief History of Wind Energy

Wind energy played an important role in World civilization history. Wind energy is first used about 500 years ago in Egypt for floating of rowboats from one coast to another. First wind mill was built in Ancient Babylon about 200 B.C., and it was a machine consisting of propellers attached to an axis which produced rotary motion. Cereal grinding in wind mills having height of 9.144 m and having wind trapping blades of 4.8768 m and is first executed in East Persia and in Afghanistan by the year of 10 A.C. Western countries had discovered wind mills at a very later time. First written records related with this subject belong to 12. Century.

Wind mills of multi-propellers were invented in USA by the second half of 19. Century. By the year of 1889, USA had 77 wind mill production factories and at the end of this century, exportation of wind mills was the greatest export item for USA economy. Until diesel motors were invented, big railway establishments had abided to great multi-propeller wind mills. By the years of 1930 and 1940, hundred thousands of wind turbines producing electricity were manufactured in USA.

Increase of the petrol cost and limitations in traditional energy sources enhanced interest to wind energy again. By the encouragements and formal research studies, lots of new turbine designs were accomplished. The equation demonstrating the relation between wind speed and generated power are given in equation 1.1 (see figure 1.3). Change of wind energy potential with respect to the wind speed is depicted in figure 1.4.

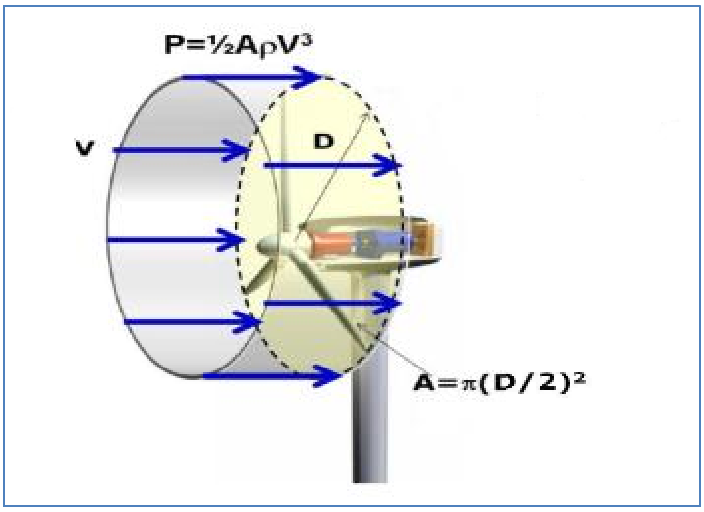

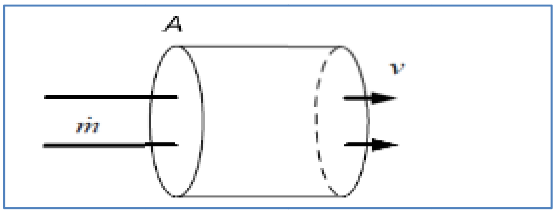

Figure 1.3. Existing wind power modified (Tanriöven, 2011)

$$P_W = \frac{1}{2} \rho A V^3 \qquad (1.1)$$

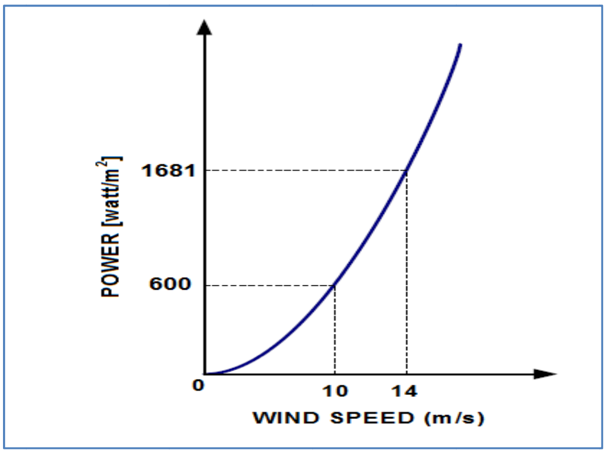

Figure 1.4. Relation of power with respect to the wind speed modified (Tanrıöven, 2011)

Front and side views of a regular wind turbine are shown in figure 1.5.

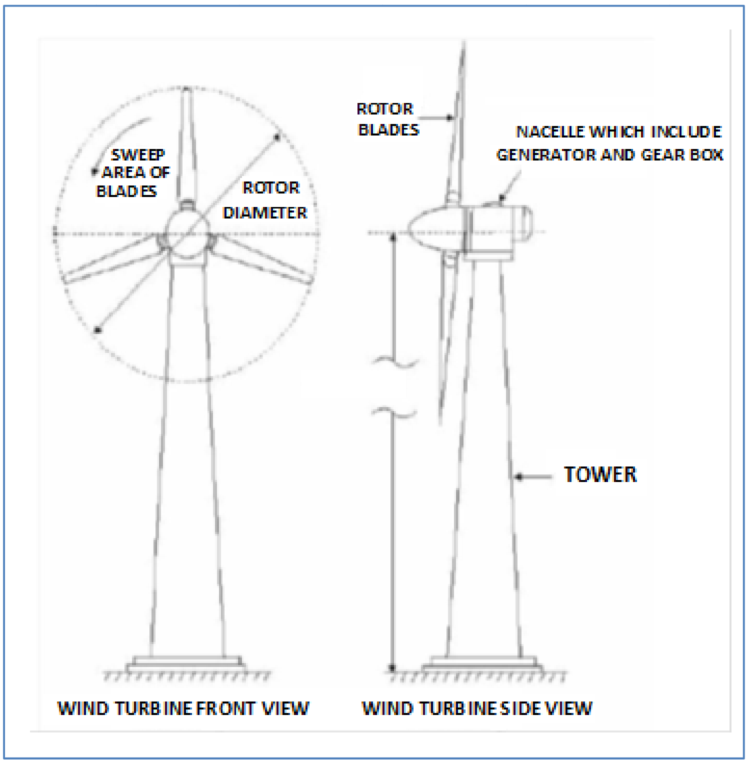

Figure 1.5. Front and side views of modified wind turbine (Yılmaz et al, 2012)

Schematic representation of stream tube is shown in figure 1.6 which represents wind tunnel of wind turbine. Related wind speeds are shown in this figure. Free stream velocity, $U_{¥}$ exhibits wind speed in front of the rotor, U_2 and U_3 symbolize wind speeds just before and after rotor; and U_W shows wind speed far on the wake.

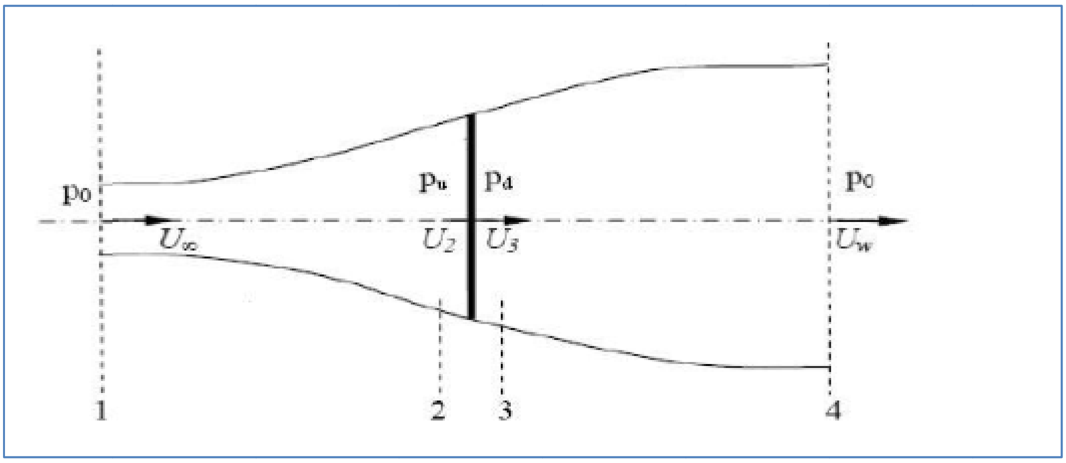

Figure 1.6. Idealized flow passing through moveable disc at stream tube

1.5. Exergy Analysis of Wind Turbines in Thermodynamic Aspect

1.5.1. Definition of Exergy

Exergy which is also known as “Available Energy” can also be considered as useful part of the energy for energy systems working at ambient temperatures. In other words, useful part of the energy is the part that can be converted to other forms of energy. Both exergy demolition and exergy loss can be assigned from “Exergy Analysis” which is also known to be “Analysis of Second Law of Thermodynamics”.

Exergy demolition is directly a result of the irreversibility within the system. During the optimization of the complex thermodynamic systems, second law of thermodynamics was proved to be a very strong tool. In the light of second law, in order to determine performance of engineering kits; availability, reversible work, irreversibility, and efficiency of second law terms are tools for conducting exergy analysis.

2. LITERATURE SURVEY

2.1. Historical Development of Wind Energy

Main source of wind energy is sun. During heating up of air and ground by sun at a certain section of Earth, other parts of Earth cool down. Daily heating and cooling variations continue around Earth. Equator region absorb much more sun energy when compared with poles. Heated air in Equator rises up and moves towards poles, and cooled air gets heavy and turns back. Air tends to pile up on 30^0 North Latitude. As a result of this, at that region pressure is high and climate is soft. Some air masses blow towards south outside of this high pressured zone and due to the Earth rotation, they tend to move towards west named to be Trade Winds.

Humans use wind energy for ages which is one of the renewable energy sources. Wind energy was used in several of geographical regions through wind mills in order to produce flour and to pump water from water wells. Contemporarily wind energy is transformed to electrical energy by modern wind turbines in order to bring this energy into use of humans. Some properties of wind energy can be sequenced as follows: Power obtained from wind energy demonstrates variation directly with the cubic of wind speed due to the Betz Theorem. Wind energy intensity depends on the locality. In order to benefit from wind energy, it must be transformed to some other forms of energy. Raw material of energy is wind and it is found in atmosphere in a large amount and free form. As long as sun and earth exist, it is possible to benefit from wind energy as a renewable energy source.

Start of the exploration of wind power and utilization from this power by human-beings endure to long before periods in the history. Running of sailing ships and running of wind mills can be demonstrated as first forms of benefitting from wind power. It is known that wind energy for the first time was used as additional power to the power of shovel convicts in Egypt in the years of 2800 B.C. Egyptians benefitted from wind power in order to inflate sailing boats owed long lengths and to float ships of having tones of weights. Until the invention of steam ships, sailing boats played an important role in intercontinental transportation and trades.

Phoenicians had performed the most important contribution to the development of intercontinental transportation. For that matter, Englishmen called western winds as trade winds. Invention and successful utilization of wind mills for grinding of grains in ancient Egypt, China and Japan in the years of 2000 B.C. are admitted. Holland is accepted to be the center of wind mills. Invention of wind mills was carried to West from Turkish People by Crusades (1096 – 1270).

2.2. Preliminary Work

Bilgili and Şahin (2009) conducted investions on the wind energy density in the southern and southernwest region of Turkey, and investigated using the Weibull and Rayleigh probability density functions, and the wind atlas analysis and application program (WasP). They used hourly wind speeds and directions collected by the General Directorate of Electrical Power Resources Survey Administration.

González et al. (2014) had given influence of terrain conditions and optimal locations on wind turbine design and power efficiency that can be acquired.

Karamanis (2011) demonstrated influence of wind speed and direction on mean power densities at variety of heights. He had handed cut – in speed and cut – out speed for diverse of wind turbine models which clearly identify that true values of them were used in our calculations of energy and exergy analysis. During the optimization of lost power estimations, the values of cut – in and cut- out speeds that were given us by wind farm exploiters were observed to be approximately equal to the values given by D. Karamanis.

Özgener (2006) exhibited impossibility of generating electricity below cut – in speed in the study “A small wind turbine system (SWTS) application and its performance analysis” by the application of measured parameters of 1.5 kW generator. This clearly supports how cut – in speed influences energy loss and exergical augmentation as in wind farm calculations. It is seen that with the cut – in speed of 4.4 m/s and below, total active power and total apparent power will be negligible.

Bhutta et al. (2012) demonstrated that coefficient of power (C_p) for various configurations is different and can be optimized with reference to tip speed ratio, $\lambda^* = (R.\Omega)/U_\infty$. They proposed that latest emerging design techniques can be helpful in this optimization. Furthermore, flow field around the blade can also be investigated with the help of these design techniques for safe operation.

Mostafaeipour et al. (2014) had focused on determining wind energy potential for the city of Zahedanins southeast part of Iran. They analyzed five years data to obtain wind power density and wind energy potential of the region by using Weibull density function.

Xydisa et al. (2009) had studied on the wind potential of a relatively flat area in central Peloponnese in Greece. Their basic aim was to compare the estimated net power output with the net power output from mountain sites in the wider central Peloponnese area. They demonstrated topological influences on energy generation capacity.

Akdağ and Güler (2010) had performed studies related with wind energy potential of Turkey and its utilization. They presented an overview of wind energy development in the world and gave motivation on the interest in wind energy investment.

Lior and Zhang (2007) aimed to attempt clarifications of the definitions and use of energy and exergy based on performance criteria, and use of the second law efficiency with an aim at the advancement of international standardization of these important concepts.

Pope et al. (2010) performed energy and exergy analysis on four different wind power systems including both horizontal and vertical axis wind turbines. They encompassed significant variability in turbine designs and operating parameters through the selection of systems. They compared two airfoils commonly used in horizontal axis wind turbines (NACA 63(2) – 215 and FX 63 – 137) with two vertical axis wind turbines (VAWTs). Their paper analyzed each system with respect to both the first and second laws of thermodynamics. Aerodynamic performance of each system was numerically analyzed by computational fluid dynamics software, Fluent.

Koroneos et al. (2001) dealed with exergy analysis of wind power. They discussed the actual use of energy from the existing available energy.

Başkut et al. (2011) presented energy and exergy efficiency results and technical availability analysis of wind turbine power plants by the data taken from the system in Çeşme/İzmir. Investigated wind turbine power plant is Turkey's first installed (1998) wind plant (1.50 MW) located in İzmir.

Başkut et al. (2010) demonstrated exergy efficiency results of the wind turbine power plants by considering meteorological variables such as density, pressure difference between state points, humidity and ambient temperature.

Xydis (2012) investigated effects of atmospheric variables as air temperature, humidity and pressure and their effects on the wind turbine output towards wind energy exploitation. He studied the wind potential around a coastal mountains area based on field measurements.

Xydis et al. (2009) studied wind potential of Central Peloponnese in Greece and the exergy analysis methodology was implemented as a wind farm sitting selection tool. They conducted a study on wind speed of the chosen regions of Central Peloponnesse and correlated based on measurements of three specific sites in the wider area using a software based on prognostic model.

Redha et al. (2011) considered thermodynamic characteristics of wind through energy and exergy analyses and both energetic and exergetic efficiencies were studied. They selected Vestas V52 wind turbine and demonstrated effect of air temperature and pressure on wind speed and wind turbine performance.

Hepbasli and Alsuhaibani et al. (2011) reviewed the studies conducted on exergetic and exergoeconomic analysis and assessed of wind energy systems and suggested possible future works to be performed. They analyzed wind energy systems in exergetic and exergoeconomic aspect.

3. MATERIALS AND METHOD

Studies of energy and exergy analysis of wind turbines of considered wind farm had been carried out in this study by using the data of 2010 year. Related data of wind farm was given hourly for each day of 2010. Data contained information on hourly speeds, electric generations, wind directions, and temperatures for five turbines considered. The altitude of considered wind farm is 800 m. Five wind turbines inside the wind farm are named as T01, T02, T03, T04 and T05.

Monthly average wind data obtained from the wind farm are used for the computation of electric generation efficiencies. Related data are given in Appendix 1. They are estimated from hourly wind data for each turbine to form monthly average data. Data formed monthly for each discrete turbine given in Appendix 1 demonstrates hourly data for each turbine, such as related wind speed, power generation, wind direction, and air temperature. However, some erroneous hourly data were determined in these computations, and Appendix 2 was presented.

Appendix 2 contained wind speed data between cut-in (4 m/s) and cut-out speeds (25 m/s) where turbines generate electricity efficiently. Other wind speeds were eliminated. Some generated data which are equal to zero and below zero were eliminated. Unrecorded wind directions which are given outside of 0^0-360^0 were eliminated. Positive generations obtained under cut-in speed were also eliminated since they generated very small amounts of energy. In T02 Turbine, for months from June to December, unrecorded wind directions were available in data provided by the company which in charge of installed wind farm, considerable electric generations occurred during these months.

3.1. Air Density

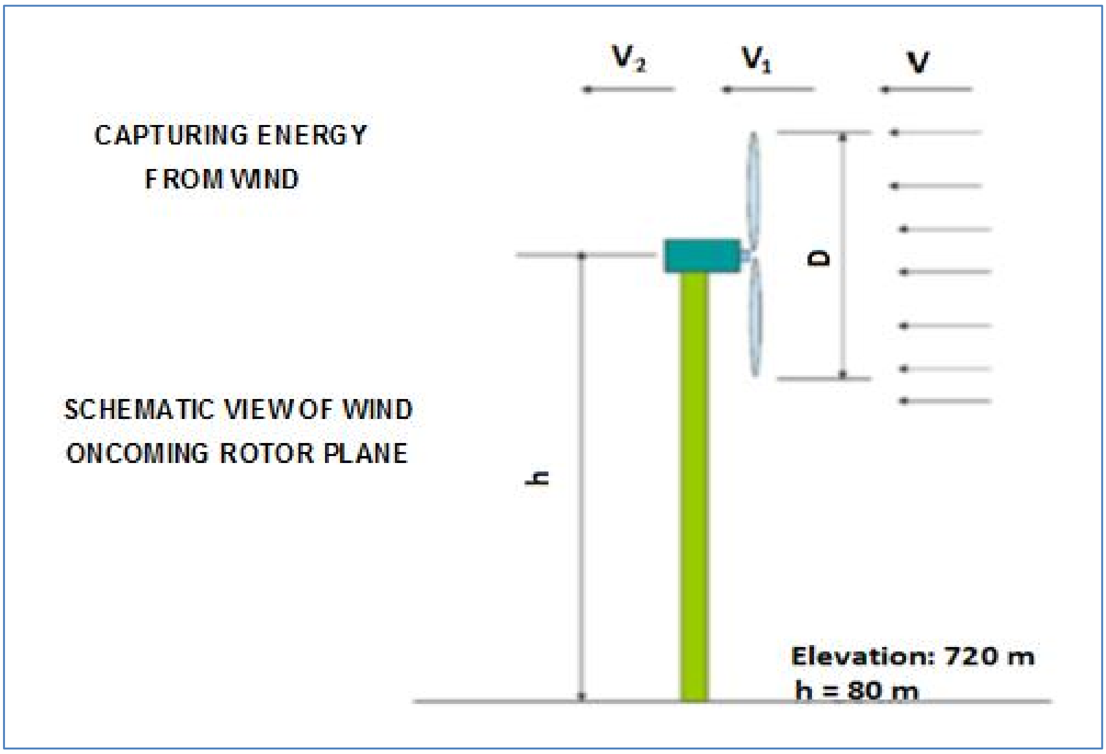

Figure 3.1. Elevation used in computations (800 m above sea level)

Density of air can be estimated as a function of air temperature, altitude (or pressure) and molecular mass by following equations:

$$P = P_o . e^{-1.18575*10^{-4} H} = 1(atm). e^{-1.18575*10^{-4} H} \tag{3.1}$$

Here, P_o → Reference Pressure (1 atm),
H → Meter (Height of Altitude)
P → Pressure at the considered height
(Tanrıöven, 2011)

Air density can be calculated by the following equation ,

$$\rho = \frac{P \, x \, MM \, x 10^{-3}}{R \, x \, T} \quad (3.2)$$

Where, “MM” is molecular mass which can be given with following equations (Tanrıöven, 2011).

Combination of Air; (100 %) ≈ Nitrogen (78.08 %) + Oxygen (20.95 %) + Argon (0.93 %) + Carbon Dioxide (0.035 %) + Neon (0.0018 %) (3.3)

Molecular mass of air mixture is given as;

MM (of air) = 0.7808x28.02 + 0.2095x32 + 0.0093x39.95 + 0.00035x44.01 + 0.000018x20.18 = 28.97 (g/mole) (Tanrıöven, 2011) (3.4)

R is the ideal gas constant equal to $8.2056 * 10^{-5} \left[\frac{m^3 . atm}{Kelvin.mol} \right]$ (3.5)

3.2. Calculation of Wind Power and Efficiency

Maximum wind power that can be obtained from wind turbine is expressed with equation 3.6 shown below where P_R designates the maximum wind power obtained from rotor (Burton et al, 2011).

$$P_R = \frac{1}{2} \rho A V_i^3 \quad (3.6)$$

Theoretical power considering some of wind energy losses is combination of maximum wind power and Betz-limit which is given as $16/27 = 0.592593$ (Burton et al, 2011). Finally, theoretical power is presented with following equation,

$$P_{TH} = \frac{1}{2} \rho A V_i^3 \; x \; 0.59 \tag{3.7}$$

By using the wind speed data in front of the rotor designated as, (U_∞), efficiency (C_p) (Also named as power coefficient) calculations are performed with following equation (Manwell et al, 2009).

$$c_p = \frac{P}{\frac{1}{2} \rho U_\infty{}^3 \pi R^2} \tag{3.8}$$

Where P designates real power obtained from wind turbine, ρ is the air density calculated by using equations (3.1) and (3.2).

The following equation is set up to calculate flow induction factor (a):

$$4a(1-a)^2 - C_P = 0 \tag{3.9}$$

At the state of wind speed on the rotor (U_D) to be given initially rather than wind speed in front of the rotor (U_∞), equation 3.10 and equation 3.11 are used to determine flow induction factor (a);

$$a = \frac{X}{X+4} \tag{3.10}$$

Where, X is determined by;

$$X = \frac{P_{real}}{0.98.0.97.\frac{1}{2}.\rho .AU_D^3} \tag{3.11}$$

Relation of thrust coefficient (C_T) with respect to the flow induction factor (a) is expressed as follows (Burton et al, 2011);

$$C_T = 4a(1 - a) \tag{3.12}$$

3.3. Computation of Wind Power Losses

Cut-in and cut-out power generations are computed by equations 3.13 and 3.14 (Yılmaz and Şahin, 2008);

$$E_{k_{lcut-in}} = \frac{1}{2}\rho A V^3{}_{lcut-in} \qquad (V_{lcut-in} < V_{cut-in}) \tag{3.13}$$

$$E_{k_{lcut-out}} = \frac{1}{2}\rho A V^3{}_{lcut-out} \qquad (V_{lcut-out} > V_{cut-out}) \tag{3.14}$$

In this formulation, $E_{k_{lcut-in}}$ *and* $E_{k_{lcut-out}}$ demonstrate kinetic energies of wind blowing at a speed lower than cut-in and higher than cut-out velocities respectively. Furthermore, A indicates the swept area by wind turbine rotor; $V_{lcut-in}$ shows wind blowing speed values lower than V_{cut-in} speed; and $V_{lcut-out}$ exhibits wind speed higher than $V_{cut-out}$ speed. When these explanations are considered, total kinetic energy loss $\left(E_{k_{losses}}\right)$ which is developed due to these boundary values can be written as follows (Yılmaz and Şahin, 2008);

$$E_{k_{losses}} = \frac{1}{2}\rho A\left[\sum_{i=1}^{n} V^3{}_{lcut-in} + \sum_{i=1}^{n} V^3{}_{lcut-out}\right] \tag{3.15}$$

Cut-in and cut-out speeds are given in table 3.1. Important specifications are demonstrated in the same table. Expression written in this table as “At enclosed table” refers the raw data that was received from the wind farm considered in present study.

Table 3.1. Specifications of wind turbines considered in the present study

1) Wind speed and direction (The height where measurements were taken should be stated.)	80 m, wind speeds are given at enclosed table
2) Atmospheric temperature	At enclosed table
3) Power obtained from turbine	At enclosed table
4) Turbine type	Vestas (V90-3.0 MW)
5) Rotor diameter or blade area	Rotor diameter:90 meter, blade area:6.362 m^2
6) Blade number	Sum of 3
7) Blade length	44 meters
8) Turbine starts to run (Cut-in velocity)	4 m/s
9) Turbine begins stopping (Cut-out velocity)	25 m/s
10) Rotational speed of rotor	16.1 rpm
11) Frequency	50 Hz
12) Voltage - current	Generator output voltage: 1000 Volt, current depends on power generated by turbine due to the variation in wind speed.
13) Turbine elevation	80 meter
14) Voltage at invertor exit, frequency, cos	Cos(Φ):1
15) Mechanical and generator efficiency of the system	
16) Generated energy	Alternating current
17) Humidity	Unsteady
18) Pressure	Unsteady
19) Running hours of turbine	At enclosed table
20) And other important technical informations	At enclosed table

Furthermore, if “$E_{k_{e-ratio}}$” is defined as the kinetic energy loss percentage due to these boundary values; this ratio can be defined as given below:

$$E_{k_{e-ratio}} = \frac{\frac{1}{2}\rho A\left[\sum_{i=1}^{n} V^{3}{}_{lcut-in} + \sum_{i=1}^{n} V^{3}{}_{lcut-out}\right]}{\frac{1}{2}\rho A\sum_{i=1}^{n} V^{3}{}_{i}} \tag{3.16}$$

In this formulation; $\sum V_i$ are the wind speeds that involve whole speeds that are taken in computations (Below cut-in speed and over cut-in speed) (Yılmaz and Şahin, 2008).

3.4. Wind Exergy

Exergy of wind turbine is given by equation (3.17).

$$W_{tr-ex} = \frac{\frac{1}{2}\rho AV^{3} - \frac{1}{2}\rho A\left[\sum_{i=1}^{n} V^{3}{}_{lcut-in} + \sum_{i=1}^{n} V^{3}{}_{lcut-out}\right] + \frac{1}{2}\rho A\left|\left[V^{3}{}_{z,comp\_top} - V^{3}{}_{z,sea\_level}\right]\right|}{\frac{1}{2}\rho AtV_{r}^{3}} \tag{3.17}$$

In this equality, while "V_r" indicates nominal wind intensity values, "t" shows time interval of measurements. This formula can be used for variety of turbines and for variety of terrain conditions. It also brings a new exergetic aspect. Besides, since it involves kinetic energy losses and gains, it can be used for appraising electric generation of turbines (Yılmaz and Şahin).

$$V_2 = V_1 \frac{\ln(Z_2 / z_0)}{\ln(Z_1 / z_0)} \tag{3.18}$$

Where, Z_2 indicates elevation of wind turbine hubs in the wind farm, and Z_1 indicates elevation of wind turbine hubs at a sea level. V_1 designates wind speed at a sea level, and V_2 designates wind speed in the territory of wind farm. Table 3.2 shows roughness lengths (z_0) for different categories (Tanrıöven, 2011).

Table 3.2. Roughness lengths

Roughness Class	Description				Roughness Length (m)
1	Plain wide terrains (Less amount of obstacles)				0.03
4	Dense enclaves or forests				1.6

Wind interpolated temperatures at a sea level for the calculations of air density can be determined considering lapse rate (Kıncay, 2008);

$$Lapse\ Rate = -\ 6.5\ ^{\circ}C / km \tag{3.19}$$

According to equation (3.19), for 800 m of elevation above sea level, around +5.2 ^{0}C temperature rise will be formed.

3.5. Estimation of Wind Directions

Wind direction estimations can be performed by completely identification of cardinal and intercardinal directions. Related directions are given in table 3.3.

Table 3.3. Wind direction values

Direction	Degree	Direction	Degree	Direction	Degree	Direction	Degree
N	0,360	E	90	S	180	W	270
NNE	22.5	ESE	112.5	SSW	202.5	WNW	292.5
NE	45	SE	135	SW	225	NW	315
ENE	67.5	SSE	157.5	WSW	247.5	NNW	337.5

3.6. Relations for Wind Aerodynamics

Relation of wind speed before rotor (U_{∞}), on the rotor (U_D) and on the wake (U_W) rotor are given by following equations (Burton et al, 2011).

$$U_D = U_{\infty}(1 - a) \tag{3.20}$$

$$U_W = U_\infty (1 - 2a) \tag{3.21}$$

Wind speed before rotor (U_∞), and on the wake (U_W) rotor are related with equation (3.22) which is defined as wind speed ratio (Ministry of Education - Turkey, 2012).

$$\lambda = \frac{U_W}{U_\infty} \tag{3.22}$$

Wind speed ratio, (λ) and flow induction factor (a) are related with equation (3.23).

$$a = 0.5 - 0.5\lambda \tag{3.23}$$

Thrust of wind is given by equation (3.24) (Manwell et al, 2009).

$$T = 2\rho A_D U_\infty^2 a(1 - a)^2 \tag{3.24}$$

Mass flow rate on the rotor, $\dot{m}$ is determined by following equation (Manwell et al, 2009).

$$\dot{m} = \rho . U_D . A \tag{3.25}$$

Rotor rotation given for a unit time is determined by equation 3.26 (Onder, 2006).

$$\Omega = 60 * \frac{\sqrt{\frac{(1-a)(4a-1)^2}{(1-3a)}} \ x \ \frac{U_D}{1-a}}{r} [rpm] \tag{3.26}$$

Tangential flow induction factor (a') can be estimated as (Burton et al, 2011);

$$a' = \frac{a.(1-a).U_{\infty}^{2}}{r^{2}.\Omega^{2}} \qquad (3.27)$$

Total circulation (Γ) which is related to the induced velocity factors (a) is given by the following equation and results of (Γ) is presented in figure 3.2 (Burton et al, 2011);

$$\Gamma = \frac{4\pi U_{\infty}^{2} a(1-a)}{\Omega} \qquad (3.28)$$

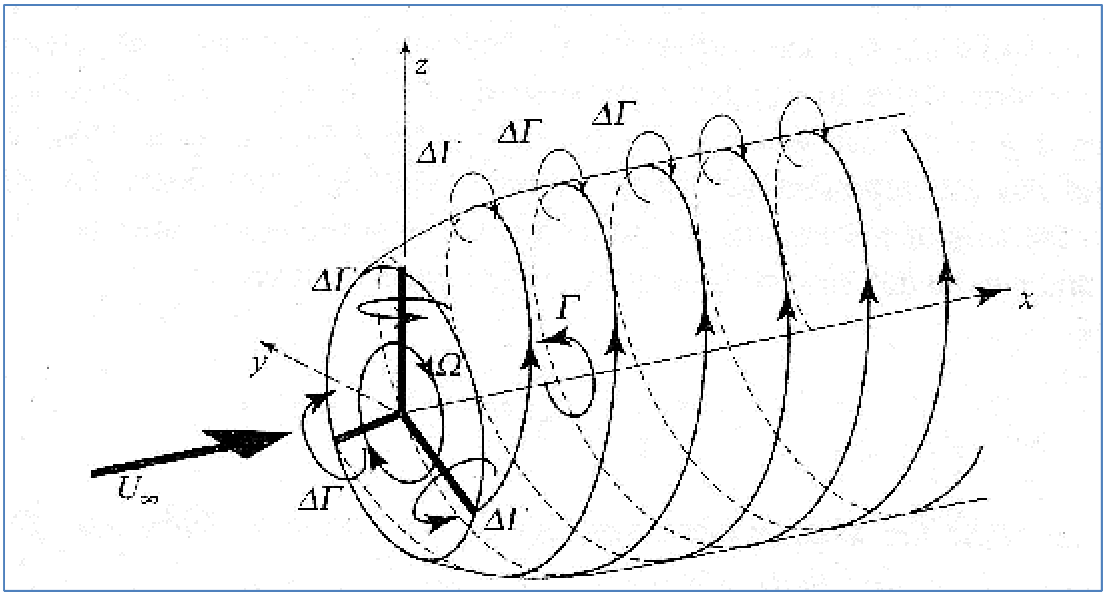

Figure 3.2. Helical vortex wake shed by rotor with three blades each with uniform circulation $\Delta\Gamma$ (Burton et al, 2011)

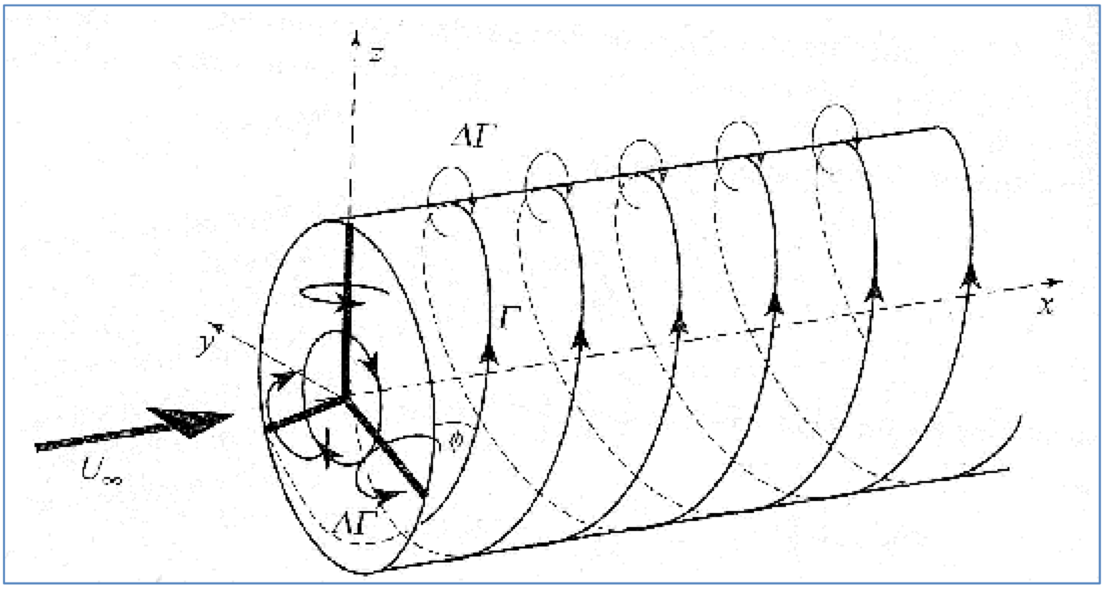

Figure 3.3. Simplified helical vortex wake ignoring wake expansion (Burton et al, 2011)

Bound circulation angle (ϕ) as shown in figure 3.3 is given by the equation below (Burton et al, 2011);

$$\sin\phi = \frac{U_\infty (1-a)}{W} \qquad and \qquad \cos\phi = \frac{r\Omega(1+a')}{W} \tag{3.29}$$

Where, W is the resultant relative velocity at the blade and defined by equation 3.30 which acts at an angle ϕ to the plane of rotation (Burton et al, 2011).

$$W = \sqrt{U_\infty^2 (1-a)^2 + r^2\Omega^2 (1+a')^2} \tag{3.30}$$

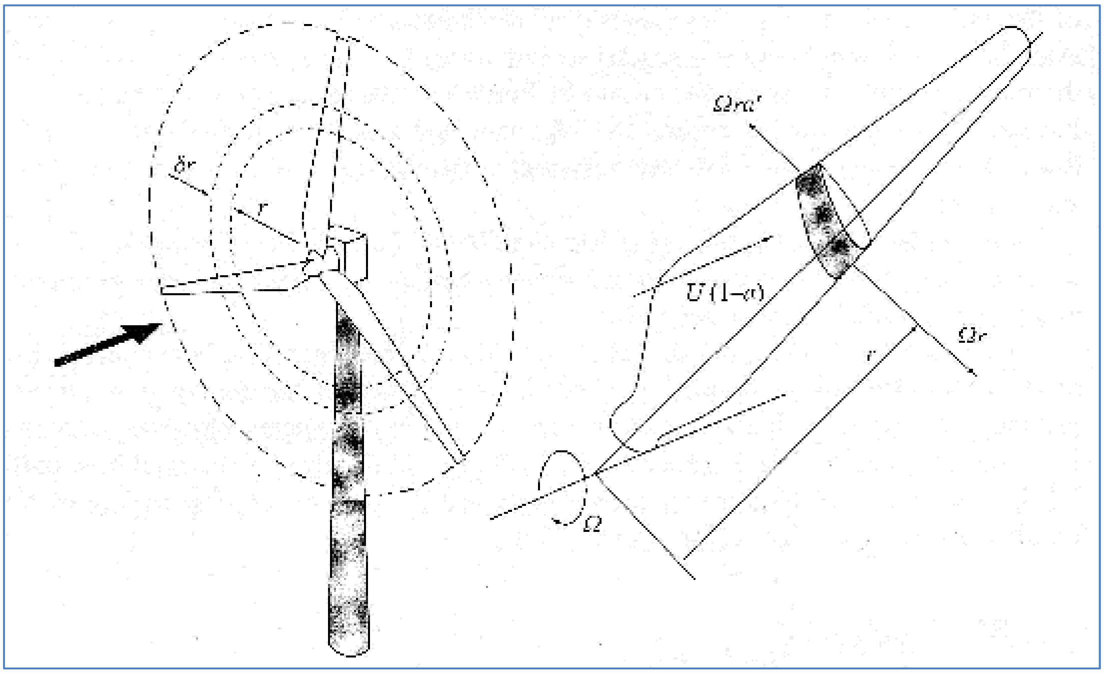

Figure 3.4. A blade element sweeps out an annular ring (Burton et al, 2011)

The angle of attack is given as follows (Manwell et al, 2009);

$$a = f - b \tag{3.31}$$

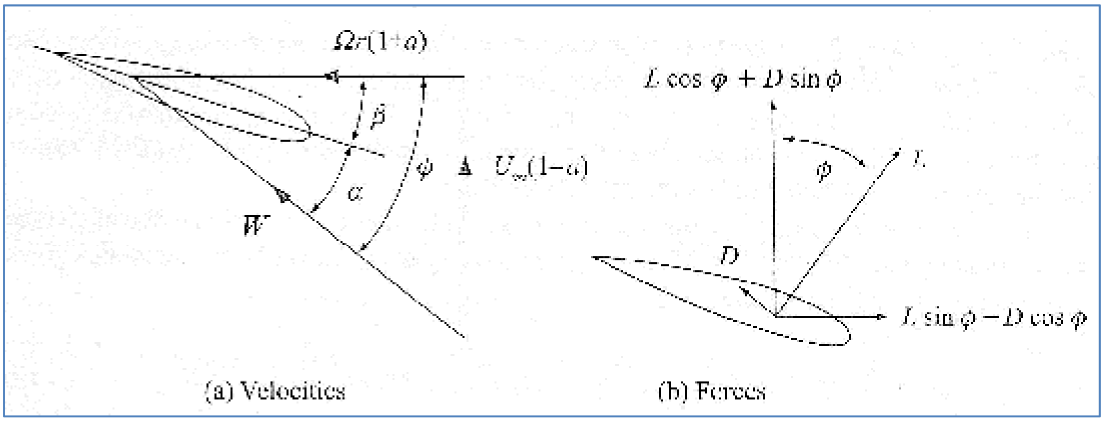

Figure 3.5. Blade Element Velocities and Forces (Burton et al, 2011)

According to the blade element theory (BEM), lift (C_l) and drag coefficients (C_d) are defined to satisfy following equations (Burton et al, 2011).

$$C_l \cos\phi + C_d \sin\phi = C_x$$
$$C_l \sin\phi - C_d \cos\phi = C_y \qquad (3.32)$$

Where $C_l = 0.1(\alpha + 4)$ and $\alpha = 0.1$ giving C_l = 0.41 (Burton et al, 2011)

And,

$$\frac{a}{1-a} = \frac{\sigma_r}{4\sin^2\phi} C_x$$
$$\frac{a'}{1+a'} = \frac{\sigma_r C_y}{4\sin\phi\cos\phi} \qquad (3.33)$$

Blade solidity, σ is defined as total blade area divided by the rotor disc area and is a primary parameter in determining rotor performance. Chord solidity, σ_r is defined as the total blade chord length at a given radius divided by the circumferential length at that radius (Burton et al, 2011);

$$\sigma_r = \frac{B}{2\pi} . \frac{c}{R} \qquad (3.34)$$

Lift force (L) on a span-wise length r of each blade, normal to the direction of W, is given by equation 3.35 (David, 2009);

$$L = \frac{1}{2} . \rho . W^2 . c . C_l . r \qquad (3.35)$$

Drag force (D) parallel to W is determined by following (David, 2009);

$$D = \frac{1}{2} . \rho . W^2 . c . C_d . r \qquad (3.36)$$

The axial thrust of an annular ring of the actuator disc is as follows (Burton et al, 2009);

$$T = \frac{1}{2}.\rho.W^2.B.c.(C_l \cos\phi + C_d \sin\phi)r \tag{3.37}$$

The torque (Q) on an annular ring is stated as (Burton et al, 2009);

$$Q = \frac{1}{2}.\rho.W^2.B.c.r.(C_l \sin\phi - C_d \cos\phi)r \tag{3.38}$$

Here, B defines the number of blades (Burton et al, 2009).

The power developed by the rotor according to the blade – element/momentum (BEM) theory, P^* is specified by equation 3.39 (Burton et al, 2009);

$$P^* = Q.\Omega \tag{3.39}$$

And, power coefficient (C_p*) for BEM theory is given by equation 3.40 (Burton et al, 2009);

$$C_P* = \frac{P^*}{\frac{1}{2}.\rho.U_\infty^3.\pi.R^2} \tag{3.40}$$

Tip speed ratio (λ^*) is defined by the equation 3.41 (Manwell, 2009).

$$\lambda^* = \frac{R.\Omega}{U_\infty} \tag{3.41}$$

Where, R is the radius of the rotor.

4. RESULTS AND DISCUSSION

4.1. Power and Efficiency Computations by Monthly Average Data

Power efficiency (C_p) was calculated using monthly average raw data given in Appendix 1.

Firstly, average air densities were determined using average air temperatures provided in Appendix 1 by equations 3.1 - 3.5. Maximum powers were obtained according to the wind speeds given in Appendix 1 using equation 3.6. Theoretical powers were also calculated according to wind speeds using equation 3.7. Finally, power efficiency (C_p) calculations were performed by equation 3.8.Values of real powers which were directly taken from the company is given in Appendix 1.

Estimations and calculations stated above were given for each discrete turbines for each months of 2010 year. Related computed data are stated in table 4.1 for turbines T01 and T02. Table 4.2 contains computed results of turbines T03, T04, T05 and according to the average data of wind speeds, power generations, wind directions, and air temperatures for all turbines are also given.

Table 4.1 Power efficiencies of T01 and T02

Date	Temperature	Density	Maximum Power	Theoretical Power	Real Power	Efficiency
	$^{\circ}C$	kg/m^3	(kW)	(kW)	(kW)	
Jan	7.6801	1.1434	1375.9169	815.3582	752.4377	0.5469
Feb	8.1528	1.1415	1645.1029	974.8758	809.8635	0.4923
May	17.3763	1.1052	1592.1378	943.4891	823.1929	0.5170
June	20.3681	1.0940	2033.9799	1205.3214	991.1619	0.4873
July	21.9068	1.0883	4239.2302	2512.1364	1605.4834	0.3787
Aug	26.3618	1.0721	2128.7950	1261.5081	747.7441	0.3513
Sep	25.6601	1.0746	1402.1259	830.8894	780.0917	0.5564
Nov	19.6671	1.0966	479.6046	284.2101	268.8630	0.5606
Dec	12.0522	1.1259	1110.7012	658.1933	628.0291	0.5654

Date	Temperature	Density	Maximum Power	Theoretical Power	Real Power	Efficiency
	$^{\circ}C$	kg/m^3	(kW)	(kW)	(kW)	
Jan	7.6631	1.1435	1966.8055	1165.5144	955.7716	0.4860
Feb	8.1877	1.1413	2219.8124	1315.4444	1115.5078	0.5025
Apr	14.5088	1.1163	1014.9111	601.4288	586.3709	0.5778
May	17.4630	1.1049	2142.0883	1269.3856	1084.7041	0.5064
June	20.4521	1.0937	3045.6743	1804.8440	1303.6618	0.4280
July	21.9243	1.0882	6782.6398	4019.3421	2068.5622	0.3050
Aug	25.3094	1.0759	3434.6791	2035.3654	1347.9105	0.3924
Sep	22.5336	1.0860	2227.6871	1320.1109	1085.3351	0.4872
Nov	17.0093	1.1066	676.9517	401.1566	376.9640	0.5569
Dec	10.2139	1.1332	1544.2887	915.1340	806.0530	0.5220

Table 4.2 Power efficiencies of T03 (Top-left), T04 (Top-right), T05 (Bottom-left) and power efficiency according to the average data of all turbines (Bottom-right)

Date	Temperature	Density	Maximum Power	Theoretical Power	Real Power	Efficiency
	$^{\circ}C$	kg/m^3	(kW)	(kW)	(kW)	
Jan	8.2245	1.1412	1905.1345	1128.9686	880.7713	0.4623
Feb	8.7931	1.1389	2219.9746	1315.5405	1024.3218	0.4614
Mar	12.5986	1.1237	1050.5815	622.5668	616.2340	0.5866
May	17.8934	1.1033	1600.0567	948.1818	905.8800	0.5662
June	20.9611	1.0918	2256.3642	1337.1047	1167.2695	0.5173
July	22.5768	1.0858	4936.6549	2925.4251	1922.5752	0.3894
Aug	25.6059	1.0748	2254.7696	1336.1598	1131.3608	0.5018
Sep	22.8647	1.0847	1625.4419	963.2249	958.3751	0.5896
Oct	18.7597	1.1000	633.0456	375.1381	320.4060	0.5061
Nov	17.3894	1.1052	534.0245	316.4590	299.1114	0.5601
Dec	10.6750	1.1313	1214.5137	719.7118	698.3232	0.5750

Date	Temperature	Density	Maximum Power	Theoretical Power	Real Power	Efficiency
	$^{\circ}C$	kg/m^3	(kW)	(kW)	(kW)	
Jan	8.2390	1.1411	2763.0143	1637.3418	1155.6235	0.4182
Feb	8.6262	1.1396	3184.7779	1887.2758	1322.8021	0.4154
Mar	12.1100	1.1256	1252.1584	742.0198	692.4607	0.5530
Apr	14.2602	1.1172	1153.0146	683.2679	629.3132	0.5458
May	16.9599	1.1068	2320.7079	1375.2343	1073.0657	0.4624
June	19.8262	1.0960	3141.5311	1861.6480	1346.7091	0.4287
July	21.1285	1.0911	7398.0647	4384.0384	2127.4713	0.2876
Aug	24.5649	1.0786	3094.8274	1833.9718	1287.2327	0.4159
Sep	21.8915	1.0883	2325.7310	1378.2109	1167.8482	0.5021
Nov	17.0431	1.1065	867.3583	513.9901	512.5969	0.5910
Dec	10.7825	1.1309	1991.4992	1180.1477	995.3280	0.4998

Date	Temperature	Density	Maximum Power	Theoretical Power	Real Power	Efficiency
	$^{\circ}C$	kg/m^3	(kW)	(kW)	(kW)	
Jan	7.5450	1.1439	2045.3745	1212.0738	953.7995	0.4663
Feb	7.9355	1.1424	2407.0438	1426.3963	1095.4809	0.4551
Mar	11.8463	1.1267	1007.2812	596.9074	585.4890	0.5813
Apr	14.0992	1.1178	875.8786	519.0392	503.8520	0.5753
May	16.7090	1.1078	1869.8518	1108.0603	902.8120	0.4828
June	19.7299	1.0964	2604.6962	1543.5237	1153.0893	0.4427
July	21.0298	1.0915	6080.6600	3603.3541	1934.5037	0.3181
Aug	24.4392	1.0790	2629.8170	1558.4101	1111.2862	0.4226
Sep	21.9426	1.0881	1976.3747	1171.1850	1006.5631	0.5093
Nov	16.9857	1.1067	666.2998	394.8443	379.7291	0.5699
Dec	10.2339	1.1331	1449.0054	858.6699	789.9731	0.5452

Date	Temperature	Density	Maximum Power	Theoretical Power	Real Power	Efficiency
	$^{\circ}C$	kg/m^3	(kW)	(kW)	(kW)	
Jan	7.8703	1.1426	1979.0339	1172.7608	939.6807	0.4748
Feb	8.3391	1.1407	2301.0221	1363.5686	1073.5952	0.4666
Mar	12.0940	1.1257	1054.1154	624.6610	623.6246	0.5916
Apr	14.4449	1.1165	914.2596	541.7835	531.4753	0.5813
May	17.2803	1.1056	1890.2908	1120.1723	957.9309	0.5068
June	20.2675	1.0943	2592.2860	1536.1695	1192.3783	0.4600
July	21.7132	1.0890	5807.9310	3441.7369	1931.7192	0.3326
Aug	25.2562	1.0761	2678.5376	1587.2816	1125.1069	0.4200
Sep	22.9785	1.0843	1888.5801	1119.1586	999.6426	0.5293
Nov	17.6189	1.1043	635.5918	376.6470	367.4529	0.5781
Dec	10.7915	1.1309	1441.3540	854.1357	783.5413	0.5436

Table 4.3 provides monthly power efficiency (C_p) for five turbines.

Table 4.3. Monthly power efficiency (C_p) for all turbines

Months	T01	T02	T03	T04	T05
January	0.5469	0.4860	0.4623	0.4182	0.4663
February	0.4923	0.5025	0.4614	0.4154	0.4551
March	0.6313	0.6045	0.5866	0.5530	0.5813
April	0.6062	0.5778	0.5931	0.5458	0.5753
May	0.5170	0.5064	0.5662	0.4624	0.4828
June	0.4873	0.4280	0.5173	0.4287	0.4427
July	0.3787	0.3050	0.3894	0.2876	0.3181
August	0.3513	0.3924	0.5018	0.4159	0.4226
September	0.5564	0.4872	0.5896	0.5021	0.5093
October	0.6353	0.5929	0.5061	0.6171	0.5953
November	0.5606	0.5569	0.5601	0.5910	0.5699
December	0.5654	0.5220	0.5750	0.4998	0.5452

4.2. Power and Turbine Efficiency for Unrecorded Wind Direction

Studies on wind data related with unrecorded wind direction eliminated from Appendix 1 are given in table 4.4. For each discrete turbines average air temperature, air density, wind speed, generated power and power efficiency data were studied.

Table 4.4. Yearly efficiency of turbines for unrecorded wind direction

Turbine no	Temperature	Density	Wind Speed	Maximum Power	Theoretical Power	Real Power	Efficiency
	$^{\circ}C$	kg/m^3	(m/s)	(kW)	(kW)	(kW)	
T01	17.1534	1.1061	8.9402	2514.0685	1489.8184	1103.2536	0.4388
T02	19.4735	1.0973	9.3914	2891.1095	1713.2501	1224.5721	0.4236
T03	17.6730	1.1041	7.9944	1794.3913	1063.3430	931.0519	0.5189
T04	16.3855	1.1090	9.9856	3512.4467	2081.4499	1386.9404	0.3949
T05	16.1699	1.1098	9.3163	2854.5230	1691.5692	1175.8678	0.4119

Variation of average wind speeds for each discrete turbines according to the unrecorded wind direction are given in figure 4.1.

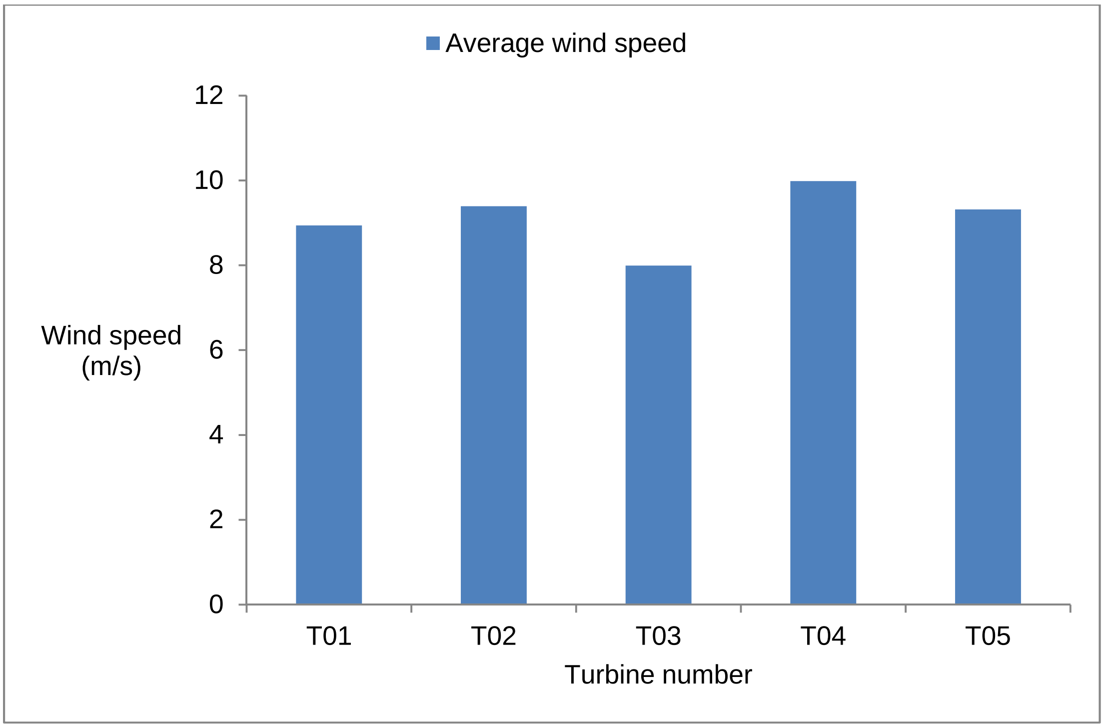

Figure 4.1. Average wind speed of turbines for unrecorded wind direction

Variation of average air temperatures and power generations for each discrete turbines according to the unrecorded wind direction are given in figures 4.2 and 4.3 respectively. Although all turbines considered in the present study is installed in same wind farm, air temperatures of turbines vary about 15%. This is due to the roughness of wind farm territory.

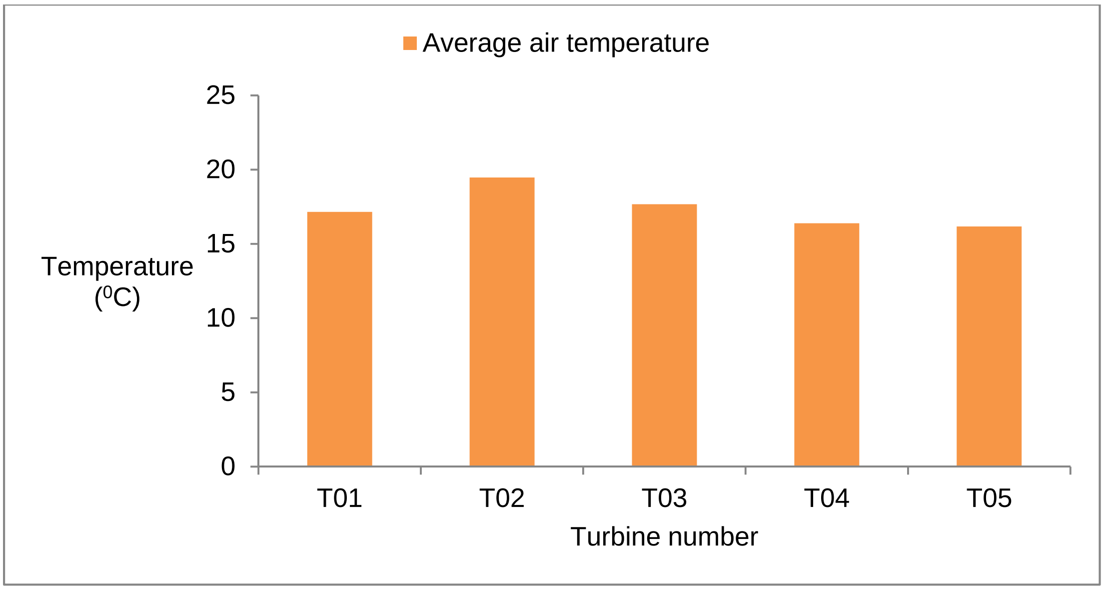

Figure 4.2. Average air temperatures for turbines according to the unrecorded wind direction

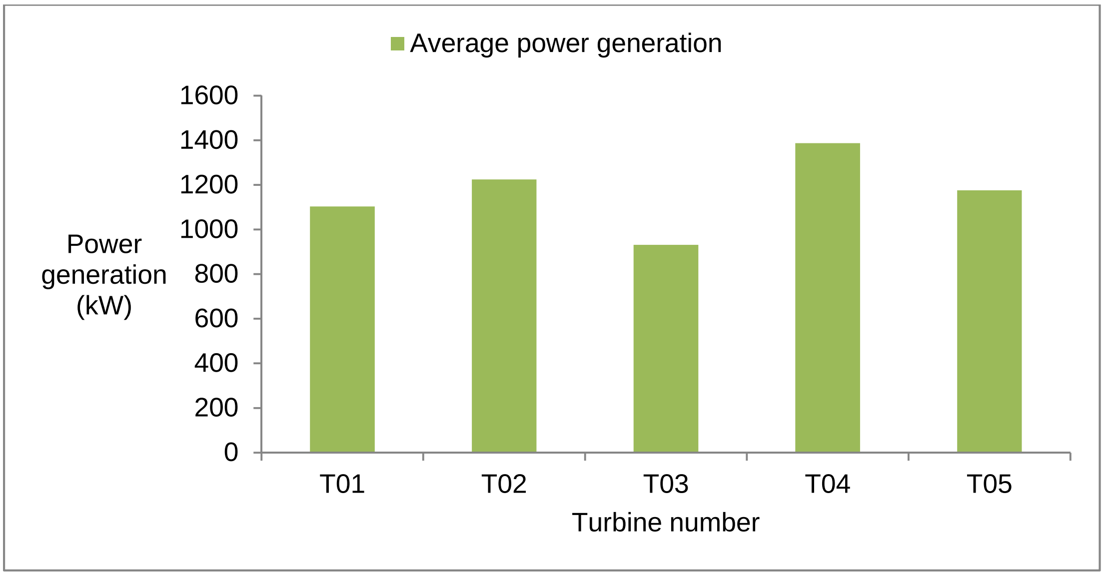

Figure 4.3. Average wind power generations of turbines for unrecorded wind direction

Variations of maximum power, theoretical power and measured power for each discrete turbines taking the unrecorded wind direction into account are presented in figure 4.4. Powers were computed using equations 3.6 and 3.7. Air densities used for the calculation of maximum power based on hourly average temperatures were performed using equations 3.1 – 3.5. The wind farm considered in this study is installed in a large valley combined with hills and crests. For this reason, topographical region of wind farm effects the wind direction as well as wind speed. That is why turbine T03 receives the lowest wind power but turbine T04 receives the highest wind power as seen in figure 4.4.

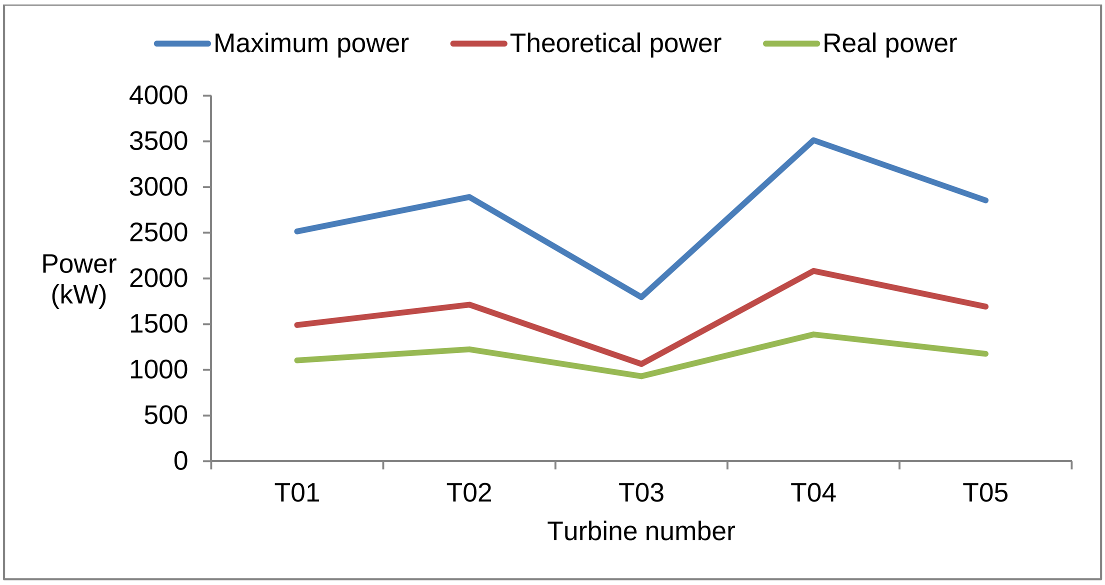

Figure 4.4. Power analysis of turbines for unrecorded wind direction

Variations of efficiencies for each discrete turbines obtained in unrecorded wind direction are given in figure 4.5. Average efficiencies were calculated using equation 3.8. Discrepancy of efficiencies of turbines is 6% as seen in figure 4.5. Turbine T03 has a maximum efficiency although it receives the lowest wind energy or wind speed. In this farm dominated wind speed throughout one year is in the range of $6m/s < U_\infty < 8m/s$. For this reason turbine blades are designed to convert maximum energy with this wind speed range.

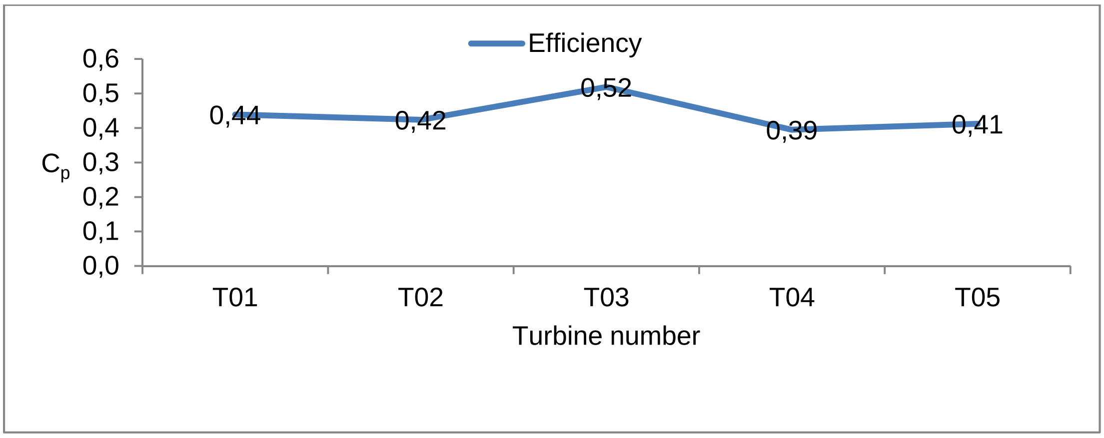

Figure 4.5. Monthly power efficiencies of turbines for unrecorded wind direction

4.3. Identification of Wind Directions for the Turbines

With the consideration of data stated in Appendix 2, figure 4.6 and figure 4.7 were formed and shown below. These figures demonstrate yearly wind blowing direction for turbines T01, T02, T03, T04 and T05. During the procurement of these figures, numbers of hourly wind direction data are stated on figures.

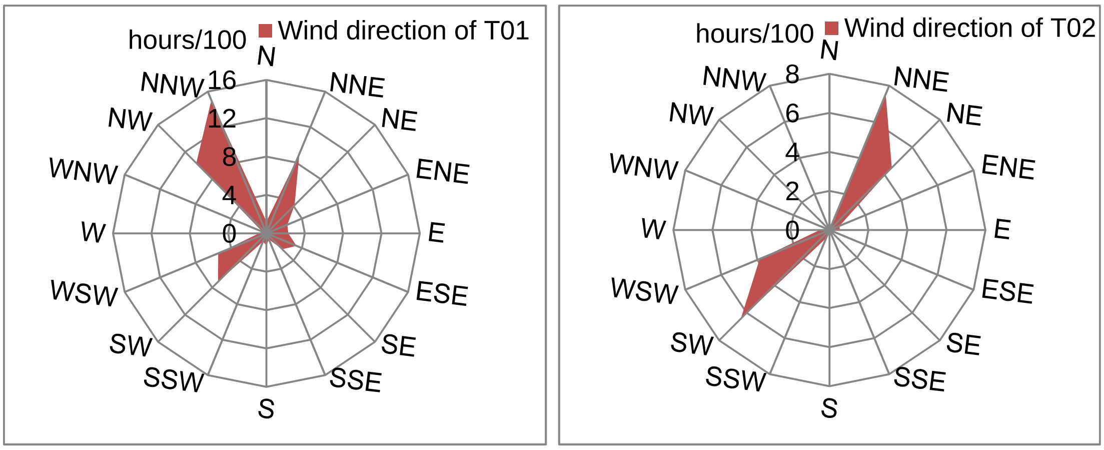

Figure 4.6. Distributions of wind direction for turbines T01 and T02

Finally, yearly wind blowing direction for T03, T04 and T05 turbines are given in figure 4.7.

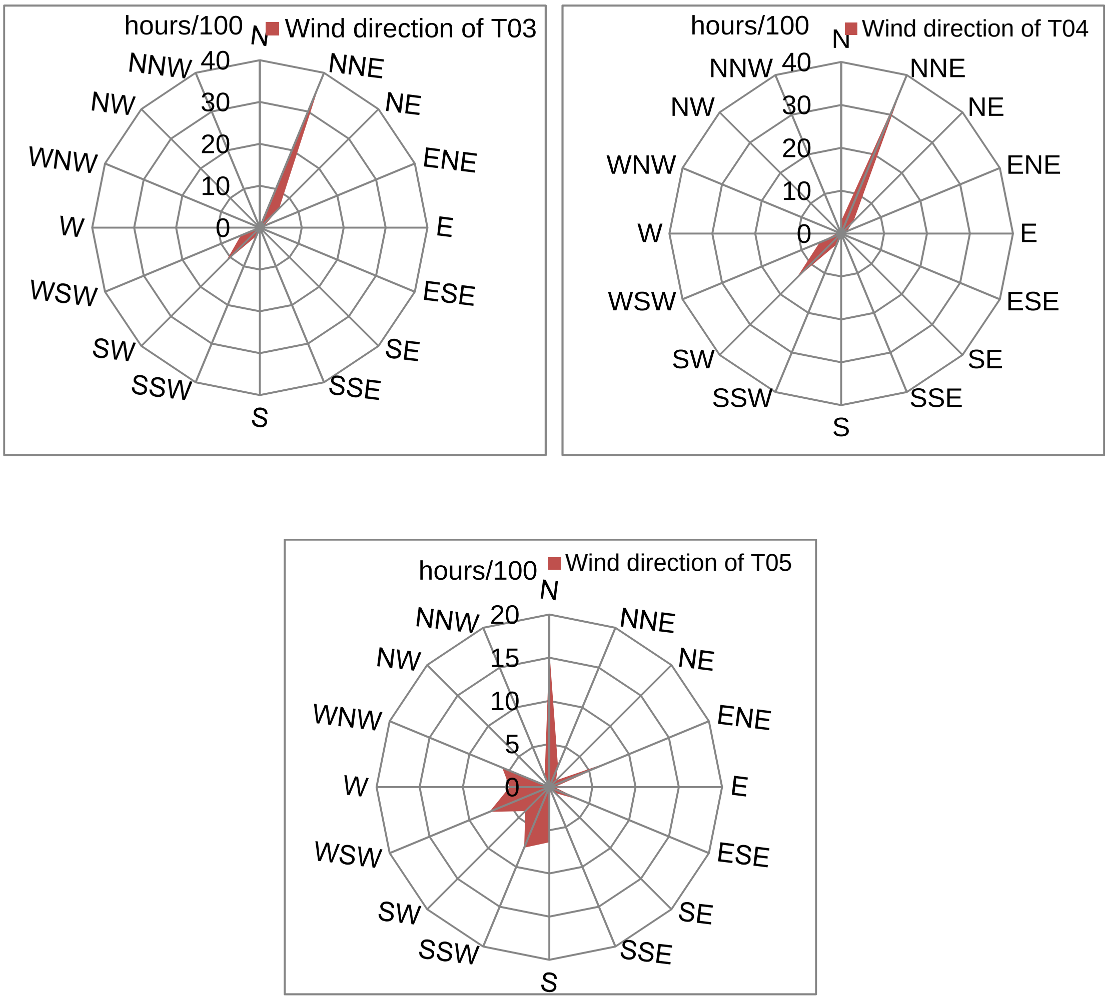

Figure 4.7. Distributions of wind direction for turbines T03, T04 and T05

Figure 4.8 and figure 4.9 involve average wind directions of T01, T02, T03 T04 and T05 turbines for each month shown with blue numbers. Red numbers indicate how many hourly data were used for determination of monthly distributions of wind directions. In Figure 4.8 (on the top and right side), all hourly wind directions measured for months between June and December were unfortunately unrecorded. Similarly, these unrecorded wind directions were also designated with red color in Appendix 1 and Appendix 2.

Figure 4.8. Monthly distributions of wind direction for turbines T01, T02, T03 and T04

Average monthly wind direction of turbine T05 is shown in figure 4.9.

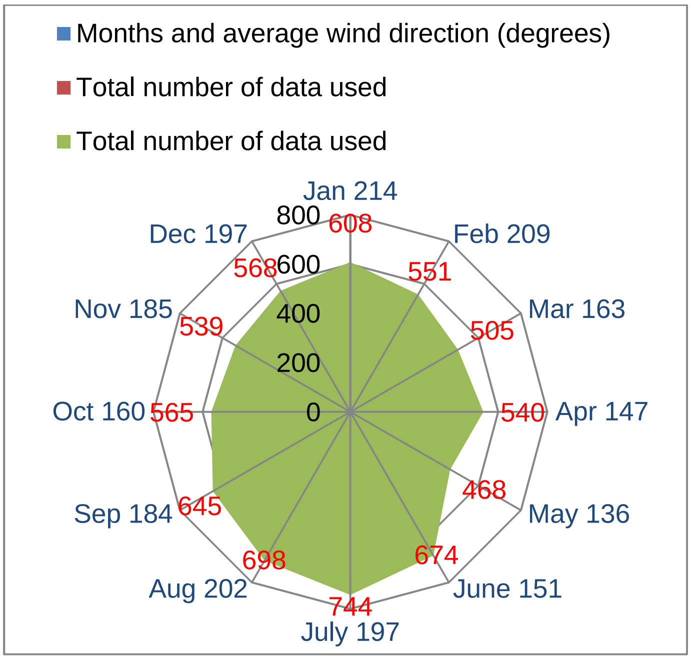

Figure 4.9. Monthly distributions of wind direction for turbine T05

Examining tables and figures about wind speed, wind direction and power generation, one can say that all turbines produce electricity every day of the year.

4.4. Introduction of Cut-In and Cut-Out Speeds

Average data in Appendix 2 are acquired with the consideration of cut-in and cut-out speeds, elimination of zero and negative values of power generation, and elimination of unrecorded wind directions (using boundary values). According to Appendix 2, average densities were formed according to the average air temperature using equations 3.1 - 3.5. Maximum wind powers were obtained using wind speeds presented in Appendix 2 and equation 3.6 was used for calculations. Theoretical wind powers were determined according to the wind speed data given in Appendix 2 with the utilization of equation 3.7. Efficiency calculations were performed by equation 3.8. Real powers were directly taken from Appendix 2 which were computed by taking average values of hourly data.

These estimations were given for each discrete turbines distributed for each months of 2010 year. Table 4.5 contains related computed data for turbines T01, T02, T03, T04, T05 and power efficiency according to the average data of all turbines.

Table 4.5. Power efficiencies of T01 (top-left), T02 (top-right), T03 (middle-left) T04 (middle-right), T05 (bottom-left) and power efficiency according to the average data of all turbines (bottom-right)

Date	Temperature	Density	Wind Speed	Maximum Power	Theoretical Power	Real Power	Efficiency
	$^\circ C$	kg/m^3	(m/s)	(kW)	(kW)	(kW)	
Jan	7.5056	1.1441	8.1478	1968.5241	1166.5328	934.9890	0.4750
Feb	7.8926	1.1425	9.1042	2742.4772	1625.1717	1130.3886	0.4122
Mar	12.0791	1.1258	7.7481	1665.6021	987.0235	787.0166	0.4725
Apr	14.1509	1.1176	6.9945	1216.5331	720.9085	604.9658	0.4973
May	17.3759	1.1052	7.7955	1665.4544	986.9359	813.0191	0.4882
June	20.0633	1.0951	8.8205	2390.4547	1416.5658	1083.5882	0.4533
July	21.9068	1.0883	10.6988	4239.2302	2512.1364	1605.4834	0.3787
Aug	27.0430	1.0696	8.6195	2178.8489	1291.1697	1019.4804	0.4679
Sep	25.6680	1.0746	7.9791	1736.3566	1028.9521	878.5708	0.5060
Oct	21.6640	1.0892	6.5388	968.5597	573.9613	513.0336	0.5297
Nov	20.2126	1.0946	6.1826	822.7963	487.5830	392.6736	0.4772
Dec	12.0818	1.1258	8.1179	1915.6358	1135.1916	881.4423	0.4601

Date	Temperature	Density	Wind Speed	Maximum Power	Theoretical Power	Real Power	Efficiency
	$^\circ C$	kg/m^3	(m/s)	(kW)	(kW)	(kW)	
Jan	7.5515	1.1439	8.9702	2626.3396	1556.3494	1129.0026	0.4299
Feb	7.9311	1.1424	9.9408	3569.5445	2115.2856	1407.0657	0.3942
Mar	12.0647	1.1258	8.2836	2035.4664	1206.2023	919.2235	0.4516
Apr	14.2137	1.1174	7.6366	1582.9072	938.0191	745.7420	0.4711
May	16.1736	1.1098	9.0517	2618.1289	1551.4838	1144.5567	0.4372
June	20.2345	1.0945	10.0211	3503.4151	2076.0978	1393.0981	0.3976
July	21.6701	1.0891	12.5965	6924.3480	4103.3174	2094.9774	0.3026
Aug	25.4159	1.0755	10.0169	3438.3358	2037.5323	1375.2438	0.4000
Sep	22.3909	1.0865	9.1485	2646.1809	1568.1072	1190.3027	0.4498
Oct	18.4181	1.1013	7.2470	1333.2673	790.0843	645.4409	0.4841
Nov	16.8024	1.1074	6.7912	1103.3348	653.8280	508.1528	0.4606
Dec	9.7383	1.1351	9.0495	2675.7459	1585.6272	1054.3497	0.3940

Date	Temperature	Density	Wind Speed	Maximum Power	Theoretical Power	Real Power	Efficiency
	$^\circ C$	kg/m^3	(m/s)	(kW)	(kW)	(kW)	
Jan	8.1438	1.1415	8.8207	2491.9362	1476.7029	1044.9531	0.4193
Feb	8.6981	1.1393	9.6454	3251.8405	1927.0166	1237.4326	0.3805
Mar	12.7037	1.1233	7.9719	1810.2018	1072.7122	838.4587	0.4632
Apr	14.6276	1.1158	6.9755	1204.6429	713.8624	615.4710	0.5109
May	17.8808	1.1033	7.8743	1713.4826	1015.3971	907.0408	0.5294
June	20.7507	1.0925	9.0317	2560.3430	1517.2403	1241.8548	0.4850
July	22.5768	1.0858	11.2645	4936.6549	2925.4251	1922.5752	0.3894
Aug	25.5241	1.0751	8.7504	2291.2106	1357.7544	1161.5017	0.5069
Sep	22.7339	1.0852	8.3018	1975.0719	1170.4130	1058.0654	0.5357
Oct	19.5235	1.0971	6.6648	1033.1433	612.2330	549.9163	0.5323
Nov	17.3718	1.1053	6.2151	844.0161	500.1577	412.7273	0.4890
Dec	10.2773	1.1329	8.3055	2064.6211	1223.4792	922.9882	0.4470

Date	Temperature	Density	Wind Speed	Maximum Power	Theoretical Power	Real Power	Efficiency
	$^\circ C$	kg/m^3	(m/s)	(kW)	(kW)	(kW)	
Jan	8.1534	1.1415	9.9955	3626.0097	2148.7465	1336.8282	0.3687
Feb	8.6141	1.1396	10.8503	4630.4274	2743.9570	1564.2445	0.3378
Mar	12.1488	1.1255	8.5720	2254.8959	1336.2346	966.2844	0.4285
Apr	13.9331	1.1185	8.0103	1828.6059	1083.6183	801.9783	0.4386
May	17.0237	1.1066	8.9069	2487.1703	1473.8787	1070.6649	0.4305
June	19.5839	1.0969	10.0863	3580.1962	2121.5977	1431.5881	0.3999
July	21.1266	1.0912	12.8792	7414.8231	4393.9692	2136.1161	0.2881
Aug	24.4869	1.0788	9.7320	3163.0096	1874.3761	1303.1872	0.4120
Sep	21.7016	1.0890	9.4050	2881.7829	1707.7232	1298.6210	0.4506
Oct	18.0375	1.1027	7.2641	1344.4770	796.7271	678.9558	0.5050
Nov	16.9637	1.1068	7.2607	1347.6001	798.5778	658.3294	0.4885
Dec	10.4133	1.1324	9.6456	3232.4255	1915.5114	1250.1878	0.3868

Date	Temperature	Density	Wind Speed	Maximum Power	Theoretical Power	Real Power	Efficiency
	$^\circ C$	kg/m^3	(m/s)	(kW)	(kW)	(kW)	
Jan	7.3802	1.1446	9.2463	2878.1279	1705.5573	1163.6981	0.4043
Feb	7.8654	1.1426	10.0255	3662.4343	2170.3314	1334.8462	0.3645
Mar	11.8182	1.1268	8.1755	1958.5249	1160.6074	860.7220	0.4395
Apr	13.6707	1.1195	7.4254	1457.8993	863.9403	668.2223	0.4583
May	16.7479	1.1076	8.3282	2035.1569	1206.0189	909.4927	0.4469
June	19.4815	1.0973	9.4910	2984.0593	1768.3314	1231.0747	0.4126
July	21.0298	1.0915	12.0539	6080.6600	3603.3541	1934.5037	0.3181
Aug	24.3409	1.0794	9.2327	2702.0582	1601.2197	1142.3703	0.4228
Sep	21.7668	1.0888	8.9074	2447.6064	1450.4334	1119.8523	0.4575
Oct	17.9968	1.1029	6.8003	1103.2245	653.7626	543.7763	0.4929
Nov	16.8605	1.1072	6.6900	1054.5006	624.8892	506.7433	0.4806
Dec	9.7438	1.1351	8.7643	2430.5950	1440.3526	1033.1305	0.4251

Date	Temperature	Density	Wind Speed	Maximum Power	Theoretical Power	Real Power	Efficiency
	$^\circ C$	kg/m^3	(m/s)	(kW)	(kW)	(kW)	
Jan	7.7469	1.1431	9.0361	2682.7822	1589.7968	1121.8942	0.4182
Feb	8.2003	1.1413	9.9132	3536.5747	2095.7480	1334.7955	0.3774
Mar	12.1629	1.1254	8.1502	1938.0622	1148.4813	874.3410	0.4511
Apr	14.1192	1.1178	7.4085	1445.7062	856.7148	687.2759	0.4754
May	17.0404	1.1065	8.3913	2079.6635	1232.3932	968.9548	0.4659
June	20.0228	1.0953	9.4901	2977.6814	1764.5519	1276.2408	0.4286
July	21.6620	1.0892	11.8986	5836.1527	3458.4608	1938.7311	0.3322
Aug	25.3622	1.0757	9.2703	2725.8495	1615.3182	1200.3567	0.4404
Sep	22.8522	1.0848	8.7484	2310.3198	1369.0784	1109.0824	0.4801
Oct	19.1280	1.0986	6.9030	1149.4790	681.1727	586.2246	0.5100
Nov	17.6422	1.1042	6.6279	1022.6737	606.0288	495.7253	0.4847
Dec	10.4509	1.1322	8.7766	2434.7295	1442.8027	1028.4197	0.4224

Variation of average wind speeds for T01, T02, T03 and T04 turbines for each month are given in figure 4.10 when boundary values were considered. The windiest month is July as seen in these figures.

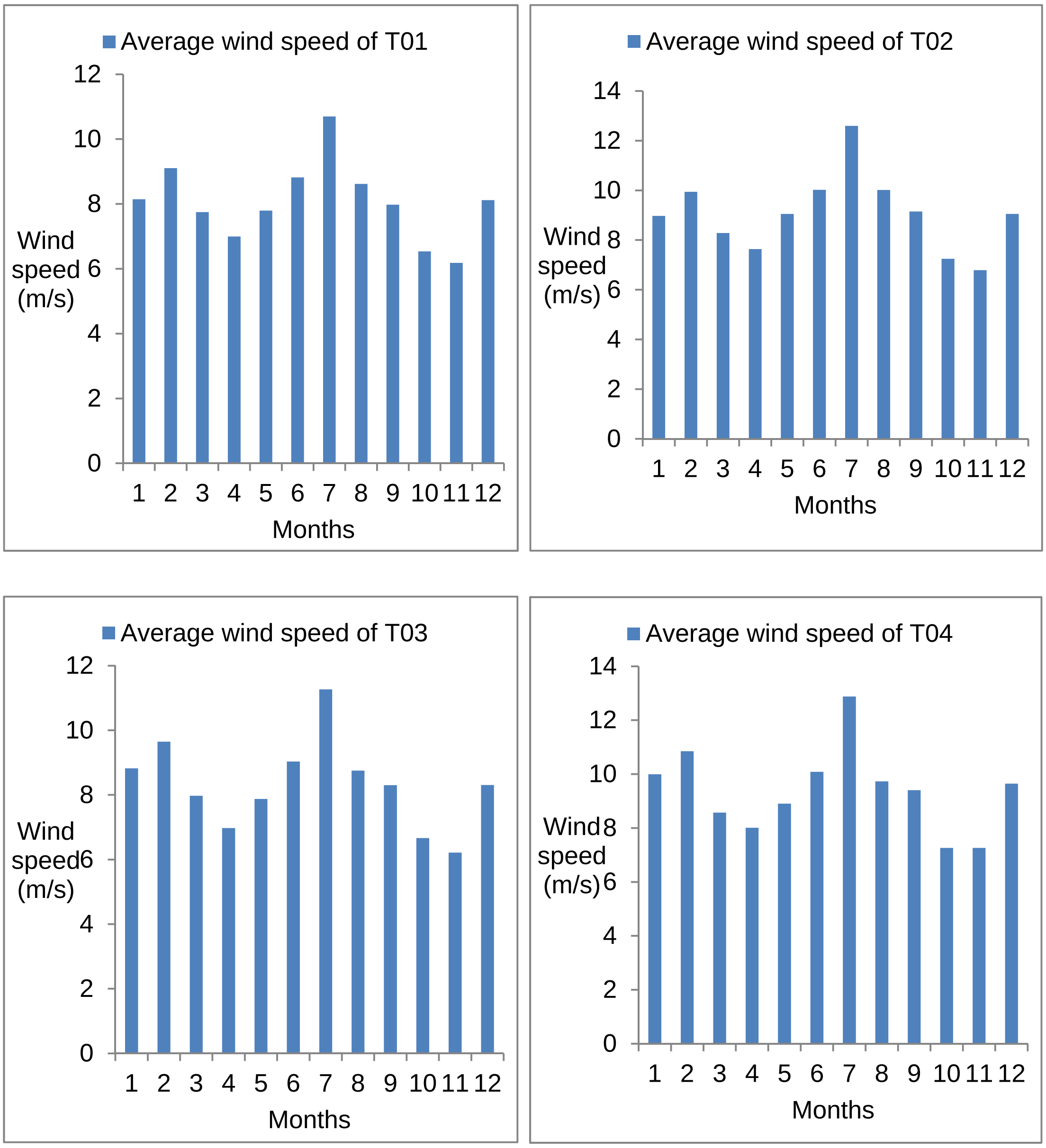

Figure 4.10. Monthly average wind speed for turbines T01, T02, T03 and T04

Figure 4.11 indicates average wind speeds of turbine T05 and monthly average wind speed according to the average wind speeds of all turbines.

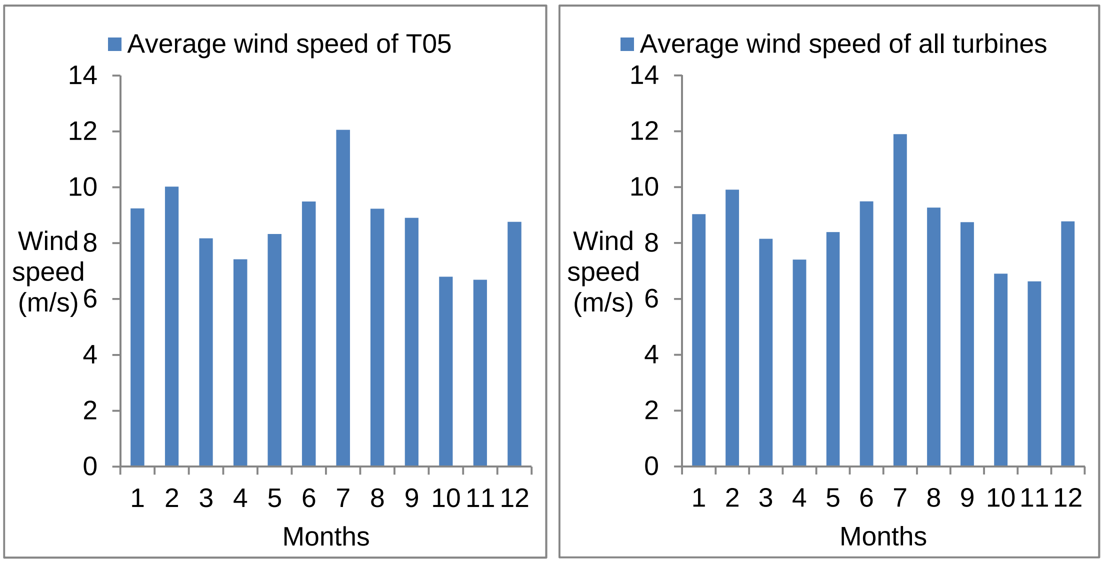

Figure 4.11. Monthly average wind speed for turbine T05 and monthly average wind speed according to the average wind speeds of all turbines

Average air temperatures of T01 and T02 turbines for each month are shown in figure 4.12 when boundary values were considered.

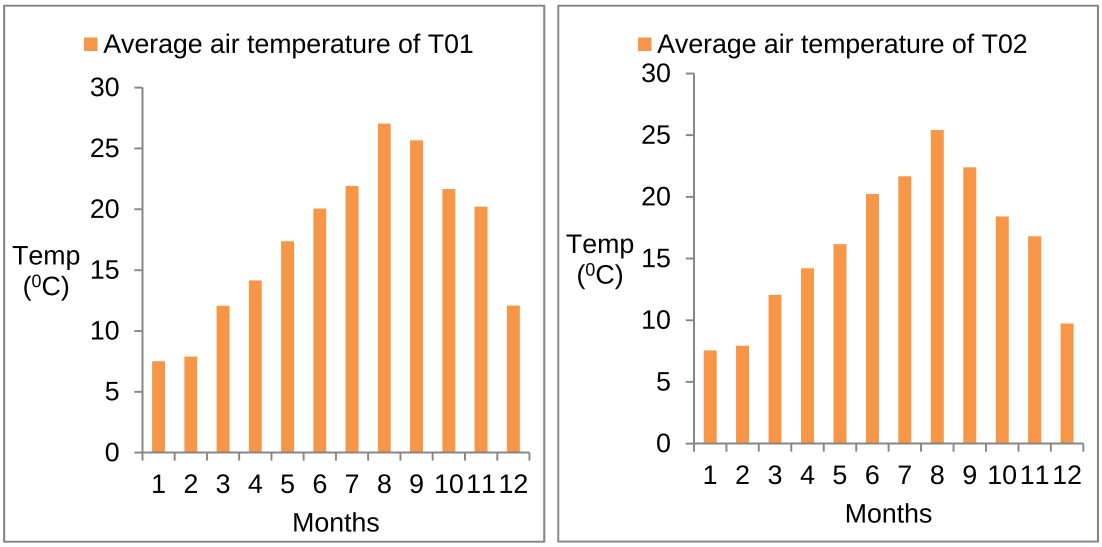

Figure 4.12. Monthly average air temperature for turbines T01 and T02

Monthly average air temperatures of T03, T04, T05 turbines and monthly average air temperatures of wind farm are presented in figure 4.13 with considering boundary values. These figures indicate that the highest temperature occurs in August.

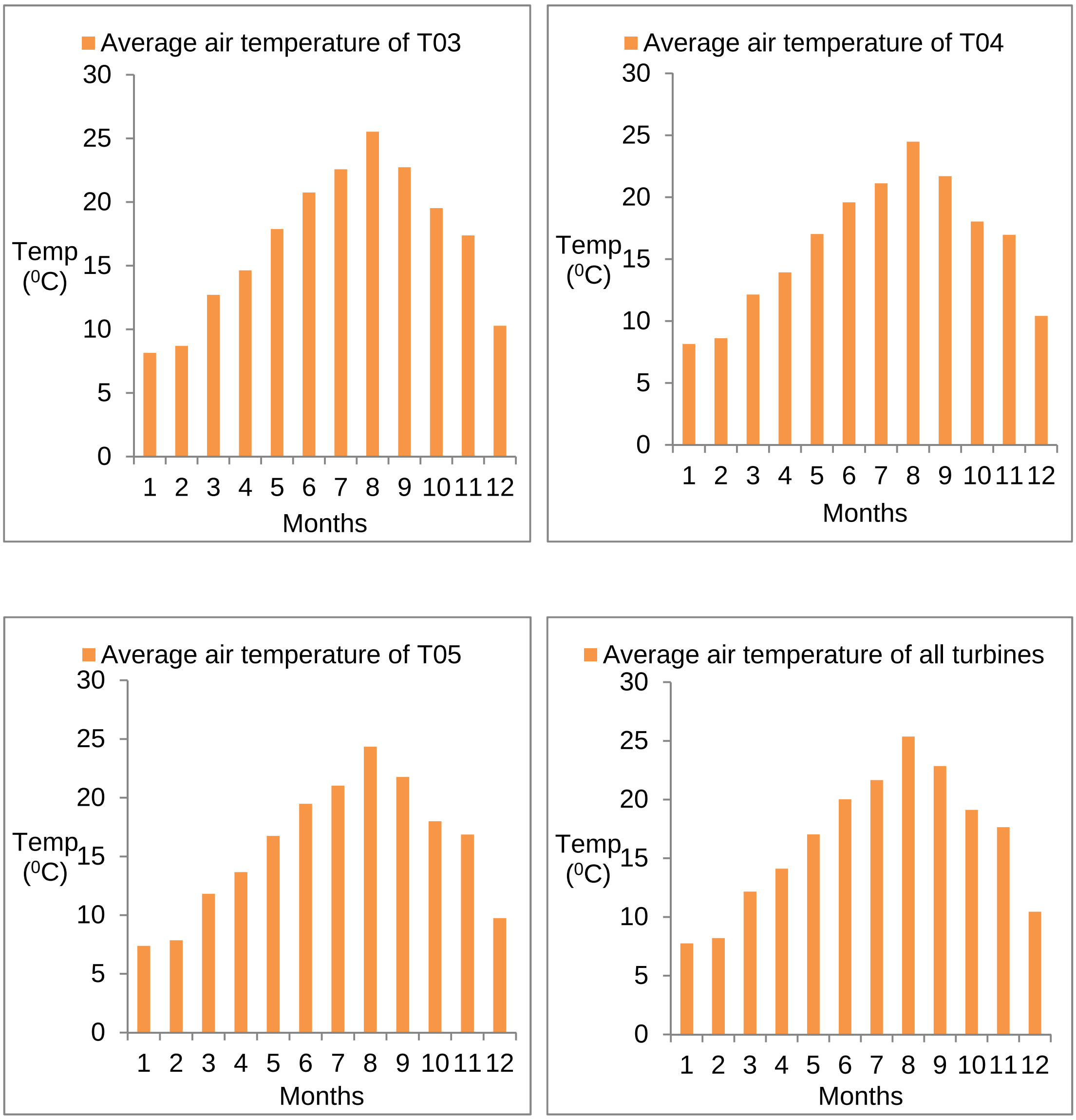

Figure 4.13. Monthly average air temperature for T03, T04, T05 turbines and monthly average air temperatures of wind farm

Variation of average measured wind power generations of T01, T02, T03 and T04 turbines for each month is indicated in figure 4.14 when boundary values were considered. Since most powerful wind occurs in July, the maximum power generation happens in this month.

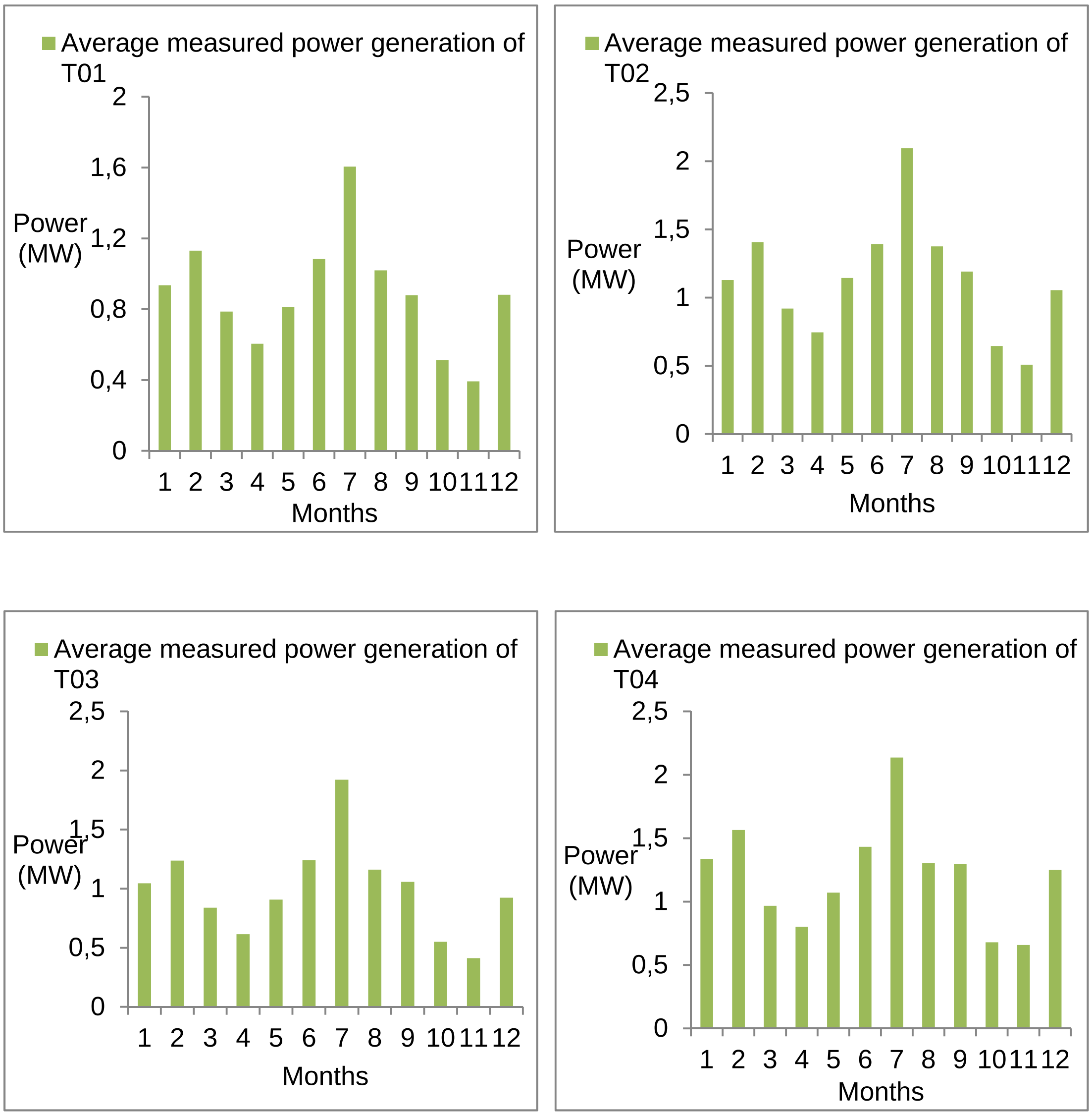

Figure 4.14. Monthly average measured wind power generations for T01, T02, T03 and T04 turbines

Variations of average power generations for T05 and average measured power generations of all turbines according to the average measured generation data of all are stated in figure 4.15 taking the boundary values into consideration. As seen in this figure the wind turbine named as T05 generated the highest electricity in July. This situation happens in all turbines since wind speed is highest in July.

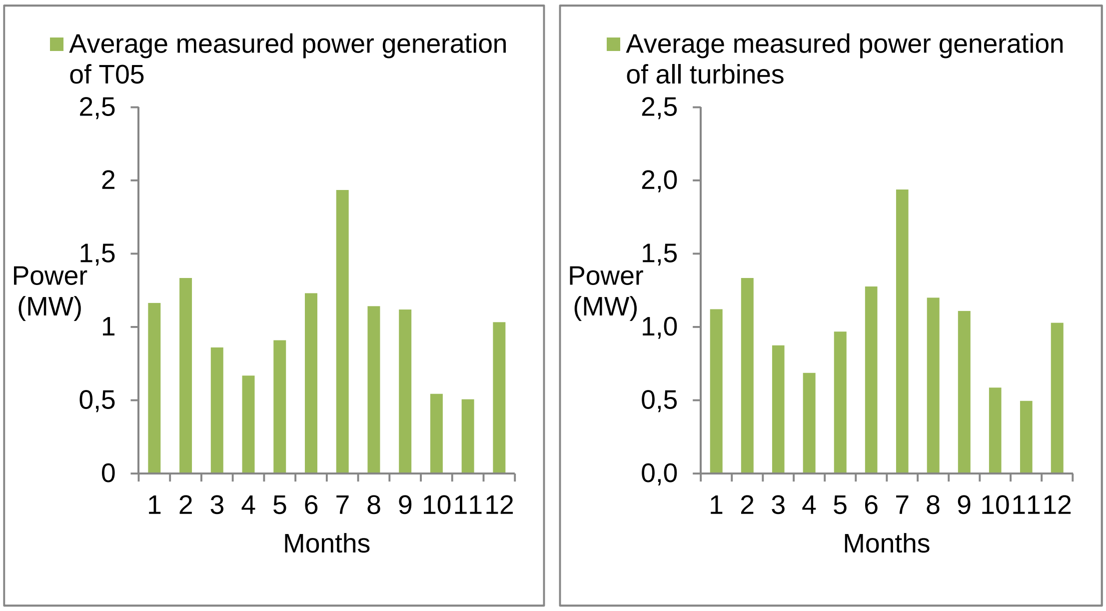

Figure 4.15. Monthly average power generation for turbine T05 and monthly average power generation of all turbines

Variation of monthly maximum wind power, theoretical power and real power generations by turbines T01, T02, T03 and T04 provided in figure 4.16 when boundary values were considered. Computations were performed according to the real generation values applying equations 3.6 and 3.7. In summary, maximum wind power generations take place in July.

Between June and December for turbine T02, since all data were given in unrecorded wind directions, computations were performed for these months without the elimination of unrecorded directions. Considerable amounts of generations occurred between these months with T02. But, wind directions for T02 in these months were unfortunately unrecorded.

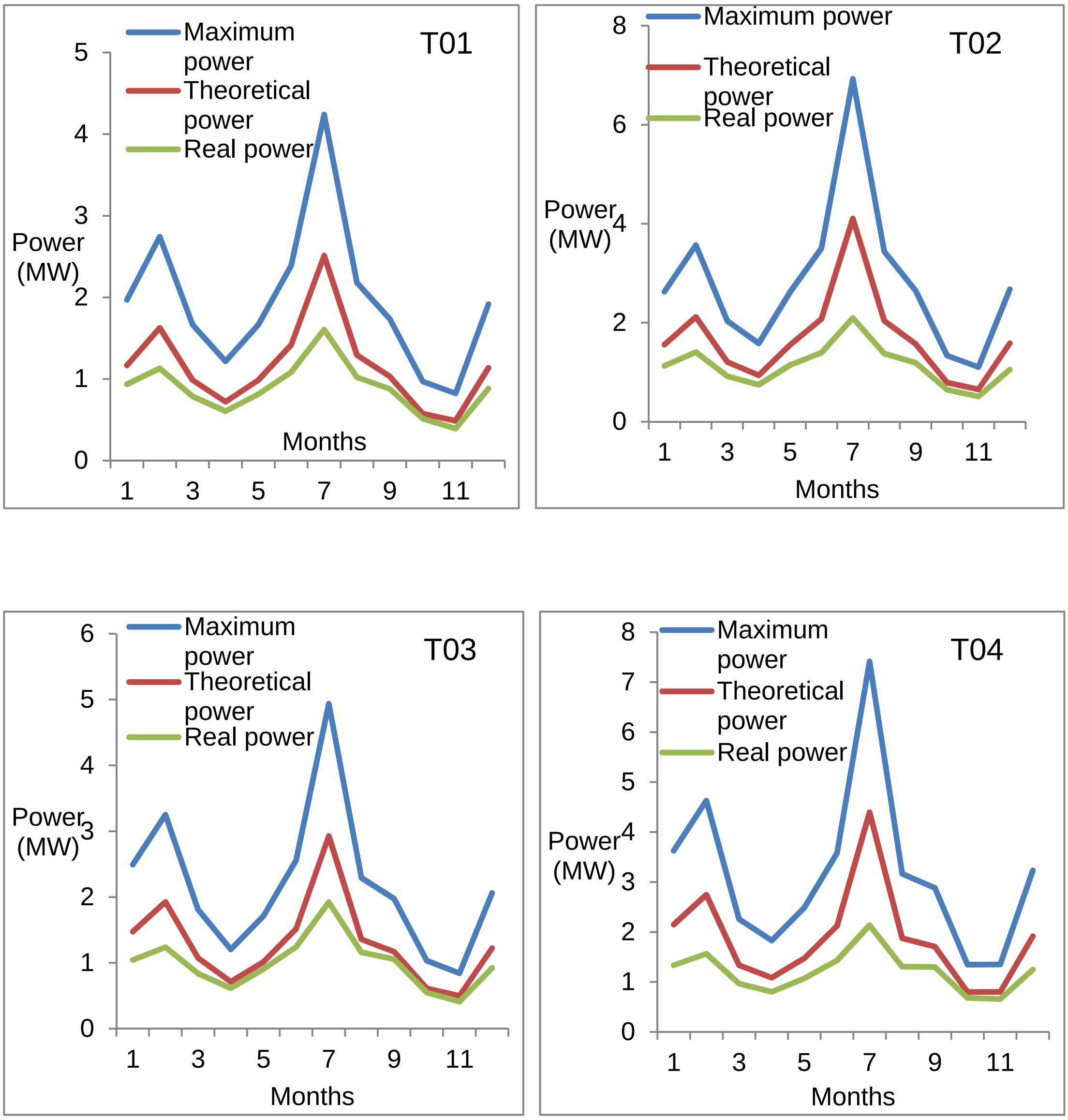

Figure 4.16. Power analysis of T01, T02, T03 and T04 turbines

It has been calculated and reported variation of maximum power, theoretical power and real power generations for turbine T05 and monthly average maximum power, theoretical power and real power generations of wind farm for each month are indicated in figure 4.17. Peak values take place in July for all parameters and variations of these parameters such as maximum, theoretical and measured powers have a similarity.

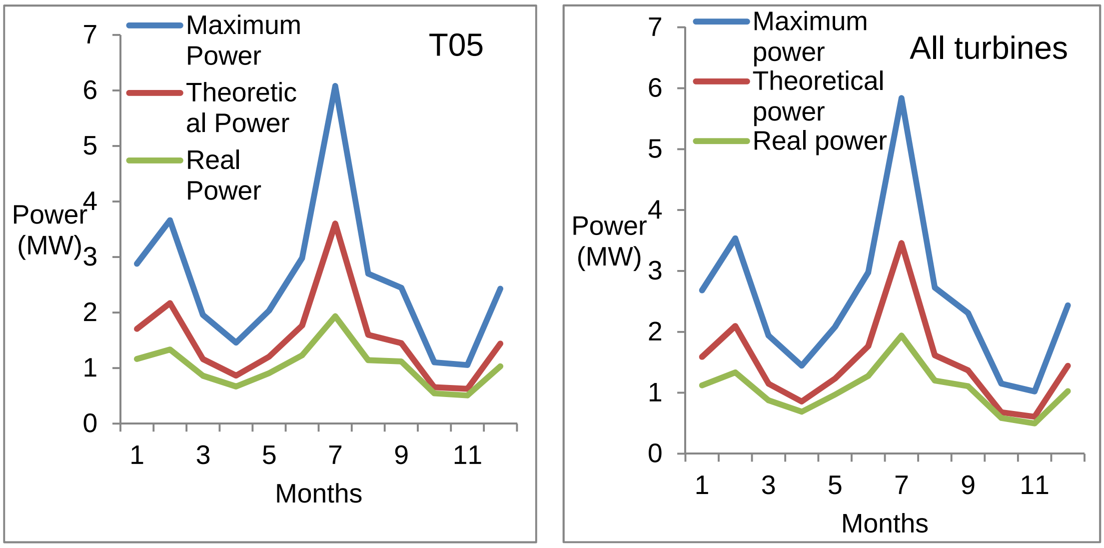

Figure 4.17. Power analysis of T05 and average power analysis according to the average powers of all turbines

Variation of efficiencies of turbines T01 and T02 for throughout one year is presented in figure 4.18 when boundary values were considered. The necessary calculations were done using equation 3.8. Calculations show that the minimum value of power coefficient, C_p occurs in July as indicated in this figure.

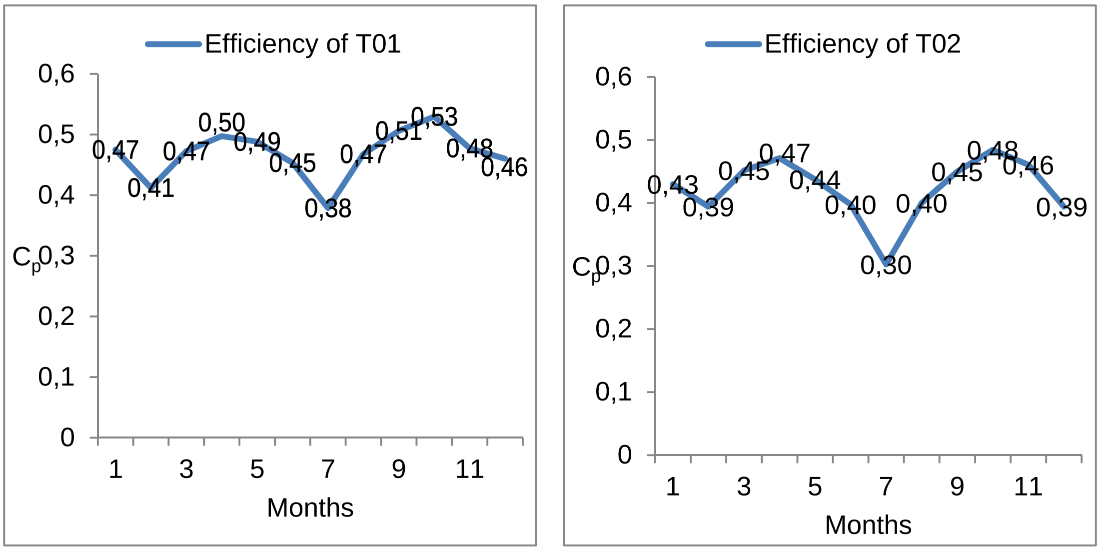

Figure 4.18. Monthly efficiencies of turbines T01 and T02

Variation of efficiencies of T03, T04, T05 and monthly average efficiencies according to the average data of all turbines for each month are given in figure 4.19.

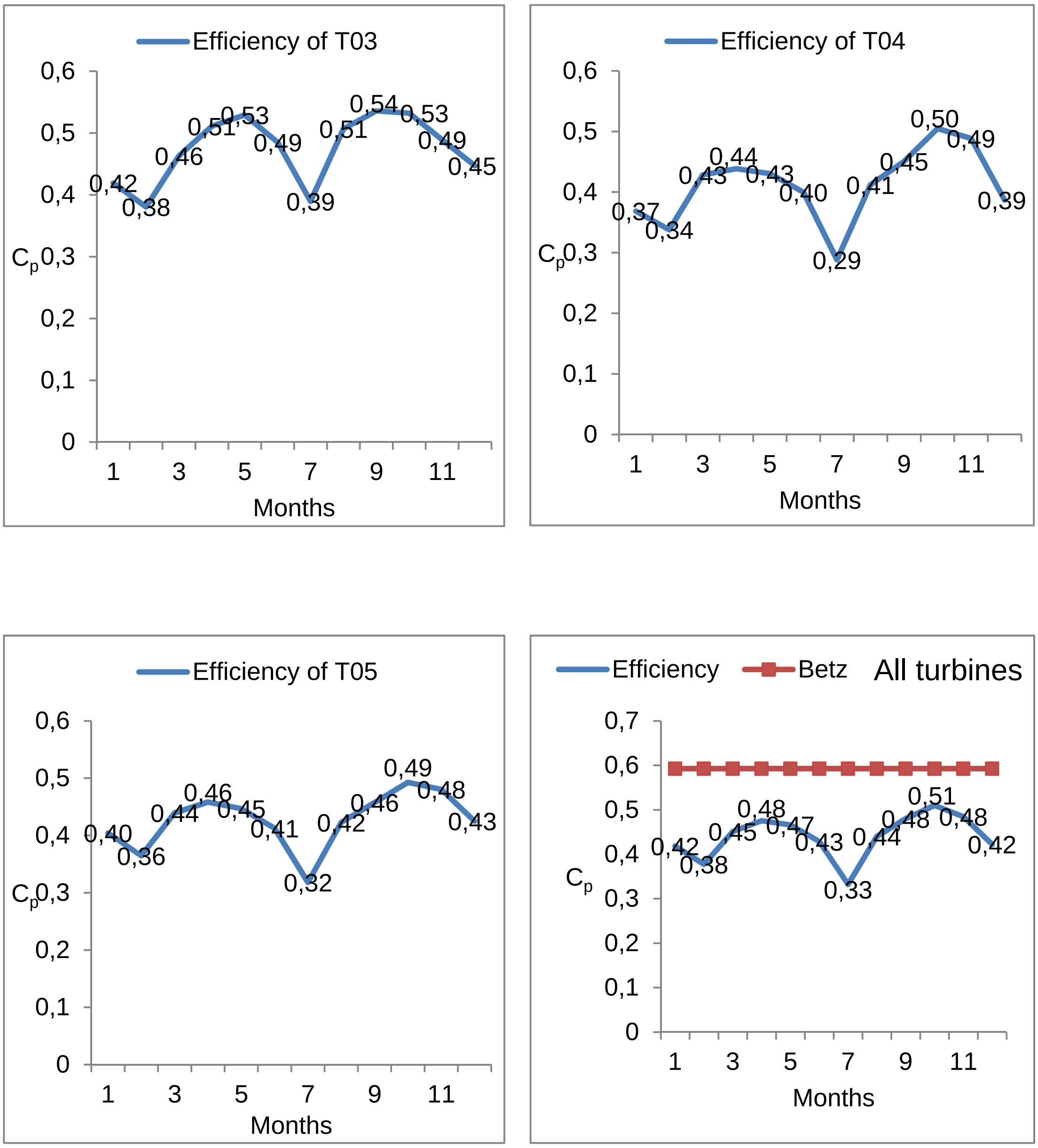

Figure 4.19. Monthly efficiencies of turbines T03, T04, T05 and monthly average efficiencies according to the average data of all turbines

Comparison of efficiencies obtained considering boundary limits for each turbine distributed for whole months stated in table 4.6. Variations of power efficiencies (C_p) have a similarity between results of turbines.

Table 4.6. Efficiency comparison for all turbines considering boundary limits

Months	T01	T02	T03	T04	T05
January	0.4750	0.4299	0.4193	0.3687	0.4043
February	0.4122	0.3942	0.3805	0.3378	0.3645
March	0.4725	0.4516	0.4632	0.4285	0.4395
April	0.4973	0.4711	0.5109	0.4386	0.4583
May	0.4882	0.4372	0.5294	0.4305	0.4469
June	0.4533	0.3976	0.4850	0.3999	0.4126
July	0.3787	0.3026	0.3894	0.2881	0.3181
August	0.4679	0.4000	0.5069	0.4120	0.4228
September	0.5060	0.4498	0.5357	0.4506	0.4575
October	0.5297	0.4841	0.5323	0.5050	0.4929
November	0.4772	0.4606	0.4890	0.4885	0.4806
December	0.4601	0.3940	0.4470	0.3868	0.4251

Figure 4.20 involves comparison of power coefficients (Efficiency) for five turbines considered. Horizontal axis demonstrates average monthly wind speed of all turbines. Figure also indicates clear vision of efficiency comparison on the desired month and the average wind speed in the related month. As seen in figure 4.20 that power efficiency (C_p) gradually decreases when wind speed increases. The reduction in efficiency is around 30 %.

As it is mentioned before the dominated wind speed throughout one year is in the range of $6 \le U_\infty \le 8\,m/s$. For this reason, blade design is more capable to convert wind power into electrical power. This is desired condition for producing more electricity.

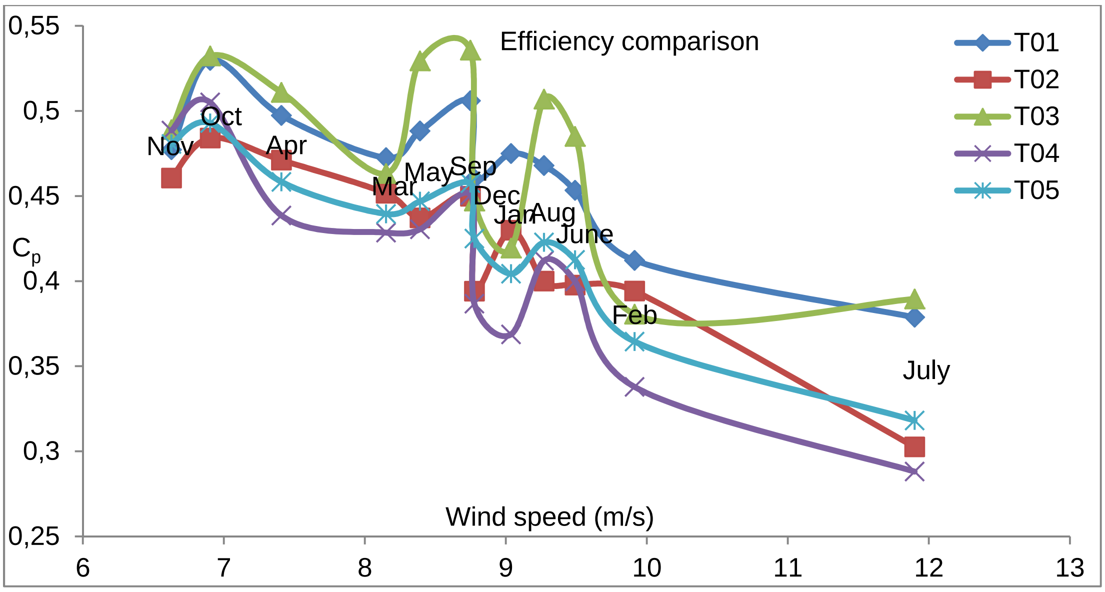

Figure 4.20. Comparison of efficiency of all turbines for one year

Figure 4.21 exhibits efficiency comparison with involving separate clear efficiency visualization of all turbines. Also, comparison of efficiencies of turbines with Betz limit can also be observed clearly in figure 4.21.

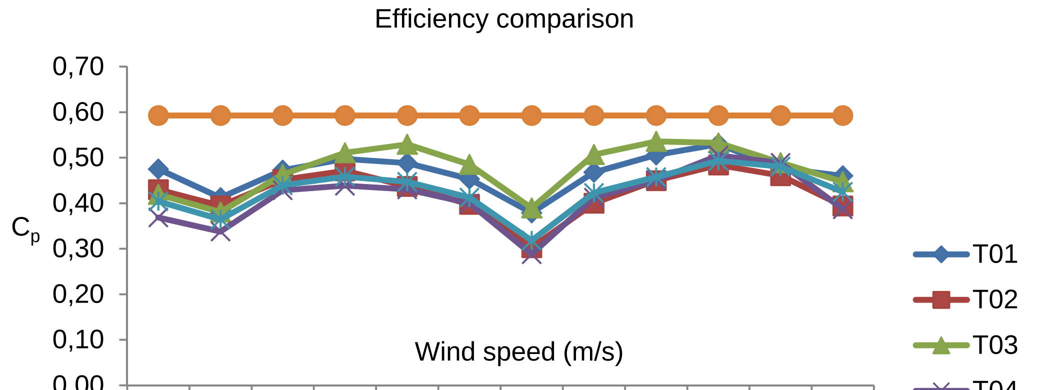

Vav	9,04	9,91	8,15	7,41	8,39	9,49	11,90	9,27	8,75	6,90	6,63	8,78
T01	0,47	0,41	0,47	0,50	0,49	0,45	0,38	0,47	0,51	0,53	0,48	0,46
T02	0,43	0,39	0,45	0,47	0,44	0,40	0,30	0,40	0,45	0,48	0,46	0,39
T03	0,42	0,38	0,46	0,51	0,53	0,49	0,39	0,51	0,54	0,53	0,49	0,45
T04	0,37	0,34	0,43	0,44	0,43	0,40	0,29	0,41	0,45	0,50	0,49	0,39
T05	0,40	0,36	0,44	0,46	0,45	0,41	0,32	0,42	0,46	0,49	0,48	0,43
Betz	0,59	0,59	0,59	0,59	0,59	0,59	0,59	0,59	0,59	0,59	0,59	0,59

Figure 4.21.Comparison of efficiency for all turbines considering average wind speeds

Figure 4.22 exhibits again comparison of turbine efficiency, however this time with involving average wind speeds of all turbines separately. Also, from figure 4.22; comparison of efficiencies of turbines with Betz limit can also be visualized clearly.

Figure 4.23 represents comparison of efficiencies of all turbines and efficiency determined according to hourly average data. Turbine constituted according to the average data of all turbines is shown as T_{all} inside the figure. Efficiencies are determined for each month which are indicated in the vertical axis.

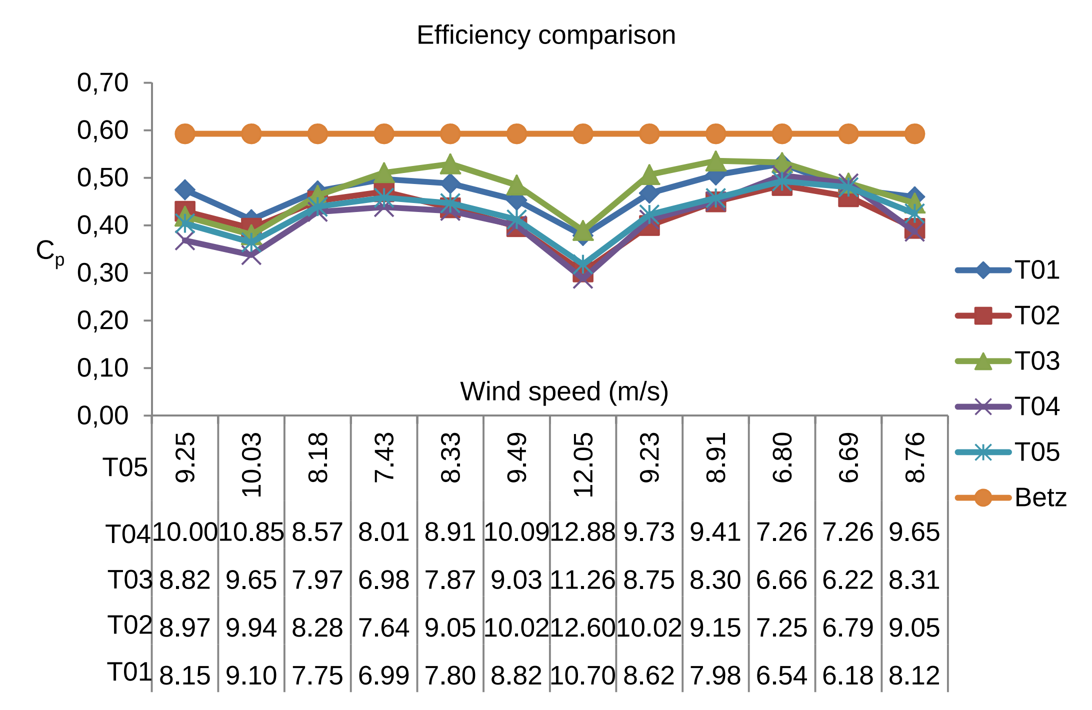

Figure 4.22. Comparison of efficiency for all turbines with separate average wind speeds related to each turbine

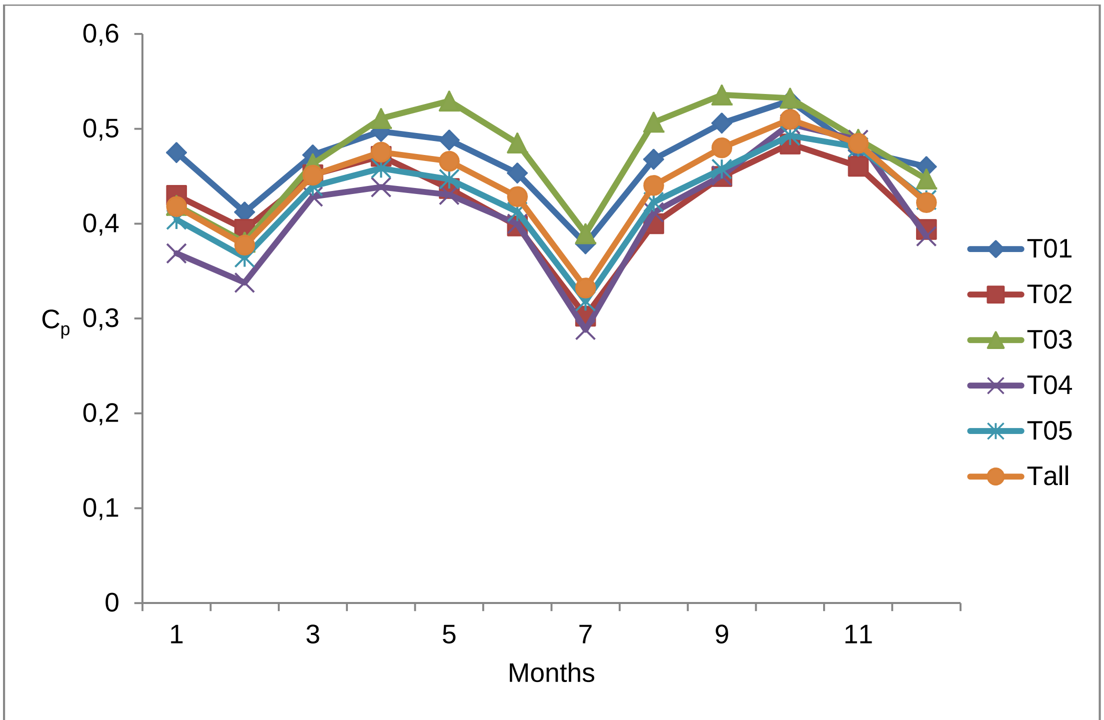

Figure 4.23. Monthly average efficiency distribution for all turbines

Comparisons of monthly efficiency of all turbines indicate that there are 20% variations between efficiency of turbines. This discrepancy may be caused by surface roughness and wind directions. Actually region of wind farm has many valleys and hills. Examination of figure reveals that the lowest turbine efficiency occurs in July although maximum power generated is gained in this month. This is due to kinetic energy of wind, in other words, conversion of wind energy into mechanical and later into electric energy is lower. Wings are supposed to be designed according to dominated wind speed of wind farm. Dominated wind speeds occurred throughout the year is in the range of $6m/s \le U_\infty \le 8m/s$.

Figure 4.24 represents comparison of flow induction factors determined according to the average efficiencies distributed for each month. Flow induction factors (a) were computed using equation 3.9. Here, flow induction factor (a) demonstrates that lower induction factor indicates lower power efficiency point.

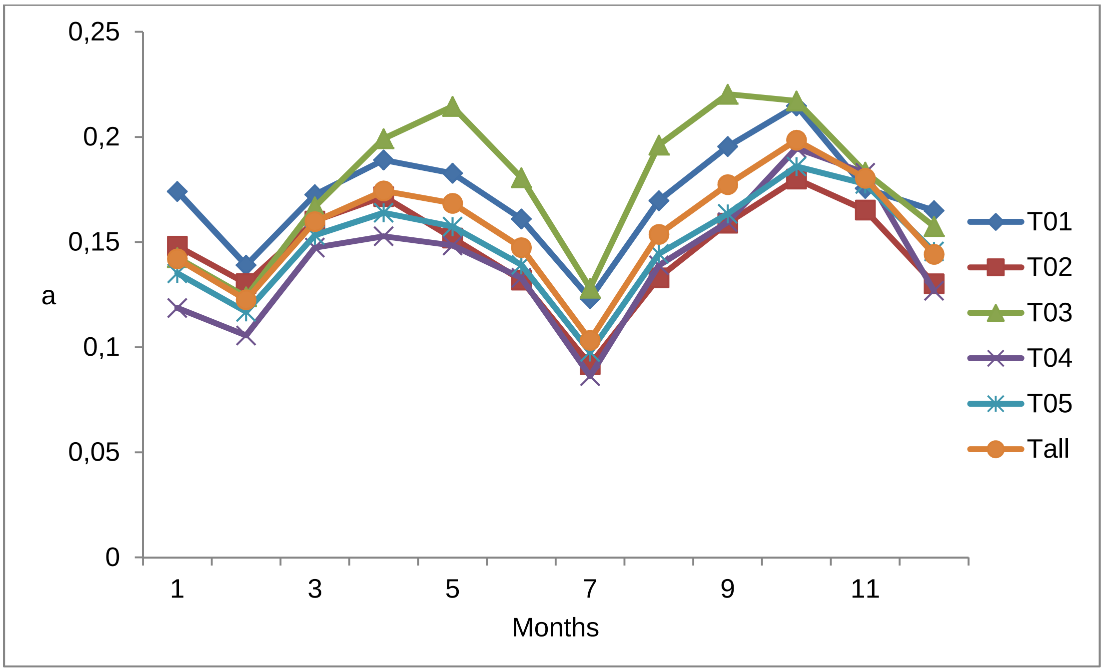

Figure 4.24. Monthly average flow induction factor (a) distribution for all turbines

Average thrust coefficient (C_T) estimations are given in figure 4.25. Equation 3.12 was used for calculations. Average thrust coefficient (C_T) distributions are given for all turbines throughout one year. According to the average data of whole turbines, thrust coefficient (C_T) distributions of turbine named as T_{all} are also provided in this figure. The coefficient of thrust force (C_T) is also lowest in July same as power coefficient (C_p). As it is known that the rotation of rotor is caused by thrust force (T).

Figure 4.26 refers to total energy generation of five turbines with an average wind speed throughout twelve months.

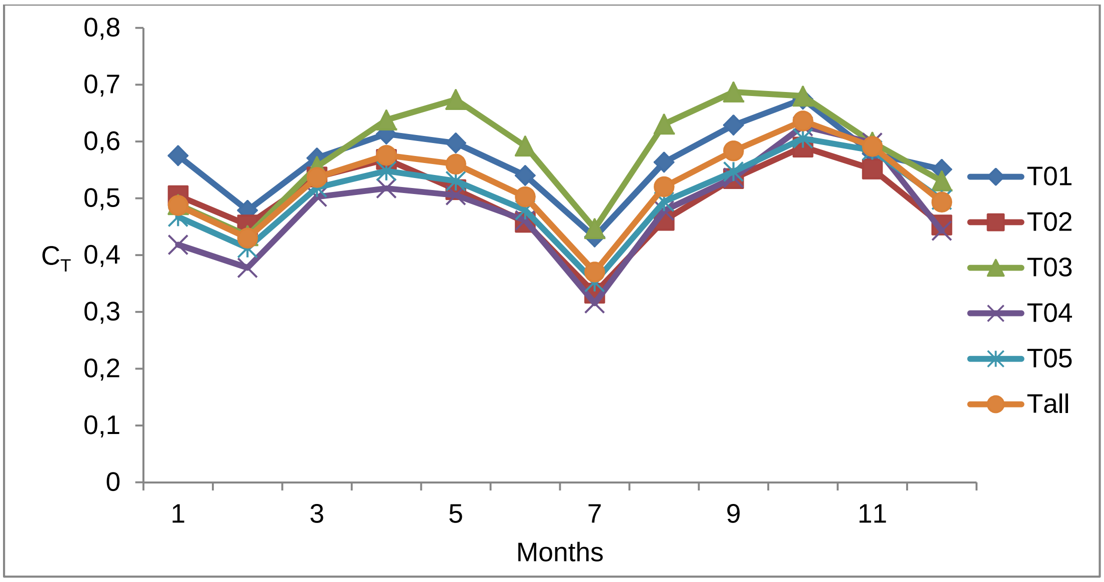

Figure 4.25. Distributions of monthly average thrust coefficient (C_T) for all turbines

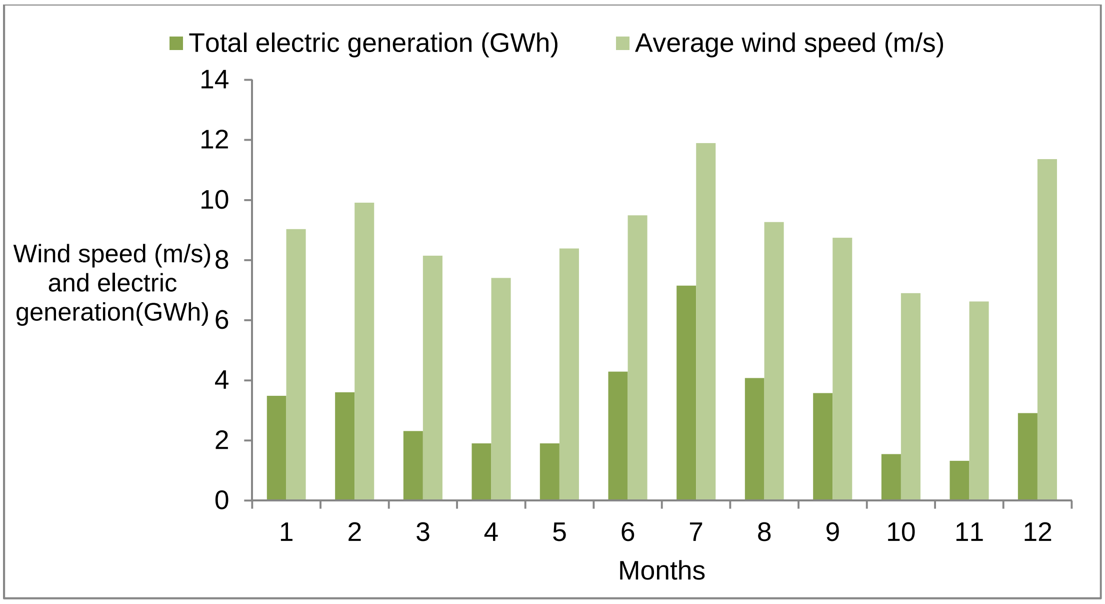

Figure 4.26. Monthly total electric generations and average wind speeds

4.5. Exergy Analysis

Table 4.7 presents calculations of exergy analysis using equation 3.17 for all turbines designed as T01, T02, T03, T04 and T05. During computation of wind speed data for sea level, equation 3.18 was used for interpolating the average speed for sea level. Roughness length was taken from table 3.2 for this equation. Equation 3.19 was used for air temperature interpolations for sea level in order to determine air density. Nominal wind speed was calculated for each month by determining maximum wind speed (V). Finally, efficiency was calculated using this maximum wind speed. Flow induction factor (a) was estimated to interpolate relations between wind speed (U_D) on rotor and free-stream wind speed ($U_{¥}$). Finally, nominal speed was determined using equation 3.26.

Table 4.7. Exergy of turbines T01, T02, T03, T04 and T05 (Continues in next page)

Turbine T01								
Date	Max power	Cut-in power	Average power	Interpolated power	Nominal power	Exergy	Exergy	Lost time
	(kW)	(kW)	(kW)	(kW)	(kW)	(1/h)	(1/s)	(minute)
Jan	27732.4	59.6	1968.5	871.7	7352.6	3.9	0.0011	15.3
Feb	32212.2	41.2	2742.5	1214.4	7366.2	4.6	0.0013	13.1
Mar	33950.1	48.6	1665.6	737.8	7218.6	4.8	0.0013	12.4
Apr	32116.0	50.5	1216.5	538.9	7318.7	4.5	0.0012	13.4
May	10620.9	54.0	1665.5	737.9	10346.6	1.1	0.0003	54.0
June	17799.7	53.1	2390.5	1059.4	8344.2	2.3	0.0006	26.2
July	22645.4	0.0	4239.2	1878.9	7720.5	3.2	0.0009	18.5
Aug	8881.1	0.2	2178.8	966.0	10945.6	0.9	0.0003	65.1
Sep	8089.8	24.8	1736.4	769.7	11266.1	0.8	0.0002	74.8
Oct	12635.4	39.4	968.6	429.3	9246.1	1.4	0.0004	42.2
Nov	4577.3	60.5	822.8	364.6	16703.2	0.3	0.0001	201.4
Dec	32977.3	48.6	1915.6	848.5	7303.1	4.7	0.0013	12.9

Turbine T02								
Date	Max power	Cut-in power	Average power	Interpolated power	Nominal power	Exergy	Exergy	Lost time
	(kW)	(kW)	(kW)	(kW)	(kW)	(1/h)	(1/s)	(minute)
Jan	28354.9	51.5	2626.3	1163.0	7599.3	3.9	0.0011	15.3
Feb	40820.1	42.8	3569.5	1580.7	7181.5	6.0	0.0017	10.1
Mar	35991.1	29.1	2035.5	901.6	7184.2	5.2	0.0014	11.6
Apr	28581.5	39.6	1582.9	701.2	6811.4	4.3	0.0012	13.9
May	12820.1	38.9	2618.1	1160.0	9788.3	1.5	0.0004	41.2
June	23080.6	43.6	3503.4	1552.6	7734.5	3.2	0.0009	18.6
July	28642.3	0.0	6924.3	3068.9	7305.5	4.4	0.0012	13.5
Aug	11395.8	0.2	3438.3	1524.2	10073.0	1.3	0.0004	45.4
Sep	10356.5	7.3	2646.2	1172.8	10630.5	1.1	0.0003	54.0
Oct	13743.8	27.0	1333.3	590.8	9078.1	1.6	0.0004	37.7
Nov	8702.3	49.1	1103.3	488.9	10776.9	0.9	0.0002	69.8
Dec	38526.3	40.0	2675.7	1185.0	6801.9	5.9	0.0016	10.2

Turbine T03								
Date	Max power	Cut-in power	Average power	Interpolated power	Nominal power	Exergy	Exergy	Lost time
	(kW)	(kW)	(kW)	(kW)	(kW)	(1/h)	(1/s)	(minute)
Jan	30894.4	52.7	2491.9	1103.5	7558.2	4.3	0.0012	14.1
Feb	37759.7	49.2	3251.8	1440.1	7246.6	5.5	0.0015	11.0
Mar	39959.2	47.0	1810.2	801.9	6978.7	5.9	0.0016	10.2
Apr	31097.5	38.8	1204.6	533.7	6422.5	4.9	0.0014	12.1
May	11042.8	37.0	1713.5	759.3	10819.6	1.1	0.0003	54.3
June	21231.8	40.5	2560.3	1134.7	7873.9	2.9	0.0008	20.9
July	25464.3	0.0	4936.7	2188.1	7449.6	3.8	0.0011	15.8
Aug	11794.6	0.1	2291.2	1015.7	9962.9	1.3	0.0004	45.7
Sep	11927.0	11.8	1975.1	875.4	9912.8	1.3	0.0004	45.7
Oct	12073.0	33.4	1033.1	457.8	9797.1	1.3	0.0004	46.6
Nov	3720.7	34.0	844.0	374.0	26854.5	0.2	0.0000	387.6
Dec	39648.8	38.1	2064.6	914.4	6754.1	6.0	0.0017	9.9

Turbine T04								
Date	Max power	Cut-in power	Average power	Interpolated power	Nominal power	Exergy	Exergy	Lost time
	(kW)	(kW)	(kW)	(kW)	(kW)	(1/h)	(1/s)	(minute)
Jan	46382.4	38.7	3626.0	1605.7	6597.1	7.3	0.0020	8.2
Feb	46557.1	39.9	4630.4	2050.6	6931.4	7.1	0.0020	8.5
Mar	46915.3	42.8	2254.9	998.8	6526.1	7.4	0.0020	8.1
Apr	50831.7	39.9	1828.6	810.1	6325.5	8.2	0.0023	7.3
May	16459.5	40.4	2487.2	1102.0	8747.9	2.0	0.0006	29.5
June	22409.1	46.9	3580.2	1586.6	7879.3	3.1	0.0009	19.4
July	21822.7	0.0	7414.8	3286.2	7859.0	3.3	0.0009	18.2
Aug	14667.2	0.4	3163.0	1402.1	8984.4	1.8	0.0005	32.8
Sep	14001.5	14.6	2881.8	1277.2	9254.1	1.7	0.0005	35.6
Oct	13412.8	33.0	1344.5	595.7	9734.2	1.5	0.0004	41.3
Nov	8911.1	37.8	1347.6	597.1	11697.9	0.8	0.0002	72.9
Dec	45790.3	37.1	3232.4	1431.6	6541.9	7.3	0.0020	8.3

Turbine T05								
Date	Max power	Cut-in power	Average power	Interpolated power	Nominal power	Exergy	Exergy	Lost time
	(kW)	(kW)	(kW)	(kW)	(kW)	(1/h)	(1/s)	(minute)
Jan	33784.6	45.8	2878.1	1274.5	7508.8	4.7	0.0013	12.7
Feb	40303.1	43.7	3662.4	1621.8	7273.9	5.8	0.0016	10.3
Mar	42559.6	49.8	1958.5	867.5	7047.8	6.2	0.0017	9.7
Apr	34191.9	38.7	1457.9	645.8	6558.5	5.3	0.0015	11.3
May	13297.0	40.2	2035.2	901.7	9424.6	1.5	0.0004	39.3
June	22168.1	49.6	2984.1	1322.4	7852.9	3.0	0.0008	19.8
July	19672.1	0.0	6080.7	2694.9	8071.1	2.9	0.0008	21.0
Aug	13425.1	0.2	2702.1	1197.7	8897.4	1.7	0.0005	35.8
Sep	13480.3	15.1	2447.6	1084.8	9148.0	1.6	0.0005	37.0
Oct	13069.3	33.0	1103.2	488.8	9029.4	1.5	0.0004	39.7
Nov	6746.6	44.3	1054.5	467.2	12850.6	0.6	0.0002	105.8
Dec	41178.4	37.6	2430.6	1076.5	6725.9	6.3	0.0018	9.5

According to the summation of the losses obtained for each month for every turbine, total losses for all turbines are depicted in table 4.8.

Table 4.8. Total times of all turbines for zero production in a year

Turbine number	Lost time (hours)
T01	9.1592
T02	5.6869
T03	11.2344
T04	4.8354
T05	5.8643

4.6. Aerodynamic Performance Analysis

Aerodynamic performance of turbines was carried out through using wind speed data of four turbines. Since there were considerable problems about the wind direction of T02, it was preferred to use data of wind speed, electric generation, wind direction and temperatures of four turbines. During calculations of aerodynamic performance, rotor speeds (U_D) were used.

Comparisons of power coefficient (C_p) and velocity ratio $(\lambda = U_W / U_\infty)$ for four turbines are given in figure 4.27. During estimation of power coefficient, C_p and velocity ratio, λ, eq. 3.10 and eq. 3.11 were used for calculations of flow induction factor (a), and by using equation 3.23, velocity ratio $(\lambda = U_W / U_\infty)$ was computed. And finally by equation 3.9, power coefficient (C_p) was calculated.

By combination of equations 3.23 and 3.9, relations between power coefficient, C_p and velocity ratio, λ can be obtained. Power coefficient (C_P) presented as $C_P = 0.5(1-\lambda^2)(1+\lambda)$ indicates that as velocity ratio, λ increases, power coefficient, C_p value also increases. But, after the peak point, as velocity ratio, λ increases the decreasing value of $(1-\lambda^2)$ term overcomes increasing value of $(1+\lambda)$ term, which results in power coefficient, C_p value to decrease.

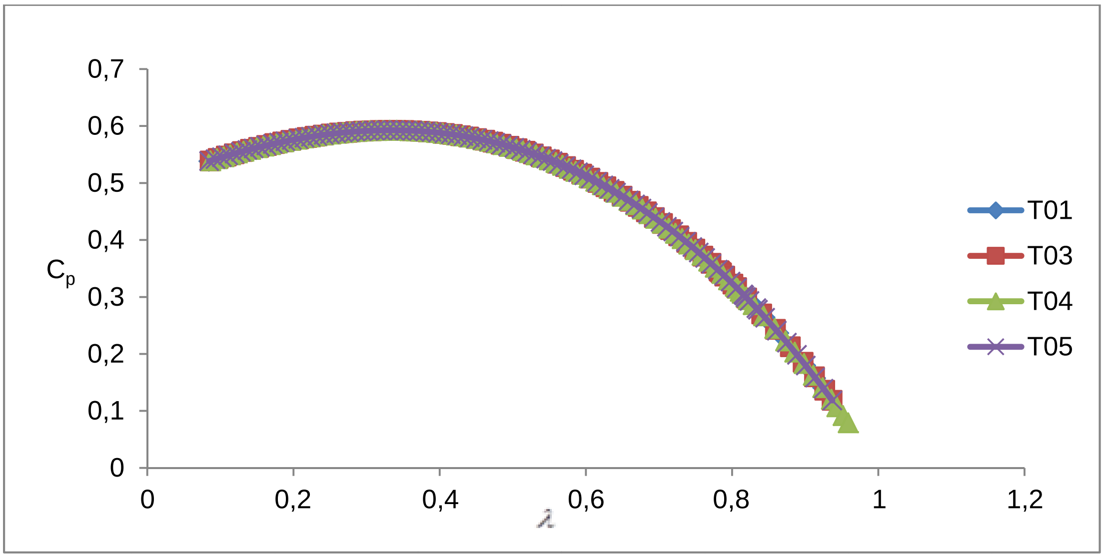

Figure 4.27. Distributions of power coefficient, C_p with velocity ratio, λ

Examining the term $1-\lambda^2$ indicates that as velocity ratio, λ increases the value of $[1-\lambda^2]$ decreases which results thrust coefficient, C_T value to decrease. Relations between thrust coefficient, C_T and velocity ratio (λ) were analyzed for four turbines and computed results were presented in figure 4.28 using equations 3.12 and 3.23. Thrust coefficient, $C_T = 1-\lambda^2$ indicates that for all turbines thrust coefficient, C_T and velocity ratio, λ are always lower than 1.

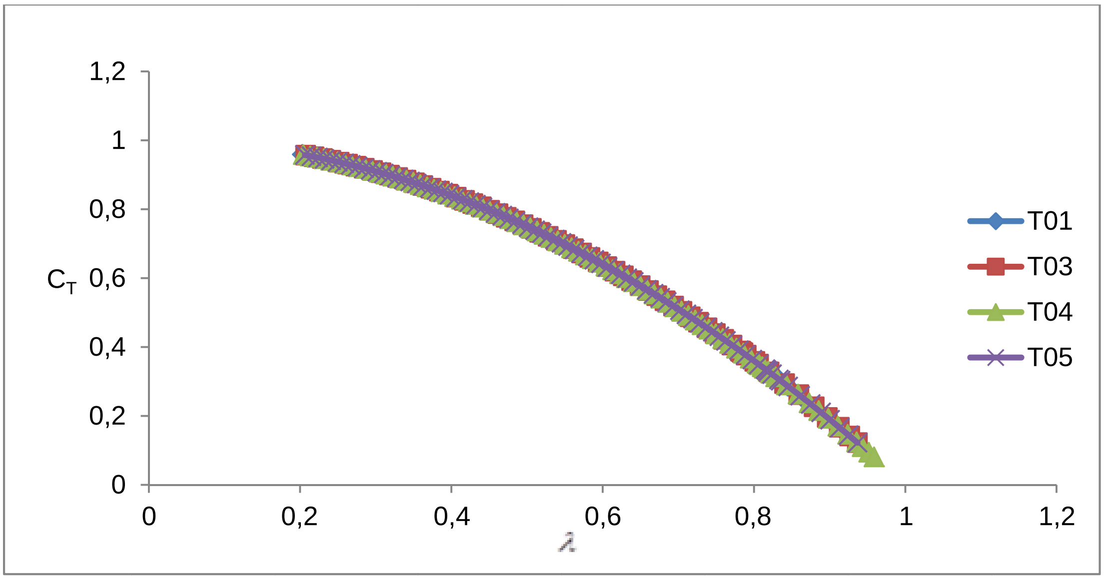

Figure 4.28. Distributions of thrust coefficient, C_T with velocity ratio, λ

As it is mentioned above, power coefficient (C_p) and flow induction factor (a) relation is calculated by equation 3.9 and results are presented in figure 4.29.

Combining equation 3.9 and 3.12 provides the following expression, $C_p = C_T - aC_T$. Both power coefficient, (C_p) and thrust coefficient (C_T) increase when flow induction factor (a) increases. These relations are presented in figures 4.29 and 4.30.

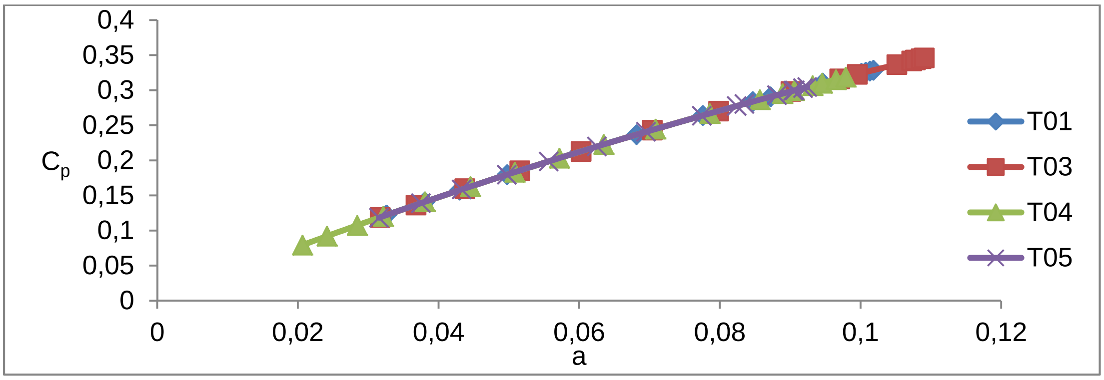

Figure 4.29. Relation of power coefficient, C_p with flow induction factor, a

As it is mentioned above, thrust coefficient (C_T) and flow induction factor (a) relation are given by equation 3.12. Flow induction factor (a) increases with increasing free-stream wind speed, $U_¥$ up to a breaking point for four turbines (see figure 4.38). Then the flow induction factor (a) decreases with increasing free-stream wind speed, $U_¥$, and (a)(1-a) term behaves in the similar trend of (a). So, when the flow induction factor (a) is given in increasing trend, thrust coefficient, C_T = 4a(1-a) also increases as shown in figure 4.30.

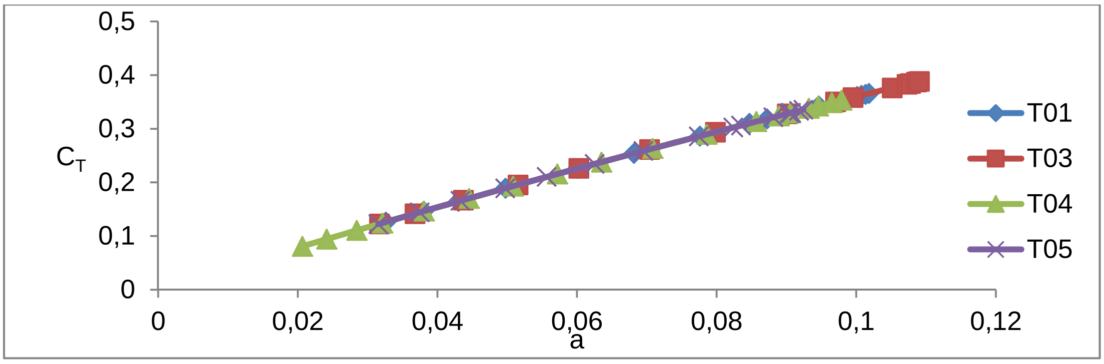

Figure 4.30. Thrust coefficient, C_T with flow induction factor, a

Wind speed far on the wake (U_W) and wind speed in front of the rotor (U_∞) are related for the exploitation of equation 3.21 indicated in figure 4.31. According to the definition of equation 3.21; after breaking point, speed will increase for the benefit of wake velocity (U_W) at a certain value of flow induction factor (a), where flow induction factor (a) starts to fall down.

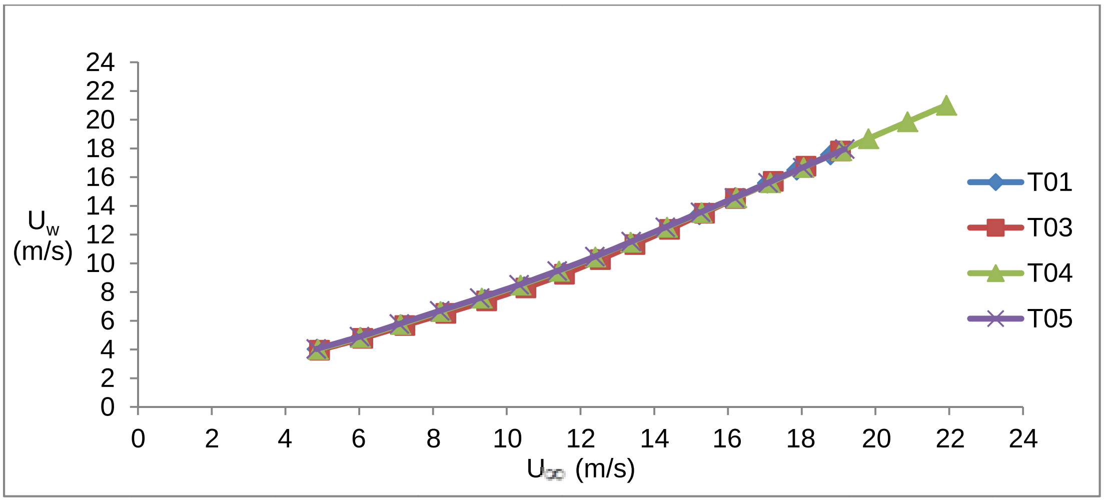

Figure 4.31. Variation of wake velocity, U_w and free-stream velocity, U_∞

Relations between velocity on the rotor (U_D) and free-stream wind speed (U_∞) are determined using equation 3.20 and obtained results are presented in figure 4.32.

Increase in air speed on the propeller (U_D) always overcomes decrease in flow induction factor (a) resulting an increase in U_∞. It is obvious that when free-stream wind speed (U_∞) increases, wind speed on the propeller (U_D) also increases. There is a linear relationship between (U_∞) and (U_D).

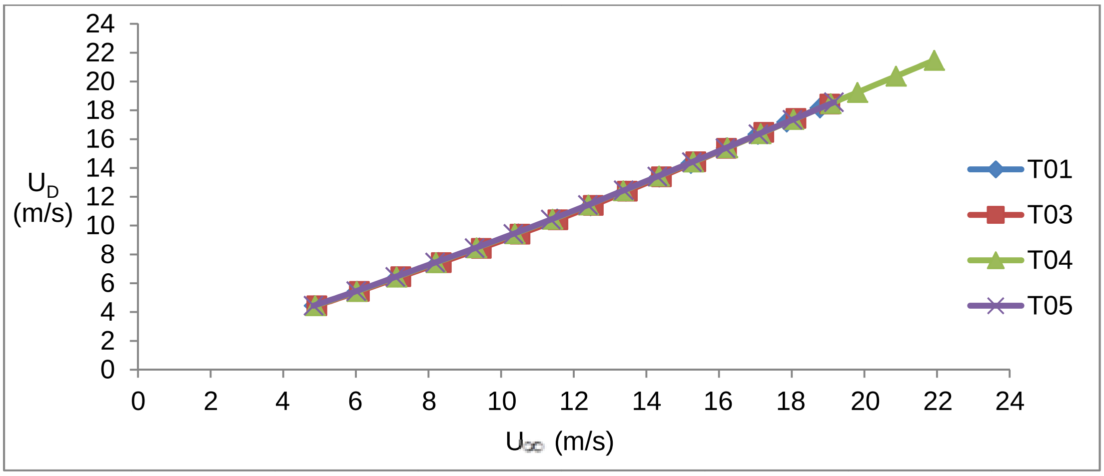

Figure 4.32. Distribution of speed on rotor, U_D with free-stream wind speed, U_∞

By using equation 3.20, free-stream wind speeds, U_∞ can be estimated. Consequently, figure 4.33 was drawn. When the figure 4.33 is carefully analyzed, it is observed that through approaching cut-in and cut-out speeds, power generations either stop or approach to a maximum limit.

Real power obtained by the turbine is a property of its own where it efficiently generates electricity between cut-in and cut-out speeds. Outside of these values its efficiency decreases as shown in the figure. So, it is best to run between wind speeds of $4\,m/s \le U_D \le 25\,m/s$.

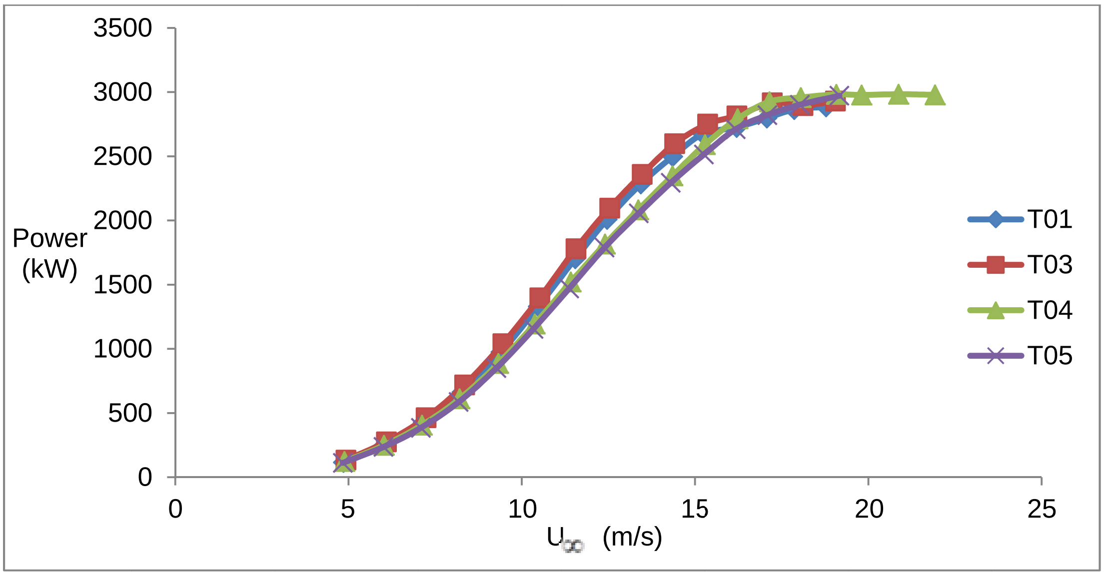

Figure 4.33. Distribution of power generation, P with free-stream wind speed, U_∞

The aerodynamic aspects of different wind turbine designs are available. The thrust force (T) in the direction normal to the wind flow direction tend to move the wing to rotate around central axis of the rotor in order to extract mechanical energy from wind power. As seen the term thrust force (T) is extremely important for the performance of wind turbine. Due to this reason, variations of thrust force (T) against free-stream wind speed, U_∞ are examined using equation 3.24 and obtained results are presented in figure 4.34.

After the peak point (see figure 4.34), as free-stream wind speed (U_∞) increases due to the decrease of the term a(1-a) in the thrust formula 3.24; sudden decrease of related term overcomes a portion of increase of free-stream wind speed, (U_∞). Thrust force increases until free-stream wind speed, $U_\infty = 14 m/s$. From this point to further up the thrust force (T) begins to decrease with free-stream wind speed, U_∞.

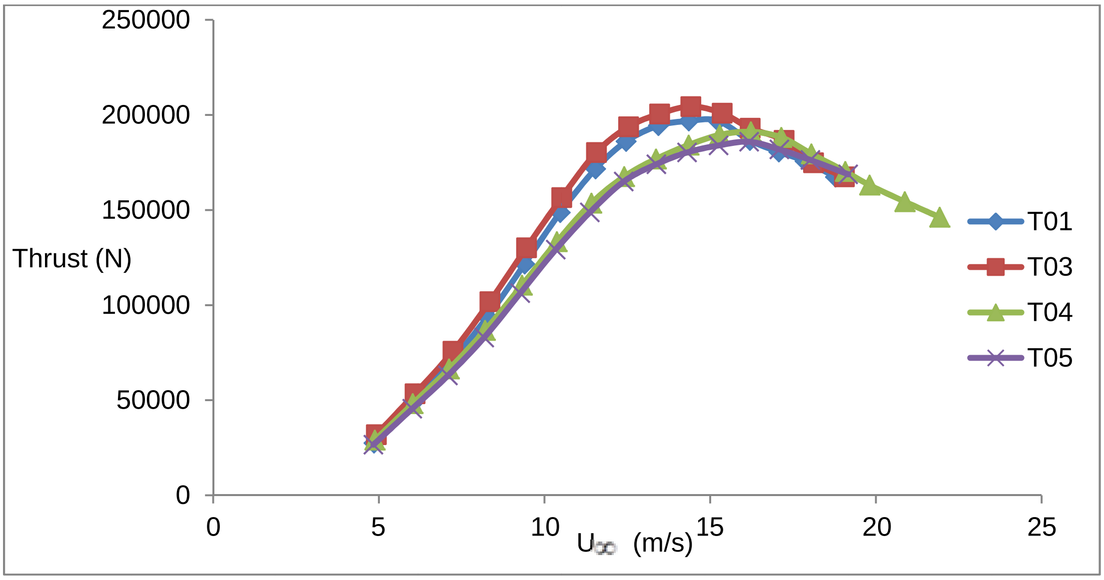

Figure 4.34. Distributions of thrust force (T) with free-stream wind speed, U_∞

Mass flow rate $(\dot{m})$ was determined through the usage of equation 3.25.

As seen in figure 4.35, mass flow rate $(\dot{m})$ is directly proportional with free-stream wind speed (U_∞), since wind flow is incompressible.

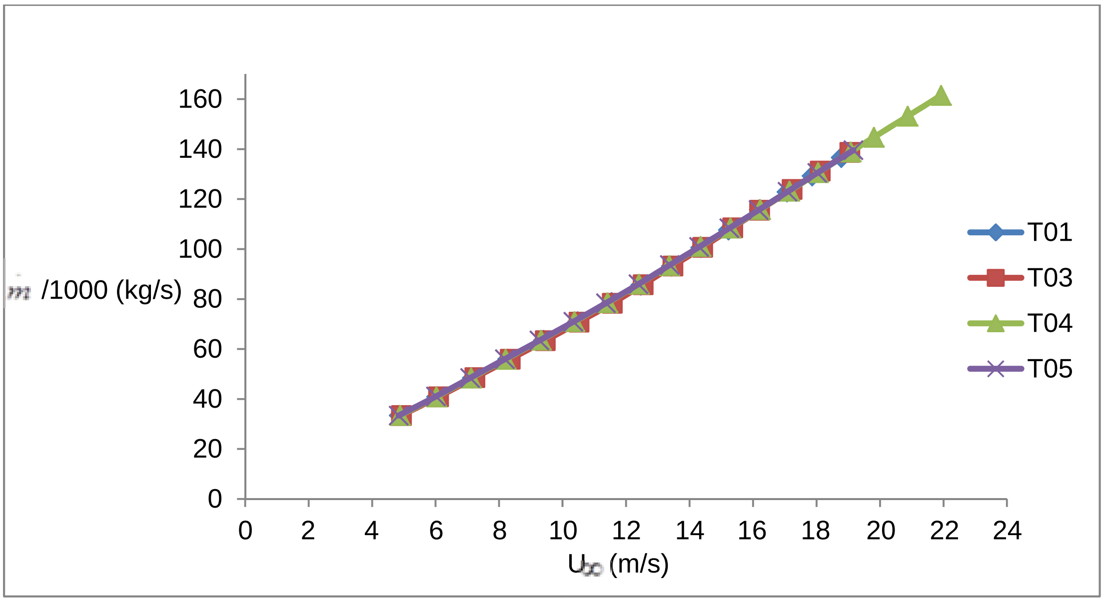

Figure 4.35. Variation of mass flow rate $(\dot{m})$ with free-stream wind speed, U_{∞}

The speed of rotor (Ω) varies with wind power (P). The results of rotor speed (Ω) with wind power (P) are determined using equation 3.26 and related results are presented in figure 4.36. For all turbines more or less there are similar relations. It is obvious that when free-stream wind speed (U_{∞}) increases, the speed of rotor (Ω) also increases.

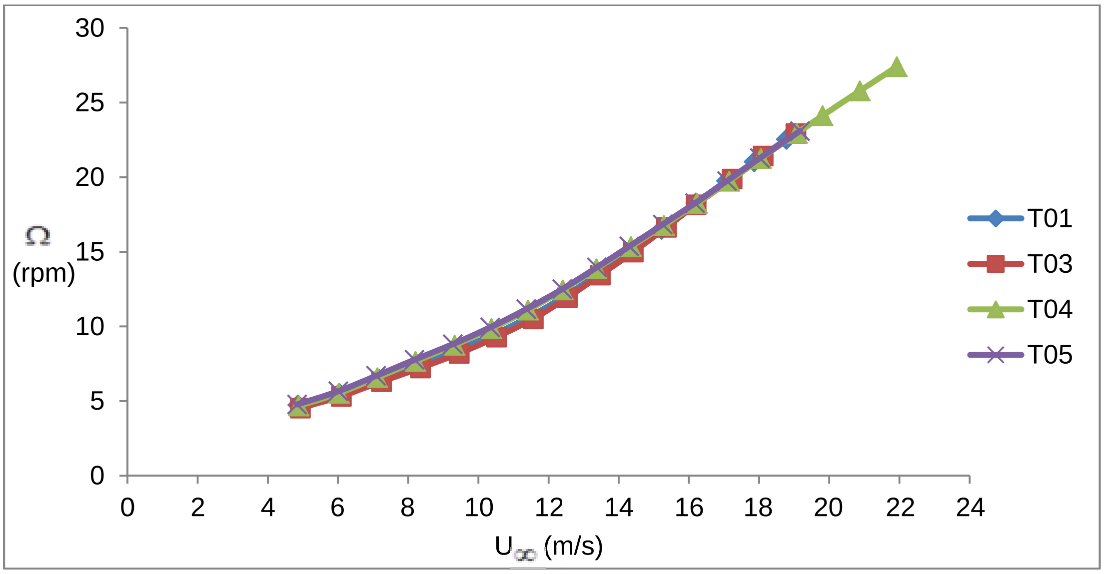

Figure 4.36. Relations between rotor speed (Ω) and free-stream wind speed (U_{∞})

Variation of tangential flow induction factor (a') with free-stream wind speed, U_{∞} provided in figure 4.37 is obtained using equation 3.27. As seen in this figure an increase of tangential flow induction factor (a') with an increase of free-stream wind speed, U_{∞} occurs until breaking point. But, after breaking point, the tangential flow induction factor (a') starts decreasing although the free-stream wind speed, (U_{∞}) continues to increase. The tangential flow induction factor (a') behaves in two different trends, namely, before and after breaking point as seen in figure 4.37. From equation 3.27, it can be observed that flow induction factor (a) and tangential flow induction factor (a') are directly functions of each other, and behave in the similar manner.

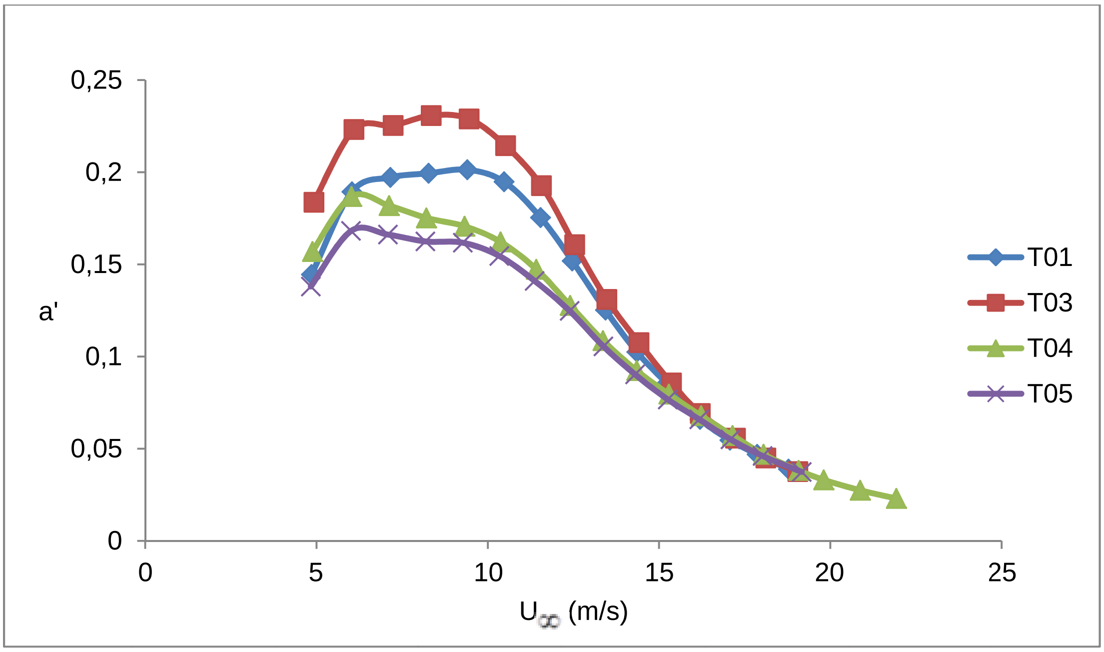

Figure 4.37. Variations of tangential flow induction factor (a') with free-stream wind speed (U_{∞})

Flow induction factors (a) and wind speeds in the forward face of the rotor (U_{∞}) were related with each other as given in figure 4.38. Maximum flow induction factors are available with free-stream wind speeds, (U_{∞}) in the range of $6\,m/s \le U_{\infty} \le 12\,m/s$.

In summary, flow induction factor (a) increases rapidly for $U_{\infty} \geq 6m/s$. On the other hand, decreases rapidly for $U_{\infty} \geq 12m/s$.

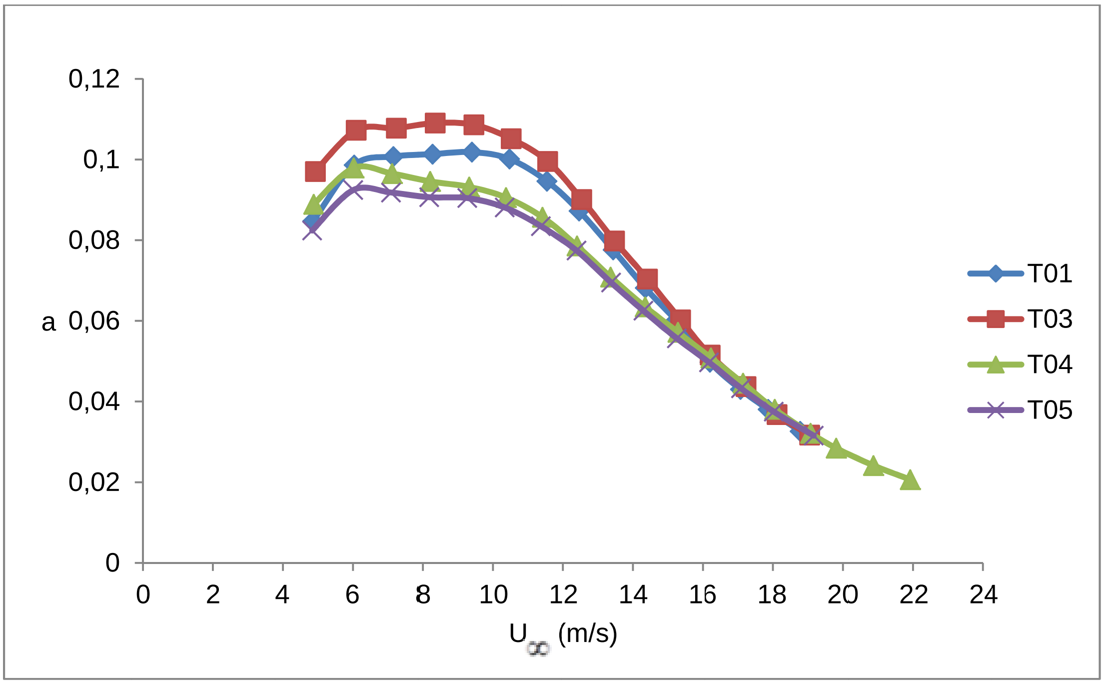

Figure 4.38. Variations of flow induction factor (a), with free-stream wind speed (U_{∞})

Power coefficients (C_p) and tangential flow induction factors (a') were related with each other as demonstrated in figure 4.39. Tangential flow induction factors (a') behave in the similar manner with the flow induction factor (a) as free-stream wind speed, U_{∞} increases since tangential flow induction factor (a') is a function of flow induction factor (a) as seen in figure 4.39.

The rate of increase in power coefficient, C_p gradually gets lower while tangential flow induction factor (a') gets a higher value.

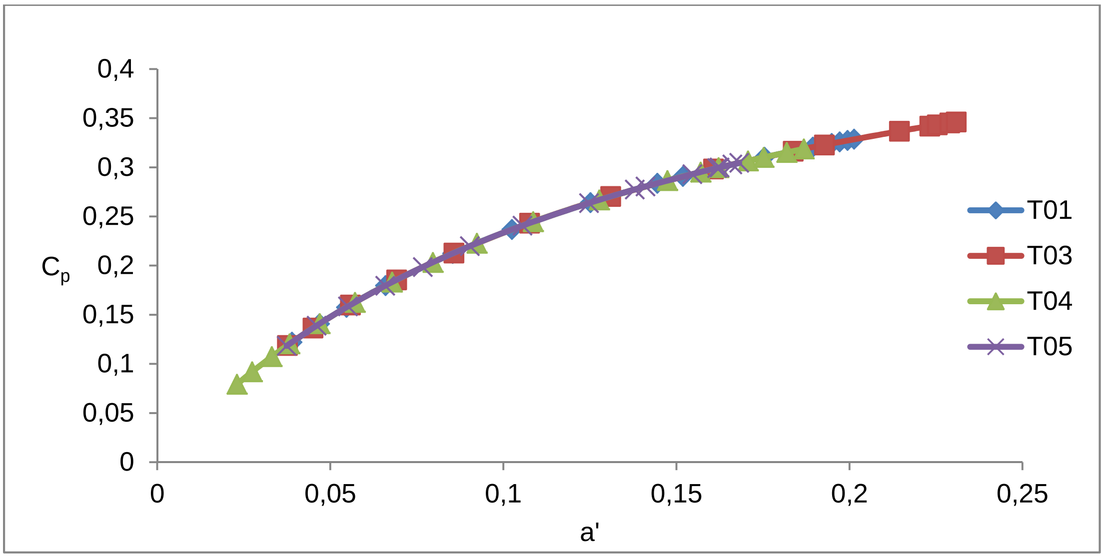

Figure 4.39. Variations of power coefficient (C_p) with tangential flow induction factor (a')

Figure 4.40 presents relations of thrust coefficients (C_T) with tangential flow induction factors (a'). As it is known that the power generation depends on the thrust force (T). In this sense, variations of thrust coefficients (C_T) with flow induction factors (a) have similar profile which the power coefficient factors, C_p has. Both the power coefficient (C_p) and thrust coefficient (C_T) of all turbines have exactly similar profiles.

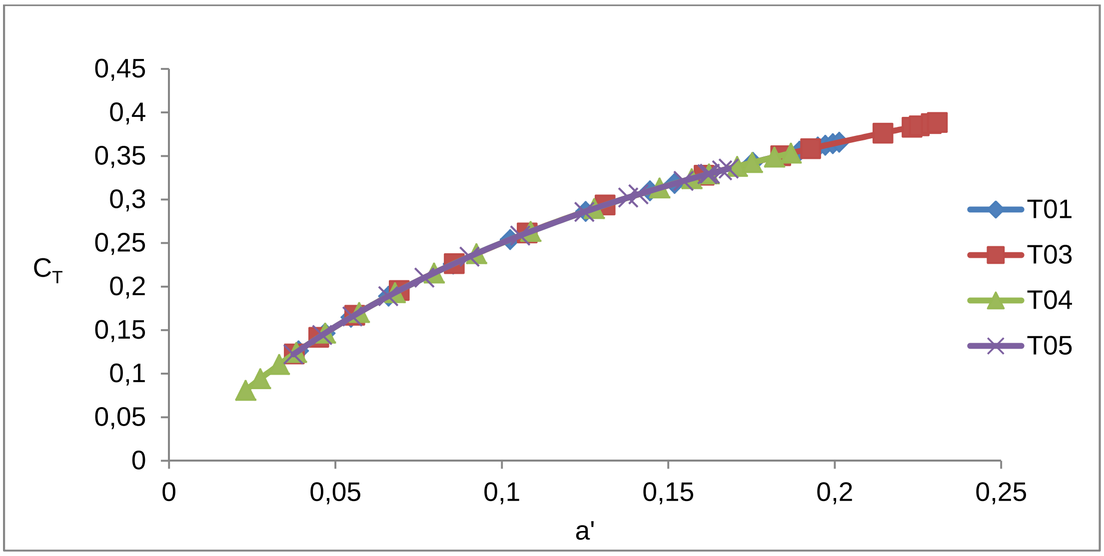

Figure 4.40. Variations of thrust coefficient, C_T with tangential flow induction factor (a')

Figure 4.41 reveals the relation of tangential flow induction factor (a') and flow induction factor (a). Tangential flow induction factor (a') is a function of flow induction factor (a). As seen in figure 4.41, tangential flow induction factor (a') and flow induction factor (a) have a same trend since free-stream wind speed (U_{∞}) increases with increasing speed of rotor (Ω) keeping, (radius of rotor, r) constant.

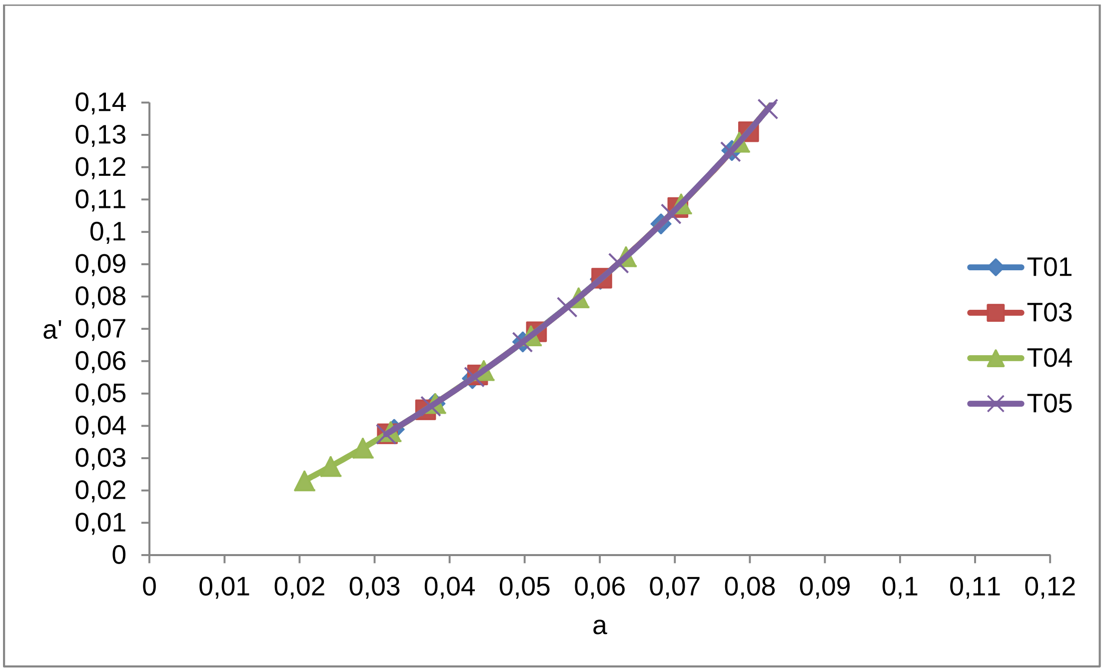

Figure 4.41. Tangential flow induction factor (a') with flow induction factor (a)

Flow induction factor (a) with velocity ratio, λ is presented in figure 4.42. Since velocity ratio (λ) is given in increasing trend, as velocity ratio (λ) increases flow induction factor (a) will decrease. This can easily be seen by considering equation 3.23, $[a = 0.5(1 - \lambda)]$.

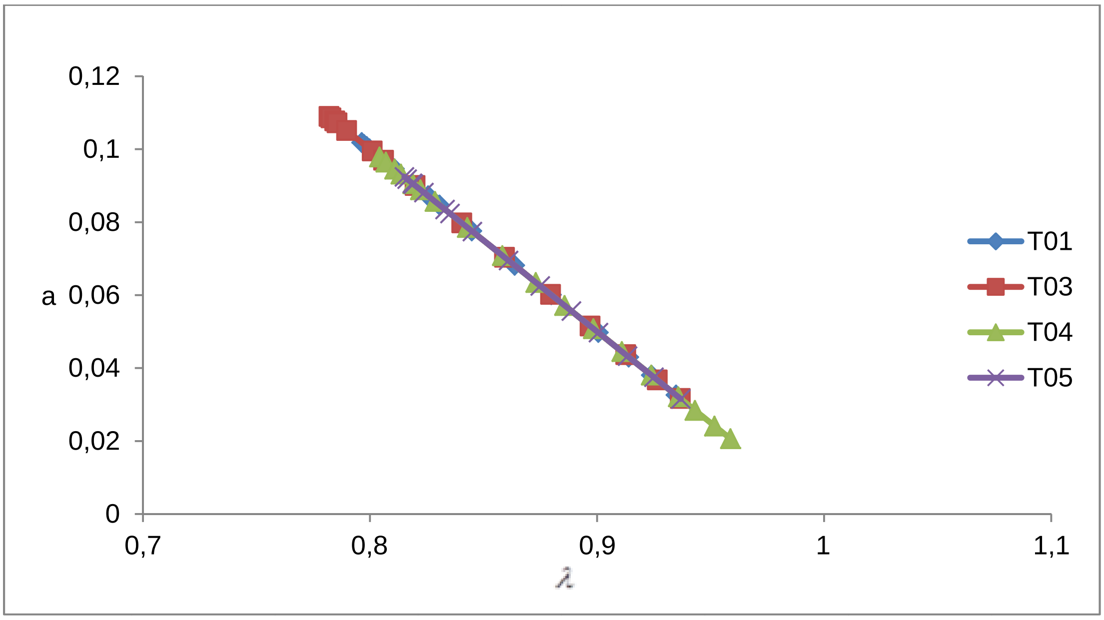

Figure 4.42. Variations of flow induction factor (a) with velocity ratio (λ)

Comparison of tangential flow induction factor (a') and velocity ratio (λ) indicated in figure 4.43. Tangential flow induction factor (a') which is a function of flow induction factor (a) increases up to the breaking point of (a). After breaking point of “a” it starts to decrease. Since trends of “a” and λ are the inverse.

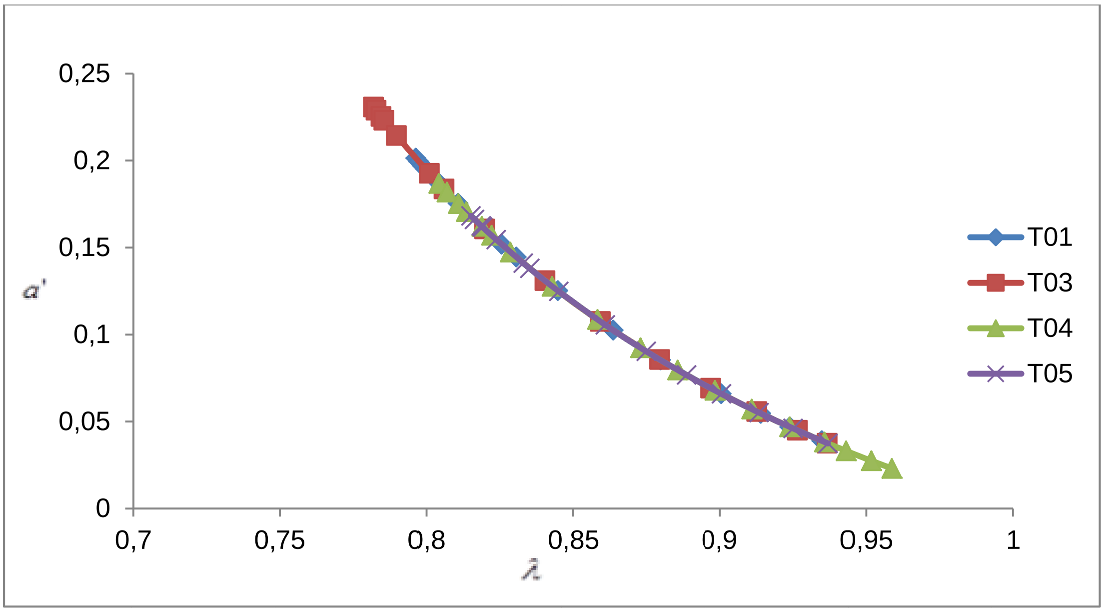

Figure 4.43. Variations of tangential flow induction factor (a') with velocity ratio ($\lambda = U_W / U_\infty$)

Through handling of equation 3.29, bound circulation angle (ϕ) formed by resultant relative velocity (W) was computed. Consequently, relation of bound circulation angle, ϕ and velocity ratio, λ was given in figure 4.44. Here, velocity ratio, λ has a trend of decreasing with increasing free stream velocity, U_∞ until breaking point, then velocity ratio, λ increases with increasing free-stream velocity, U_∞ after breaking point. Here, bound circulation angle (ϕ) has a trend of increasing until breaking point with increasing free stream velocity (U_∞), then bound circulation angle, ϕ has a trend of decreasing with increasing free-stream velocity (U_∞) after breaking point.

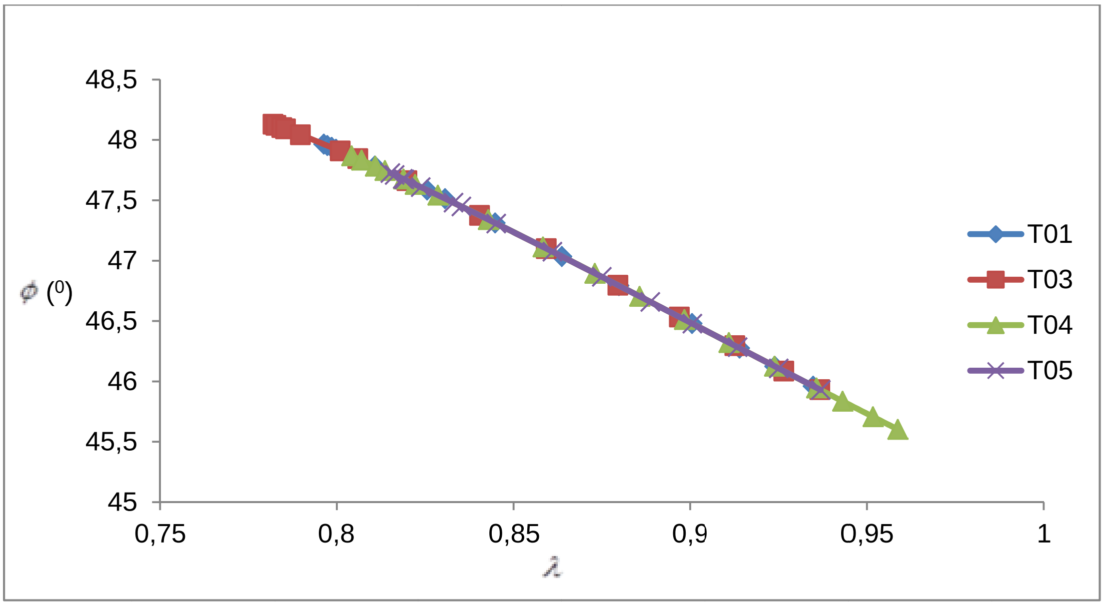

Figure 4.44. Variation of bound circulation angle, ϕ and velocity ratio, λ

Through handling of equation 3.29, bound circulation angle (ϕ) formed by resultant relative velocity (W) was computed. In addition, relations of bound circulation angle, ϕ with free-stream wind speed, U_∞ were presented in figure 4.45. Free-stream wind speed, U_∞ profile is given in increasing trend. When free stream wind speed, U_∞ increases, tangential flow induction factor (a') increases until breaking point, then tangential flow induction factor (a') decreases with increasing free stream wind speed, U_∞ . Due to approaching breaking point for smaller values of free-stream wind speed, U_∞ , as free-stream wind speed, U_∞ gets higher values (Ω/W) term decreases, but $(1+a')$ term increases. However, the term (Ω/W) suppresses the term $(1+a')$ to have smaller values in arccosine which results in larger angles with increasing free-stream wind speed, U_∞ . After breaking point, opposite slope of curve occurs and bound circulation angle (ϕ) decreases with increasing free-stream wind speed, U_∞ and bound circulation angle (ϕ) is defined as $\phi = \frac{180}{\pi}.\arccos(\frac{45\Omega(1+a')}{W})$. Finally, one can conclude that the highest bound circulation angle, ϕ occurs with free-stream wind speed (U_∞) in the range of $6m/s \geq U_\infty \geq 13m/s$ as seen in figure 4.45.

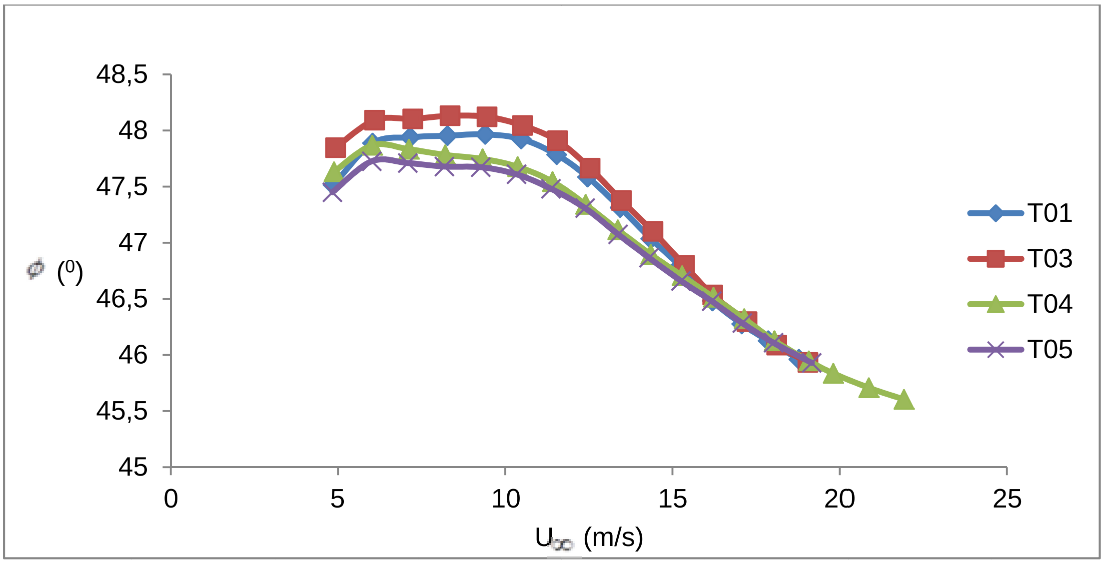

Figure 4.45. Variations of bound circulation angle, ϕ with free stream wind speed, U_∞

Bound circulation angle, ϕ is analyzed as a function of the tangential flow induction factor (a') and results are presented in figure 4.46. Slope of bound circulation angle, ϕ with the tangential flow induction factor (a') gradually slows down while the tangential flow induction factor (a') continues to increase. Agreements between results of turbines are very well.

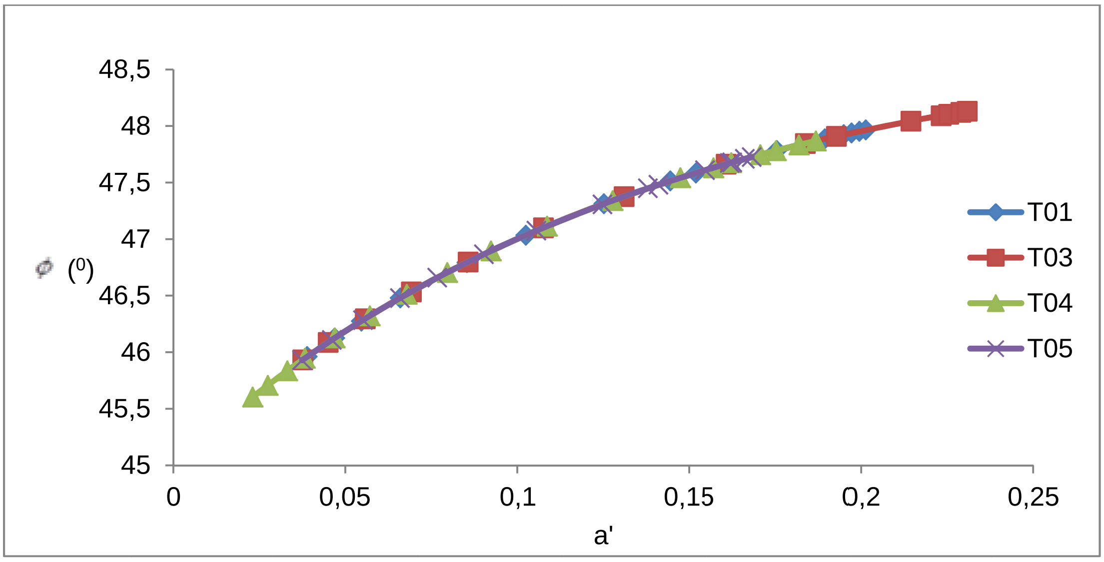

Figure 4.46. Variation of bound circulation angle, ϕ with tangential flow induction factor, a'

Variations of bound circulation angle (ϕ) with flow induction factor (a) is also analyzed and results are presented in figure 4.47. As indicated in this figure, bound circulation angle (ϕ) against flow induction factor (a) changes linearly which is similar to the relation of bound circulation angle (ϕ) and tangential flow induction factor, a'.

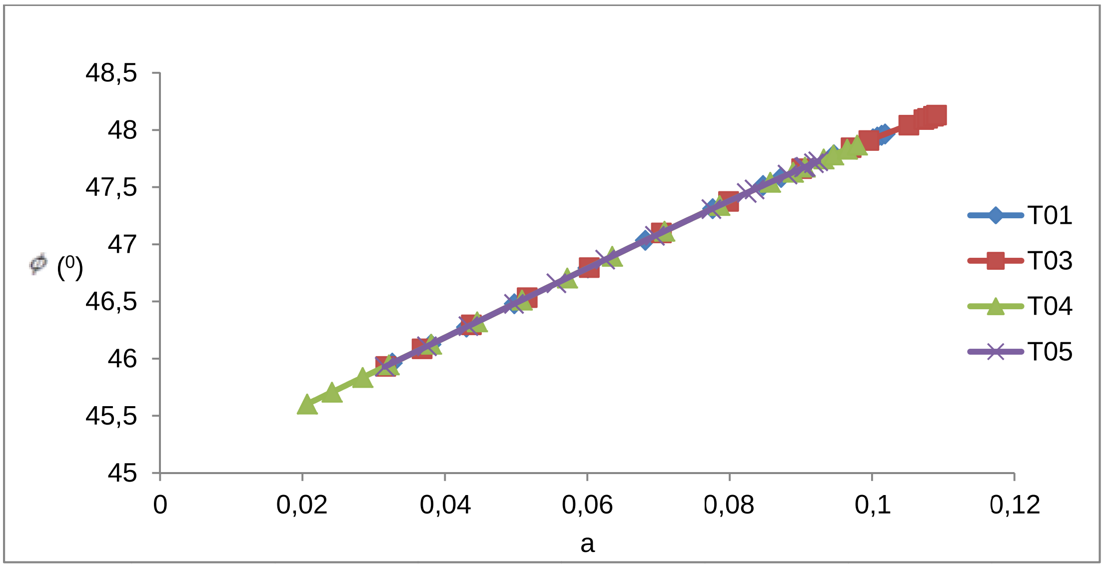

Figure 4.47. Variation of bound circulation angle, ϕ with flow induction factor (a)

One of the important parameter is bound circulation angle (ϕ). It is necessary to see variation of this angle (ϕ) with speed of rotor (Ω) as seen in figure 4.48. For lower speed of rotor (Ω) there is only 1% of difference between angles (ϕ) of all turbines. Highest value of bound circulation angle (ϕ) occurs for the rotation speed (Ω) in the range of $46^{\circ} \geq \phi \geq 48^{\circ}$. When rotor speed (Ω) increases this bound circulation angle (ϕ) gradually decreases. More or less all turbines have the same bound circulation angle (ϕ) for speed of $\Omega \geq 15\,rpm$.

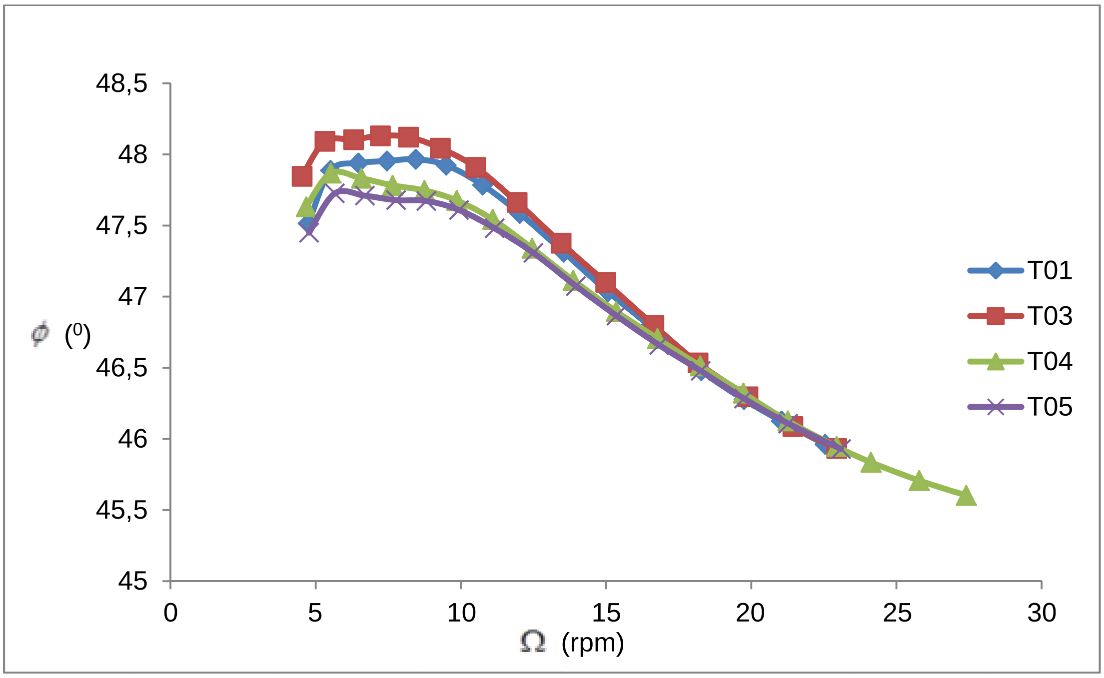

Figure 4.48. Variation of bound circulation angle (ϕ) with rotor speed (Ω)

Variation of bound circulation (ϕ) angle with the resultant relative velocity (W) at the blade is given in figure 4.49.

Plot of bound circulation angle (ϕ) and resultant relative velocity (W) at the blade has similar shape of curves plotted for bound circulation angle (ϕ) and rotor speed (Ω) shown in figure 4.48 due to the free-stream wind speed (U_{∞}). Namely, magnitude of free-stream wind speed (U_{∞}) effects both rotor speed (Ω) and resultant relative velocity (W).

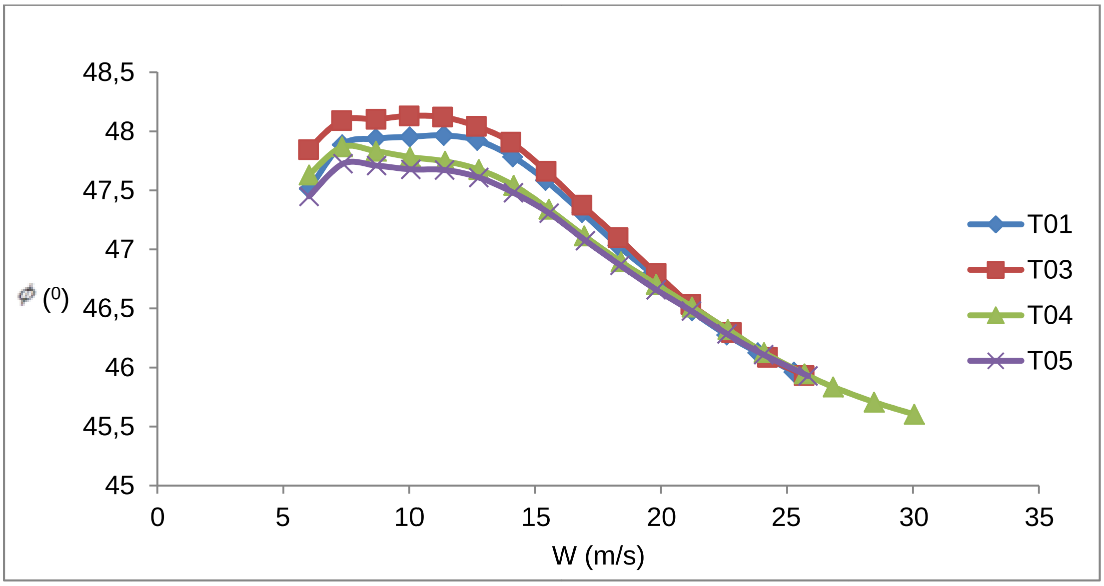

Figure 4.49. Variation of bound circulation angle, ϕ with resultant relative velocity, W

Resultant relative velocity, W and free-stream wind velocity, U_∞ distribution was given in figure 4.50.

Resultant relative velocity (W) depends on the free-stream wind speed (U_∞). Higher free-stream wind speed, U_∞ causes higher resultant relative velocity (W) as seen in figure 4.50.

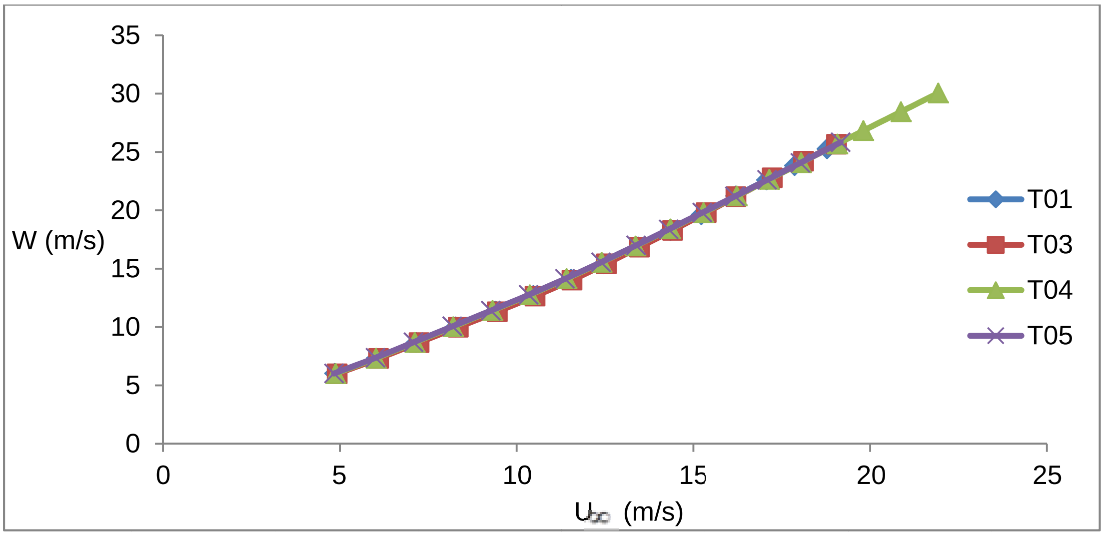

Figure 4.50. Variation of resultant relative velocity, W with free-stream wind velocity, U_∞

Total circulation (Γ) which is related to the induced velocity factors (a) and presented by the following equation;

$$\Gamma = \frac{4\pi U_{\infty}^{2} a(1-a)}{\Omega} \tag{3.28}$$

All variables including total circulation (Γ) depends on the free-stream wind speed (U_{∞}). Variations of total circulation (Γ) against wind speed (U_{∞}) are shown in figure 4.51. The magnitude of circulation (Γ) begins to increase up to wind speed of $U_{\infty} = 11 m/s$. From this free-stream wind speed (U_{∞}) further on, the value of total circulation (Γ) begins to decrease. There are 30 % differences between turbines for the highest magnitude of total circulation (Γ).

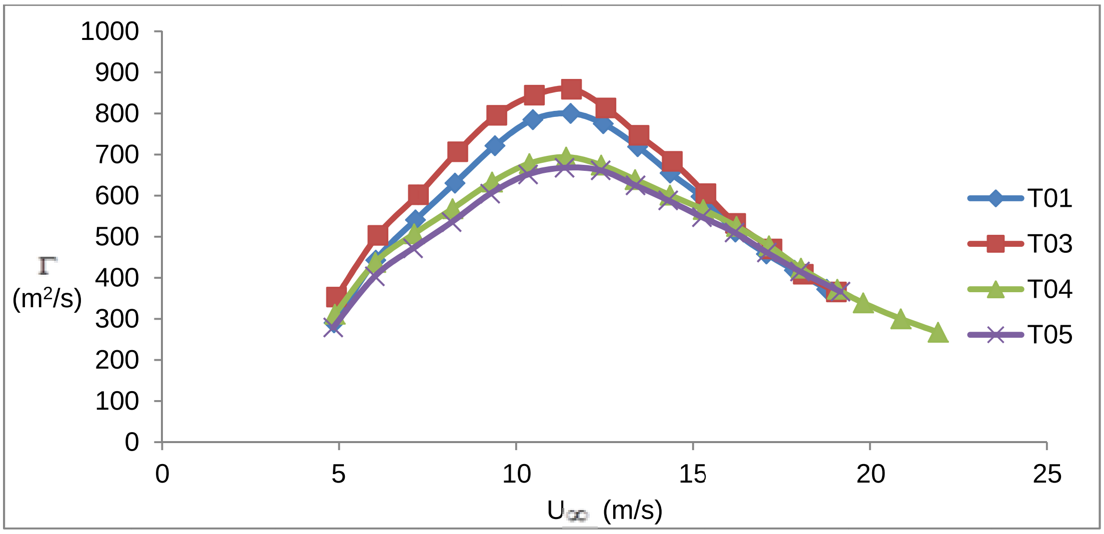

Figure 4.51. Variations of total circulation, Γ with free-stream wind speed, U_{∞}

Figure 4.52 presents the variation of power coefficient for BEM theory, C_p* with tip speed ratio, λ^*. Equations 3.40 and 3.41 give calculations of these two parameters.

Results of power coefficient for BEM theory, Cp* with tip speed ratio, λ^* decreases gradually. Results of all turbines agree well with each other.

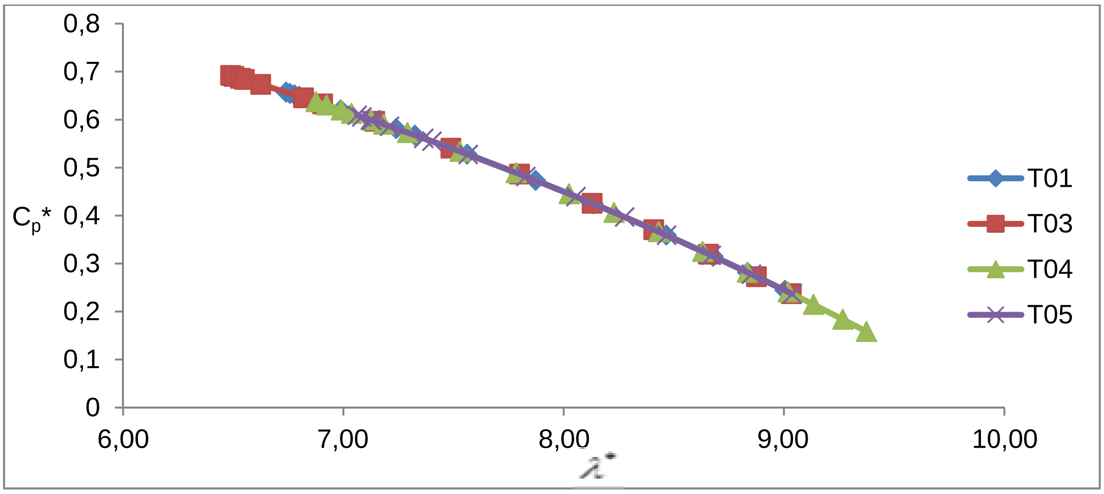

Figure 4.52. Variation of power coefficient for BEM theory, C_p* with tip speed ratio, λ^*

Figure 4.53 consists of variation of power coefficient for BEM theory, C_p* with wind speed (U_D) on the rotor.

Power coefficient for BEM theory, C_p* is approximately constant with wind speed on the rotor, U_D in the range of $5\,m/s \le U_D \le 10\,m/s$ and power coefficient for BEM theory, C_p* has maximum value. But power coefficient for BEM theory, C_p* values vary with turbine about 30 % in this maximum range. All turbines have same power coefficient for BEM theory, C_p* values having U_D higher than 15 m/s.

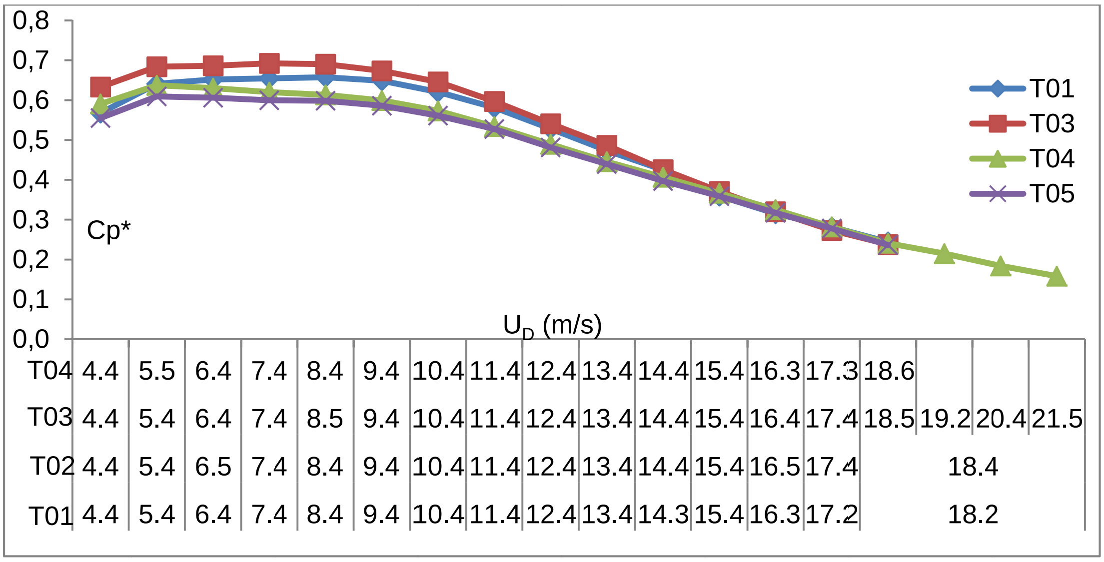

Figure 4.53. Distributions of power coefficient for BEM theory, C_p* with wind speed on the rotor, U_D

5. CONCLUSIONS

Cut-in and cut-out speeds with other important specifications were presented in table 3.1. Expression written in the table as “At enclosed table” refers the raw data that was received from wind farm.

According to the data obtained from wind farm, firstly analyses were performed without taking cut-in and cut-out speeds into consideration. Monthly averages wind data were used in estimations of related parameters. At very low speeds, turbine cannot generate electricity where it is expressed in its specifications as cut-in speed. Averages of maximum power and real power generally increase with increasing free-stream wind speeds (U_∞) when cut-in speeds are considered, however efficiencies decrease to meaningful values. The magnitude of circulation (Γ) begins to increase up to wind speed of $U_\infty = 11 m/s$. From this free-stream wind speed (U_∞) further on, the value of total circulation (Γ) begins to decrease. There are 30 % differences between turbines for the highest magnitude of total circulation (Γ). One of the important parameter is bound circulation angle. For lower speed of rotor (Ω) there is only 1% of difference between angles (φ) of all turbines. Highest value of bound circulation angle (φ) occurs for the rotation speed (Ω) in the range of $46^\circ \geq \varphi \geq 48^\circ$. When rotor speed increases this bound circulation angle (φ) gradually decreases. More or less all turbines have the same bound circulation angle (φ) for speed of $\Omega \geq 15 rpm$. Power coefficient for BEM theory, Cp* is approximately constant with wind speed on the rotor, U_D in the range of $5 m/s \leq U_D \leq 10 m/s$ and power coefficient for BEM theory, Cp* has maximum value. But power coefficient for BEM theory, Cp* values vary with turbine about 30 % in this maximum range.

It is observed that maximum power generations occur in July for all turbines, when average wind speed (U_∞) is maximum and air temperature is also high in this month compared with other months for all turbines. In addition, non-stop generations take place in this month for all turbines.

The total electric generation of five turbines was 38.09176 GWh in one year (2010). Turbine T04 generated 9.03 GWh electricity. The maximum power was generated by turbine T04, on the other hand, turbine T01 generated 6.12 GWh electricity. Although both turbines are installed in the same wind farm, the difference of electric production in between turbines T01 and T04 is 33% in the year of 2010. This wind farm is situated in the valley containing many hills, crests and roughness. This topographic condition of the farm effects wind directions and magnitude of wind speed, U_{∞}.

Aerodynamic performance of turbines was carried out through using wind data. Obstacles around each turbine that cause impacts on measured wind speed U and wind direction. In order to avoid the effect of obstacles and roughness around the turbine stations, the roughness of the terrain should be examined for each turbine station and considered for correction of the wind speed. The present wind turbines have a height of 80 meter and diameter of rotor is 90 meter. The distance in vertical direction between ground surface and the tip of the blade is 35 m. Any hills or obstacles between forward face of the rotor and bellowing wind may convey the main flow to a higher level than tower of the turbine. Under this condition, they cannot receive some part of the available wind power for conversion.

REFERENCES

AKDAĞ, S., A., and GÜLER, Ö., 2010. Evaluation of Wind Energy Investment Interest and Electricity Generation Cost Analysis for Turkey. Applied Energy, 87: 2574 – 2580

BASKUT, O., OZGENER, O., OZGENER, L., 2010. Effects of Meteorological Variables on Exergetic Efficiency of Wind Turbine Power Plants. Renewable and Sustainable Energy Reviews, 14: 3237 – 3241

BASKUT, O., OZGENER, O., OZGENER, L., 2011. Second Law Analysis of Wind Turbine Power Plants: Cesme, Izmir example. Energy, 36: 2535 – 2542

BAŞKURT, Ö. 2010, Rüzgâr Güç Tesislerinde Ekserji Analizi, E.U. Turkey

BHUTTA, M., M., A., HAYAT, N., FAROOQ, A., U., ALİ, Z., JAMIL, S. R., HUSSAIN, Z., 2012. Vertical Axis Wind Turbine – A Review of Various Configurations and Design Techniques. Renewable and Sustainable Energy Reviews, 16: 1926 – 1939

BOSTON UNIVERSITY MECHANICAL ENGINEERING DEPARTMENT, (Unpublished)

BURTON, T., JENKINS, N., SHARPE, D., BOSSANYI, E., 2011. Wind Energy Handbook. John Wiley & Sons, Ltd., United Kingdom, p. 1-49

GOLDING, E. W. 1955, “The Generation of Electricity by Wind Power”, E&F, N, Spon Limited: London

GONZÁLEZ, J., S., PAYÁN, M. B., SANTOS, J., M., R., GONZÁLEZ-LONGATT, F. 2014. A Review and Recent Developments in the Optimal Wind - Turbine Micro - Siting Problem. Renewable and Sustainable Energy Reviews, 30: 133 – 144

HEPBASLI, A., and ALSUHAIBANI, Z., 2011. Exergetic and Exergoeconomic Aspects of Wind Energy Systems in Achieving Sustainable Development. Renewable and Sustainable Energy Reviews, 15: 2810 – 2825

KORONEOS, C., SPACHOS, T., MOUSSIOPOULOS, N., 2003. Exergy Analysis Of Renewable Energy Sources. Renewable Energy, 28: 295 – 310

KORONEOS, C., SPACHOS, T., MOUSSIOPOULOS, N., 2001.Exergy Analysis of Renewable Energy Sources. Elsevier, p. 295 – 310

KARAMANIS, D., 2011. Management of Moderate Wind Energy Coastal Resources. Energy Conversion and Management, 52: 2623 – 2628

KINCAY, O., 2008. Rüzgâr enerjisine dayalı elektrik santralleri lisans başvurusunda izlenecek yol. Yıldız Teknik Üniversitesi Makine Mühendisliği Bölümü, İstanbul, p.7 - 10

LIOR, N. and ZHANG, N. 2007. Energy, Exergy, and Second Law Performance Criteria. Energy, 32: 281 – 296

MANWELL, J., F., MCGOWAN, J., G., ROGERS, A., L., 2009. Wind Energy Explained Theory, Design and Application. John Wiley & Sons, Ltd., United Kingdom, p. 91-115

MOSTAFAEIPOUR, A., JADIDI, M., MOHAMMADI, K., SEDAGHAT, A., 2014. An Analysis of Wind Energy Potential and Economic Evaluation in Zahedan, Iran. Renewable and Sustainable Energy Reviews, 30: 641 – 650

OZGENER, O., 2006. A Small Wind Turbine System (SWTS) Application And Its Performance Analysis. Energy Conversion and Management, 47: 1326 – 1337

ONDER, M., 2006. Yatay Eksenli Rüzgâr Türbin Kanadının Bilgisayar Destekli Tasarımı: Yüksek Lisans Tezi, Gazi Üniversitesi, Fen Bilimleri Enstitüsü, Ankara, 28 - 35p.

POPE, K., DINCER, I. NATERER, G., F., 2010. Energy and Exergy Efficiency Comparison of Horizontal and Vertical Axis Wind Turbines. Renewable Energy, 35: 2102 - 2113

REDHA, A., M., DİNÇER, İ., GADALLA, M., 2011 .Thermodynamic Performance Assessment of Wind Energy Systems: An Application. Energy, 36: 4002 - 4010

SPERA, D., A., 2009. Wind Turbine Technology Fundamental Concepts of Wind Turbine Engineering. ASME, USA, p. 281-293

ŞAHİN, A. Dinçer, İ, Rosen, M, 2005, New Spatio - Temporal Wind Exergy Maps, İTÜ, Turkey

ŞAHİN, B., and BİLGİLİ, M., 2009. Investigation of Wind Energy Density in the Southern and Southwestern Region of Turkey. Journal of Energy Engineering, 135:12-20.

TANRIÖVEN, M., 2011. Rüzgâr ve Güneş Enerjili Güç Sistemleri. Yıldız Teknik Üniversitesi Elektrik Mühendisliği Bölümü, İstanbul, p. 7

XYDIS, G., 2012. Effects of Air Psychrometrics on the Exergetic Efficiency of a Wind Farm at a Coastal Mountainous Site - An Experimental Study. Energy, 37: 632 – 638

XYDIS, G., KORONEOS, C., LOIZIDOU, M. 2009. Exergy Analysis in a Wind Speed Prognostic Model as a Wind Farm Sitting Selection Tool: A Case Study in Southern Greece. Applied Energy, 86: 2411–2420

XYDIS, G., NANAKI, E., A., KORONEOS, C., J., 2014. Comparative Wind Farm Planning on a High Plateau: Dust Dispersion as a Sitting Constraint. Land Use Policy, 39: 22 – 33

Yenilenebilir Enerji Teknolojileri, Rüzgâr Türbinlerinde Üretilen Alternatif Akımın Temelleri (MİLLİ EĞİTİM BAKANLIĞI), 2012. Ankara, p. 10 – 12

YILMAZ, S., and ŞAHİN, A., D., 2008. Rüzgâr Enerjisinde Ekserji İncelemesi, VII. Ulusal Temiz Enerji Sempozyumu. UTES, p. 715 - 724

YILMAZ, T., B., and AVCI, B., 2012. Rüzgâr Türbini Kanat Tasarımı ve Analizi Bitirme Projesi, Dokuz Eylül Üniversitesi Mühendislik Fakültesi Makine Mühendisliği Bölümü, İzmir – Turkey, p.5

CURRICULUM VITAE

Akın İLHAN was born in Şanlıurfa by the year of 1983. His mother is teacher, father is civil engineer. He completed his elementary and secondary education in Tarsus/Mersin. He graduated from Tarsus American College (Tarsus/Mersin) in 2001. Akın İLHAN fulfilled higher education in Çukurova University Mechanical Engineering Department by the year of January 2008. He served for his military service in Konya – Karapınar Atış Poligon Grup Komutanlığı until January 2009.

After January 2009, Akın İLHAN took charge in various private sector companies. He started his career in Doğuş İnşaat ve Ticaret A.Ş. as mechanical engineer in the project of Boyabat Dam and Hydro Electrical Plant Construction. He continued his job through the ends of 2010 year. By the year of 2011, he worked as Machine Supply and Maintenance Chief (Azerbaijan – Xaçmaz and Azerbaijan – Baku Cities respectively) in the company of Azer İnşaat Servis LLC in road construction projects. At the start of 2012 year, for a short time he worked in Volvo Group Automotive Ltd. Şti. (İstanbul) as Service Area Manager of Volvo Trucks for southern cities of Turkey. By the ends of 2012 year, Akın İLHAN took charge in Lilpar İnşaat Tur. Loj. Gıda San. ve Tic. Ltd. Şti. as corporate executive and shareholder of the same company. He quitted from this job through the ends of 2013. He continued with his career as Academic Personnel in Amasya University Technology Faculty Mechanical Engineering Department (as Research Assistant – September 2013). He still continues with this work.

Akın İLHAN started his M.Sc. Education in September 2012 at the department of Mechanical Engineering of Çukurova University Natural and Applied Sciences Institute.

APPENDICES

Appendix 1 represents average data of all turbines distributed for months when boundary values weren’t considered (Section 4.1). By the whole data obtained from wind farm, following averages were obtained without any elimination.

Appendix 1. Monthly average wind data (Without considering boundary values)

	Hourly Wind Data (m/s)					Hourly Generation Data (kWh)					Hourly Wind Direction Data (º)					Hourly Temperature Data (Cº)				
Turbine no	T01	T02	T03	T04	T05	T01	T02	T03	T04	T05	T01	T02	T03	T04	T05	T01	T02	T03	T04	T05
Date	Hourly Average Wind Speed (m/s)	Hourly Average Wind Speed (m/s)	Hourly Average Wind Speed (m/s)	Hourly Average Wind Speed (m/s)	Hourly Average Wind Speed (m/s)	Hourly Average Generation (kWh)	Hourly Average Generation (kWh)	Hourly Average Generation (kWh)	Hourly Average Generation (kWh)	Hourly Average Generation (kWh)	Hourly Average Wind Direction (º)	Hourly Average Wind Direction (º)	Hourly Average Wind Direction (º)	Hourly Average Wind Direction (º)	Hourly Average Wind Direction (º)	Hourly Average Temperature (Cº)	Hourly Average Temperature (Cº)	Hourly Average Temperature (Cº)	Hourly Average Temperature (Cº)	Hourly Average Temperature (Cº)
January	**7.2324**	**8.1470**	**8.0663**	**9.1306**	**8.2529**	**752.4377**	**955.7716**	**880.7713**	**1155.6235**	**953.7995**	**166.4066**	**187.3761**	**168.2285**	**183.9066**	**207.1631**	**7.6801**	**7.6631**	**8.2245**	**8.2390**	**7.5450**
February	7.6806	8.4876	8.4939	9.5778	8.7172	809.8635	1115.5078	1024.3218	1322.8021	1095.4809	175.3007	174.1389	140.8252	186.1716	201.5466	8.1528	8.1877	8.7931	8.6262	7.9355
March	**6.2308**	**6.7863**	**6.6488**	**7.0454**	**6.5504**	**546.8749**	**677.0642**	**616.2340**	**692.4607**	**585.4890**	**137.5198**	**108.5498**	**112.5236**	**116.1778**	**157.2111**	**12.0721**	**11.8432**	**12.5986**	**12.1100**	**11.8463**
April	5.9539	6.5873	6.1258	6.8715	6.2686	454.3213	586.3709	483.5192	629.3132	503.8520	85.2488	90.9441	88.1096	86.8949	154.1246	14.4949	14.5088	14.8611	14.2602	14.0992
May	**7.6794**	**8.4786**	**7.6967**	**8.7029**	**8.0960**	**823.1929**	**1084.7041**	**905.8800**	**1073.0657**	**902.8120**	**455.9177**	**675.8872**	**379.5238**	**322.8945**	**387.6637**	**17.3763**	**17.4630**	**17.8934**	**16.9599**	**16.7090**
June	8.3611	9.5665	8.6612	9.6589	9.0731	991.1619	1303.6618	1167.2695	1346.7091	1153.0893	309.8879	1000.0000	44.4481	43.9176	152.3224	20.3681	20.4521	20.9611	19.8262	19.7299
July	**10.6988**	**12.5136**	**11.2645**	**12.8696**	**12.0539**	**1605.4834**	**2068.5622**	**1922.5752**	**2127.4713**	**1934.5037**	**329.8005**	**1000.0000**	**27.2878**	**20.4794**	**196.8814**	**21.9068**	**21.9243**	**22.5768**	**21.1285**	**21.0298**
August	8.5465	10.0122	8.7045	9.6624	9.1507	747.7441	1347.9105	1131.3608	1287.2327	1111.2862	296.7843	1000.0000	26.3498	22.4024	205.2694	26.3618	25.3094	25.6059	24.5649	24.4392
September	**7.4302**	**8.6397**	**7.7810**	**8.7583**	**8.2962**	**780.0917**	**1085.3351**	**958.3751**	**1167.8482**	**1006.5631**	**202.6249**	**1000.0000**	**46.7326**	**43.7237**	**183.7405**	**25.6601**	**22.5336**	**22.8647**	**21.8915**	**21.9426**
October	5.5233	6.2463	5.6559	6.2741	5.8394	371.7414	506.3546	320.4060	534.7630	415.8938	96.0997	1000.0000	253.2081	91.6636	161.9880	20.9839	18.3065	18.7597	17.9587	17.9302
November	**5.1614**	**5.7721**	**5.3357**	**6.2695**	**5.7415**	**268.8630**	**376.9640**	**299.1114**	**512.5969**	**379.7291**	**190.8414**	**1000.0000**	**182.0529**	**180.0286**	**186.5208**	**19.6671**	**17.0093**	**17.3894**	**17.0431**	**16.9857**
December	6.7690	7.5387	6.9623	8.2111	7.3805	628.0291	806.0530	698.3232	995.3280	789.9731	209.0102	1000.0000	193.9014	193.3274	192.6279	12.0522	10.2139	10.6750	10.7825	10.2339
Yearly	**7.2723**	**8.2313**	**7.6164**	**8.5860**	**7.9517**	**731.6504**	**992.8550**	**867.3456**	**1070.4345**	**902.7060**	**221.2869**	**247.3792**	**138.5993**	**124.2990**	**198.9216**	**17.2314**	**16.2846**	**16.7669**	**16.1159**	**15.8689**

Appendix 2 represents average data of all turbines distributed for months when boundary values were considered (Section 4.4). By the whole data obtained from wind farm, following averages were obtained by performing eliminations on data outside of boundary limits (Eliminations on speeds below cut-in, zero or negative generations and unrecorded wind directions).

Appendix 2. Monthly average wind data (Considering boundary values)

	Hourly Wind Data (m/s)					Hourly Generation Data (kWh)					Hourly Wind Direction Data (º)					Hourly Temperature Data (Cº)				
Turbine no	T01	T02	T03	T04	T05	T01	T02	T03	T04	T05	T01	T02	T03	T04	T05	T01	T02	T03	T04	T05
Date	Hourly Average Wind Speed (m/s)	Hourly Average Wind Speed (m/s)	Hourly Average Wind Speed (m/s)	Hourly Average Wind Speed (m/s)	Hourly Average Wind Speed (m/s)	Hourly Average Generation (kWh)	Hourly Average Generation (kWh)	Hourly Average Generatio n (kWh)	Hourly Average Generation (kWh)	Hourly Average Generation (kWh)	Hourly Average Wind Direction (º)	Hourly Average Wind Direction (º)	Hourly Average Wind Direction (º)	Hourly Average Wind Direction (º)	Hourly Average Wind Direction (º)	Hourly Average Temperatu re (Cº)	Hourly Average Temperatur e (Cº)	Hourly Average Temperatur e (Cº)	Hourly Average Temperatur e (Cº)	Hourly Average Temperatur e (Cº)
January	8.1478	8.9702	8.8207	9.9955	9.2463	934.9890	1129.0026	1044.9531	1336.8282	1163.6981	161.6512	187.7583	164.6394	187.2648	214.0952	7.5056	7.5515	8.1438	8.1534	7.3802
February	9.1042	9.9408	9.6454	10.8503	10.0255	1130.3886	1407.0657	1237.4326	1564.2445	1334.8462	174.1532	177.1821	136.9686	185.5210	209.3203	7.8926	7.9311	8.6981	8.6141	7.8654
March	7.7481	8.2836	7.9719	8.5720	8.1755	787.0166	919.2235	838.4587	966.2844	860.7220	129.5461	100.6323	98.8287	110.5427	162.6416	12.0791	12.0647	12.7037	12.1488	11.8182
April	6.9945	7.6366	6.9755	8.0103	7.4254	604.9658	745.7420	615.4710	801.9783	668.2223	73.8275	74.1808	70.4101	74.6980	146.5428	14.1509	14.2137	14.6276	13.9331	13.6707
May	7.7955	9.0517	7.8743	8.9069	8.3282	813.0191	1144.5567	907.0408	1070.6649	909.4927	163.2090	38.2035	42.3755	43.3347	136.2634	17.3759	16.1736	17.8808	17.0237	16.7479
June	8.8205	10.0211	9.0317	10.0863	9.4910	1083.5882	1393.0981	1241.8548	1431.5881	1231.0747	315.8384	1000.0000	39.0754	39.5662	151.1177	20.0633	20.2345	20.7507	19.5839	19.4815
July	10.6988	12.5965	11.2645	12.8792	12.0539	1605.4834	2094.9774	1922.5752	2136.1161	1934.5037	329.8005	1000.0000	27.2878	20.4785	196.8814	21.9068	21.6701	22.5768	21.1266	21.0298
August	8.6195	10.0169	8.7504	9.7320	9.2327	1019.4804	1375.2438	1161.5017	1303.1872	1142.3703	326.2478	1000.0000	24.0455	20.9217	202.1376	27.0430	25.4159	25.5241	24.4869	24.3409
September	7.9791	9.1485	8.3018	9.4050	8.9074	878.5708	1190.3027	1058.0654	1298.6210	1119.8523	212.7814	1000.0000	36.0657	33.7141	183.7344	25.6680	22.3909	22.7339	21.7016	21.7668
October	6.5388	7.2470	6.6648	7.2641	6.8003	513.0336	645.4409	549.9163	678.9558	543.7763	80.8479	1000.0000	90.8638	78.7559	160.3192	21.6640	18.4181	19.5235	18.0375	17.9968
November	6.1826	6.7912	6.2151	7.2607	6.6900	392.6736	508.1528	412.7273	658.3294	506.7433	191.4677	1000.0000	188.4941	190.3438	184.6502	20.2126	16.8024	17.3718	16.9637	16.8605
December	8.1179	9.0495	8.3055	9.6456	8.7643	881.4423	1054.3497	922.9882	1250.1878	1033.1305	215.3998	1000.0000	206.0652	203.9406	197.4932	12.0818	9.7383	10.2773	10.4133	9.7438
Yearly	8.0623	9.0628	8.3185	9.3840	8.7617	887.0543	1133.9297	992.7488	1208.0822	1037.3694	197.8975	115.5914	93.7600	99.0902	178.7664	17.3036	16.0504	16.7344	16.0156	15.7252